

**Quantitative investigations of *FXN*
transcription and epigenetic
modifications, including histone
acetylation and methylation, in FRDA
human and mouse tissues.**

A thesis submitted for the degree of Master of
Philosophy (M.Phil)

by

Daniah M. Trabzuni

Division of Biosciences
School of Health Sciences and Social Care
Brunel University

October 2008

Declaration

This declaration is to certify that all of the work contained within this thesis is
the author's own original work, except where otherwise specified within the text.

Daniah Trabzuni

Acknowledgments

All Praise is to Almighty Allah for His love, care, provision and answering my prayers for giving me the strength, perseverance and patience to carry out this work successfully. I thank Allah for the mercy which He has bestowed upon me throughout my entire life and in particular while working on this thesis so I can reach the best places and meet the best people.

My thanks to my principle supervisor Dr. Mark Pook for his supervision, and my appreciation to my second supervisor Dr. Suling Li.

I am as ever, truly fortunate to have a loving family who always support me. My parents, I am indebted and thankful for your constant and invaluable support, encouragement and prayers for me. My siblings, Dina, Fadi and Sulafa: I am highly thankful for your continuous support, encouragement and emotional help during difficult times.

I am truly grateful to my best friend Faiqa Ahmad. My deep thanks and appreciation to you for your continuous support at all levels: psychologically, emotionally and professionally at all times. You have given me the strength, patience, guidance to continue and produce this thesis.

I give my sincere appreciation and special thanks to my chairman Dr. Brian Meyer at King Faisal Specialist Hospital and Research Centre, for being a true support over the years and every time I needed him. Moreover, I am grateful to all my friends who helped, and supported me with their valuable suggestions throughout this thesis. Especially the long hours I have spent with them to reach this point and the help we have given each other to improve our outcomes whenever it was possible. I greatly appreciate your help; I just cannot find words to thank you all enough.

Finally, I would like to express my profound gratitude to King Faisal Specialist Hospital and Research Centre and the Ministry of Higher Education, Kingdom of Saudi Arabia for providing me with my scholarship.

Abstract

Friedreich ataxia (FRDA) is an autosomal recessive neurodegenerative disorder characterized by progressive gait and, limb ataxia, cardiomyopathy, diabetes mellitus, optic atrophy and hearing loss. It is most often caused by homozygous expanded (GAA)·(TTC)n repeats within intron 1 of the *FXN* gene, resulting in severely reduced levels of frataxin protein. The exact mechanisms of how the expanded (GAA)·(TTC)n repeats reduce *FXN* transcription are not fully understood. However, many studies have suggested that the expanded repeat may induce epigenetic modifications that cause the *FXN* transcription inhibition to occur.

In the past few years, epigenetic modifications have been given considerable attention as an important mechanism that is contributing to the aetiology of FRDA. This thesis investigated histone acetylation and methylation in three different regions of the *FXN* gene: *FXN* promoter, upstream GAA and downstream GAA, using chromatin immunoprecipitation (ChIP) and quantitative reverse transcriptase PCR (qRT-PCR) of the human and transgenic mouse brain tissues. Furthermore, the frataxin mRNA levels were investigated in autopsied brain tissues from an FRDA patient and *FXN* transgenic mouse brain, heart and liver tissues. In addition, a preliminary study that investigated the effect of a histone deacetylase inhibitor (HDACi) on *FXN* transcription and histone modifications (acetylation) of transgenic mouse brain, heart and liver tissues was conducted.

Results showed an overall significant decrease in the acetylation pattern of H3K9ac and H4K16ac residues in all three regions within *FXN* gene. Moreover, a significant increase in the di- and trimethylation pattern of the H3K9me2 and the H3K9me3 residues was identified in all three regions of the *FXN* gene. The results were comparable between the FRDA patient and transgenic mouse (YG8, YG22) brain tissues. The *FXN* mRNA levels showed a significant decrease in all transgenic mouse brain, heart and liver tissues, which is comparable with the *FXN* mRNA level of the FRDA patient brain and heart tissues.

Results for the preliminary HDACi study showed an approximate 20-30 % increase in the *FXN* mRNA level in different transgenic mouse tissues after 3 days intake at 150mg/kg dose. In addition, there was an increase in the acetylation pattern of the H3K9ac and the H4K12ac in the HDACi treated transgenic mouse brain tissues.

These studies will aid the understanding of *FXN* epigenetic modifications and their contribution to FRDA disease; this is an exciting challenge leading to a new effective FRDA therapeutic pathway.

Table of contents

Declaration

Acknowledgments

Abstract.....	1
Table of Contents.....	3
List of figures.....	7
Abbreviations.....	11

1 Introduction

1.1 Ataxia.....	15
1.1.1 Inherited progressive ataxia disorders.....	15
1.2 Friedreich ataxia (FRDA).....	16
1.2.1 The identification of FRDA.....	16
1.2.2 Clinical Features.....	16
1.2.3 Pathology.....	18
1.2.4 Epidemiology and prevalence.....	20
1.2.5 Genetic background.....	20
1.3 Epigenetics.....	53
1.3.1 The definition of epigenetics.....	53
1.3.2 Molar and Molecular epigenetics.....	55
1.3.3 Mechanisms of molecular epigenetic regulations.....	57
1.3.4 The relationship between the different mechanisms of epigenetic regulations.....	67

1.3.5	Molecular epigenetic mechanisms in Friedreich ataxia	70
1.4	Therapeutic approaches.....	74
1.4.1	Antioxidant and iron chelation-based approaches.....	74
1.4.2	Gene based approach.....	74
1.4.3	Molecules that increase frataxin mRNA or protein.....	76
1.4.4	Gene therapy approach.....	76
1.5	<i>In vitro</i> and <i>in vivo</i> modules.....	77
1.5.1	<i>In vitro</i> models.....	77
1.5.2	<i>In vivo</i> models.....	77
1.6	The aim of the study.....	80

2 Materials and Methods

2.1	Genotyping of mice.....	81
2.1.1	DNA Extraction.....	81
2.1.2	(GAA) PCR.....	81
2.1.3	(FXN) knockout PCR.....	83
2.2	RNA Extraction using TRIZOL®Reagent.....	84
2.2.1	Tissue Homogenisation.....	84
2.2.2	Phase separation.....	85
2.2.3	RNA precipitation and wash.....	85
2.2.4	RNA Quality Check.....	86
2.3	cDNA Synthesis.....	86
2.3.1	cDNA Synthesis.....	86
2.3.2	cDNA Quality Check.....	87

2.4	Chromatin immuno-precipitation assay (ChIP).....	89
2.4.1	Tissue Homogenisation.....	89
2.4.2	DNA and Protein Cross-Linking.....	89
2.4.3	DNA Shearing.....	90
2.4.4	DNA immuno-precipitation.....	90
2.4.5	DNA Phenol /Chloroform Extraction.....	92
2.4.6	DNA Quality Check.....	93
2.5	Relative Quantitative PCR.....	94
2.5.1	cDNA Quantification.....	94
2.5.2	ChIP genomic DNA Quantification.....	95

3 Results

3.1	Genotyping of mice.....	97
3.1.1	Screening for the (GAA) _n ·(TTC) _n repeats.....	97
3.1.2	Screening for the <i>Fxn</i> knockout alleles	97
3.2	<i>FXN</i> mRNA level in the human brain and transgenic mouse brain, heart and liver tissues.....	99
3.2.1	RNA Extraction quality Check.....	100
3.2.2	cDNA Synthesis quality Check.....	100
3.2.3	Relative Quantitative, qRT-PCR.....	102
3.3	Histone modifications of <i>FXN</i> in human and transgenic mouse brain tissues.....	108
3.3.1	Chromatin immuno-precipitation assay (ChIP).....	108
3.3.2	Relative Quantitative, qRT-PCR	111
3.4	HDACi effect on mRNA level of <i>FXN</i> in transgenic mouse brain, heart and liver tissues.....	117

3.5 HDACi effect on histone modifications of <i>FXN</i> in transgenic mouse brain tissues.....	121
---	------------

4 Discussion.....123

List of references.....	127
--------------------------------	------------

Appendix 1.....	135
------------------------	------------

List of figures

Figure 1.1:	Overview of the main sites of neuronal loss and organ dysfunction in Friedreich ataxia.....	19
Figure 1.2:	Dorsal root ganglion neurons of an embryonic rat (100X).....	20
Figure 1.3:	Ideogram of the human chromosome 9.....	21
Figure 1.4:	<i>FXN</i> gene structure.....	22
Figure 1.5:	Northern blot analysis of frataxin mRNA in poly (A) RNA from total mouse embryos.....	23
Figure 1.6:	Frataxin expression at E16.5.....	23
Figure 1.7:	Frataxin expression in developing dorsal root ganglia.....	24
Figure 1.8:	Structure of frataxin.....	27
Figure 1.9:	Suggested pathogenesis of FRDA.....	29
Figure 1.10:	Diagram showing the Pandolfo hypothesis.....	30
Figure 1.11:	Iron binding.....	31
Figure 1.12:	Diagram showing some of the ways that an amino-acid mutation can disrupt a protein's structure or function.....	32
Figure 1.13:	Unusual DNA structures formed by all expandable repeats.....	38
Figure 1.14:	Model for the role of different biology processes <i>in vivo</i>	39
Figure 1.15:	Three hypotheses to explain early events in repeat expansions.....	41

Figure 1.16:	A model for replication blockage by (GAA) n •(TTC) n repeats leading to their expansion.....	42
Figure 1.17:	Gap repair model for repeat expansions in non-dividing cells.....	44
Figure 1.18:	Loss of stabilizing interruptions within expandable repeats.....	46
Figure 1.19:	Recombination models for repeat expansions.....	47
Figure 1.20:	Cleavage of a stable DNA structure on the lagging-strand template.....	48
Figure 1.21:	Transcription-coupled RNA-DNA hybrid formation in a (GAA) n •(TTC) n repeat.....	51
Figure 1.22:	Schematic representation of the frataxin minigene.....	52
Figure 1.23:	The external environment interacts with the internal environment to influence fetal development with both immediate and life-long consequences.....	56
Figure 1.24:	Nucleosome structure.....	57
Figure 1.25:	Properties of euchromatic regions.....	58
Figure 1.26:	Properties of heterochromatic regions.....	59
Figure 1.27:	Methylation of cytosine.....	63
Figure 1.28:	The interaction of DNA methylation, histone modification and other factors such as small RNAs contribute to an overall regulation of the gene expression and allows cells to remember their identity.....	68
Figure 1.29:	Interaction between RNA, histone modification and DNA methylation in heritable silencing.....	69
Figure 1.30:	Model for chromatin organization in the region containing residue 13 in normal and FRDA alleles.....	71

Figure 1.31:	The current understanding as to why GAA repeats reduce frataxin message levels.....	73
Figure 1.32:	Two steps mating strategy.....	78
Figure 3.1:	GAA genotyping PCR product.....	98
Figure 3.2:	<i>Fxn</i> knockout PCR.....	99
Figure 3.3:	RNA extraction.....	100
Figure 3.4:	cDNA quality check PCR 1.....	101
Figure 3.5:	cDNA quality check PCR 2.....	101
Figure 3.6:	qRT-PCR analysis of <i>FXN</i> mRNA in human brain tissue...	103
Figure 3.7:	qRT-PCR analysis of <i>FXN</i> mRNA in transgenic mouse brain tissues.....	104
Figure 3.8:	qRT-PCR analysis of <i>FXN</i> mRNA in transgenic mouse heart tissues.....	105
Figure 3.9:	Quality check of the qPCR product 1.....	106
Figure 3.10:	Quality check of the DNA qPCR product 2.....	107
Figure 3.11:	Schematic representation of 2.2 kb at the 5'end of the <i>FXN</i> gene.....	109
Figure 3.12:	DNA sonication.....	110
Figure 3.13:	ChIP DNA quality check PCR.....	110
Figure 3.14:	Histone acetylation analysis in human brain tissue.....	112
Figure 3.15:	Histone methylation analysis in human brain tissue.....	113
Figure 3.16:	Histone acetylation analysis in transgenic mouse brain tissue.....	114

Figure 3.17:	Histone methylation analysis in transgenic mouse brain tissue.....	115
Figure 3.18:	Quality check of the DNA qPCR product 1.....	116
Figure 3.19:	HDACi effect on FXN mRNA of YG8 brain tissues.....	118
Figure 3.20:	HDACi effect on FXN mRNA of YG8 liver tissues.....	119
Figure 3.21:	HDACi effect on FXN mRNA of YG8 heart tissues.....	119
Figure 3.22:	HDACi effect on FXN mRNA of YG8 brain tissues.....	120
Figure 3.23:	Histone acetylation in YG8 mouse brain tissues.....	122
Figure 3.24:	Histone acetylation in YG8 mouse brain tissues.....	122

Abbreviations

α	Alpha
AMV	Avian Myeloblastosis Virus
ATP	Adenosine triphosphate
AVED	Ataxia with isolated vitamin E deficiency
BAC	Bacterial artificial chromosome
β	Beta
cDNA	Complementary DNA
CHCl₃	Chloroform
ChIP	Chromatin immunoprecipitation
CNS	Central nervous system
CpG	Cytosine phosphate guanine
CTCF	CCCTC-binding factor
DM1	Myotonic dystrophy
DNA	Deoxyribonucleic Acid
DNMTs	DNA methyltransferases
DRG	Dorsal root ganglia
DSBs	Double-strand breaks
dsRNA	Double-stranded RNA
EDTA	Ethylene diamine tetra acetic acid
EGFP	Enhanced green fluorescent protein
ES	Embryonic stem cells
EtBr	Ethidium bromide
Fe²⁺	Ferrous iron
Fe³⁺	Ferric iron
FRDA	Friedreich ataxia
<i>Fxn</i>	Mouse frataxin
<i>FXN</i>	Human frataxin
GAPDH	Glyceraldehyde 3-phosphate dehydrogenase
H	Heart

H₂O₂	Hydrogen peroxide
H3	Histone 3
H3K14ac	Histone 3 lysine 14 acetylated
H3K27	Histone 3 lysine 27
H3K27me2,3	Histone 3 lysine 27 di- or trimethylated
H3K4	Histone 3 lysine 4
H3k4me2,3	Histone 3 lysine 4 di- or trimethylated
H3K9ac	Histone 3 lysine 9 acetylated
H3K9me3	Histone 3 lysine 9 trimethylated
H4	Histone 4
H4K12ac	Histone 4 lysine 12 acetylated
H4K16ac	Histone 4 lysine 16 acetylated
H4K20ac	Histone 4 lysine 20 acetylated
H4K5ac	Histone 4 lysine 5 acetylated
H4K8ac	Histone 4 lysine 8 acetylated
HATs	Histone acetyltransferases
HBA2	Hemoglobin, alpha 2
HDACs	Histone deacetylases
HDACi	Histone deacetylases inhibitor
H-DNA	Helical DNA
HEPES	N-2-hydroxyethylpiperazine-N'-2-ethanesulfonic Acid
HMSN	Hereditary motor and sensory neuropathy
HP1	Heterochromatin protein 1
IAA	Isoamyl-alcohol
ISC	Iron-sulphur clusters
IscU2	Iron scaffold protein
ISPs	ISC-containing proteins
KCl	Potassium Chloride
KO	knockout
ΔYFH1	Knockout yeast frataxin homolog gene
MeCP2	Methyl CpG binding protein 2
Mg⁺²	Magnesium

MMR	Mismatch repair
MPP	Mitochondrial processing peptidase
MRI	Magnetic resonance imaging
mRNA	Mature ribonucleic Acid
MRS	Magnetic resonance spectroscopy
MSH2	DNA mismatch repair protein Msh2
MSH3	DNA mismatch repair protein Msh3
MSH6	DNA mismatch repair protein Msh6
MZ	Monozygotic twins
NaCl	Sodium chloride
NaHCO₃	Sodium Bicarbonate
NER	Nucleotide excision repair
NP-40	Nonidet P-40
OD	Optical density
OH[.]	Hydroxyl radical
OIZ	Okazaki initiation zone
P	Pancreas
PBS	Phosphate Buffered Saline
PcG	Polycomb group
PCR	Polymerase chain reaction
PEV	Position effect variegation
pH	Negative logarithm of the concentration (mol/L) of the H ₃ O ⁺ [H ⁺] ion; scale is commonly used over a range 0 to 14
Pol II	RNA Polymerase II enzyme
RNA	Ribonucleic Acid
RNAi	RNA interference
RPI	ROCHE protease Inhibitor
RT	Room temperature
SACO	Serial analysis of chromatin occupancy
SAGE	Serial analysis of gene expression
SC	Spinal cord
SCAs	Spinocerebellar ataxias

SDS	Sodium dodecyl sulphate
SDS 2.1	Sequence Detection System computer program
shRNA	Short hairpin RNA
TBE	Tris-Borate-EDTA Buffer
TNRs	Trinucleotide repeats
Tris-HCl	Tris-hydroxymethylaminomethane
TRIZOL	The brand name of a solution used in RNA/DNA/protein extraction from Invitrogen. The correct name of the method is Guanidinium thiocyanate-phenol-chloroform extraction
TrxG	Trithorax complexes
UK	United Kingdom
WT	wild-type
YAC	Yeast artificial chromosome
° C	degree centigrade
3D	Three dimensions

Chapter 1

Introduction

1.1 Ataxia

The word ataxia originates from the Greek language meaning "lack of order". It is a neurological dysfunction of motor coordination that can affect muscle movements (Taroni and DiDonato 2004). Ataxia may affect the fingers and hands, the arms or legs, the body, speech or eye movements. It is a specific clinical manifestation implying dysfunction of parts of the nervous system that coordinate movement. This includes *cerebella*, *sensory*, and *vestibular* ataxia. Several possible causes exist for these patterns of neurological dysfunction, such as hereditary ataxia. Dystaxia refers to difficulty in controlling voluntary movements (Harding 1984).

1.1.1 Inherited progressive ataxia disorders

There are different types of progressive ataxias. The inherited ataxias are characterized by problems of balance and coordination, hearing and vision as well as swallowing, slurred speech, weakening of the heart, diabetes, scoliosis (Box *et al.* 2005). There are two groups of hereditary ataxias. Firstly, autosomal recessive ataxias, such as Friedreich ataxia (FRDA) and ataxia with isolated vitamin E deficiency (AVED) disorders. These are mainly categorized by inactivating mutations leading to loss of cellular protein function, which will affect the energy process and oxidative stress in living cells. Secondly, autosomal dominant spinocerebellar ataxias (SCAs). These are categorized primarily by an expansion of CAG-triplet repeats in the coding region of the potential gene; this will cause an excess production of longer polyglutamine mutant protein, termed gain of function effect (Taroni and DiDonato 2004; Thompson 2008).

The most common inherited progressive, neurodegenerative ataxia disorder in the United Kingdom is Friedreich ataxia (FRDA) (Harding 1981; Delatycki *et al.* 2000; Puccio and Koenig 2002; Gomez-Sebastian *et al.* 2007).

1.2 Friedreich ataxia (FRDA)

Friedreich ataxia is a slow progressive, demoralizing ataxia (De Biase *et al.* 2007b) which can lead to life in a wheelchair and early death as a result of cardiomyopathy. It is a rare autosomal recessive disease, affecting males and females equally (Andermann *et al.* 1976; Campuzano *et al.* 1996; Delatycki *et al.* 2000; Pandolfo 2003).

1.2.1 The identification of FRDA

The identification of FRDA began in the 1850s, when Nicholaus Friedreich, a professor of medicine, noted his observations on ataxia on nine members of three families (Friedreich 1876; Friedreich 1877; Chakravarty 2003). In 1863, the disease was first described by Friedreich in his published papers as a ‘degenerative atrophy of the posterior columns of the spinal cord’ causing progressive ataxia, sensory loss and muscle weakness, frequently associated with scoliosis, foot deformity and heart disease (Friedreich 1863a,b; Friedreich 1863c; Pandolfo 1998). By the end of the nineteenth century a significant number of cases were diagnosed as having FRDA and the disorder was first discussed at the Medical Society of London in 1880.

1.2.2 Clinical Features

In Professor Nicholaus Friedreich’s time, and later in the nineteenth century, there was a debate on the different diagnostic criteria for FRDA. It was extremely important to have a strict set of diagnostic criteria to make sure that all of the patients diagnosed with FRDA were fully suitable for further FRDA research studies.

A different set of diagnostic criteria for FRDA proposed by Geoffroy (Geoffroy *et al.* 1976) and Harding (Harding 1981) are shown in Table 1.1. The diagnostic criteria of Harding are more liberal, allowing the diagnosis of FRDA in the early stages of the disease (Delatycki *et al.* 2000).

Previously, patients observed with the following symptoms were considered to be affected with FRDA. In most cases, the onset is around puberty (Harding 1981; Muller-Felber *et al.* 1993; Pandolfo 2003). Early and late onset also exist (De Michele *et al.* 1994; De Michele *et al.* 1996; Pandolfo 2003).

Table 1.1: Different diagnostic criteria for FRDA proposed by Geoffroy (Geoffroy *et al.* 1976) and Harding (Harding 1981). The table is adapted from (Delatycki *et al.* 2000).

Criteria	Geoffroy <i>et al.</i>, 1976	Harding, 1981
Primary (essential for diagnosis)	1-Onset before the end of puberty. (never after the age of 20years) 2-Progressive ataxia of gait. 3-Dysarthria. 4-Loss of joint position or vibration sense. 5-Absent tendon reflexes in the legs. 6-Muscle weakness.	1-Age of onset of symptoms before the age of 25 years 2-Progressive unremitting ataxia of limbs and of gait. 3-Absence of knee and ankle jerks.
Secondary	1-Extensor plantar responses. 2-Pes cavus. 3-Scoliosis. 4-Cardiomyopathy.	1-Dysarthria. 2-Extensor plantar responses.
Additional		If secondary criteria are absent, the following have to be present: 1-An affected sib fulfilling primary and secondary criteria. 2-Median motor nerve conduction velocities of greater than 40 m/s thus excluding cases of type I hereditary motor and sensory neuropathy (HMSN).

The main neurological symptoms are: loss of tendon reflexes in the lower limb, spasm in lower limb, distal amyotrophy, scoliosis, dysarthria, nystagmus, pes cavus, loss of sensory nerve action, loss of the central and peripheral sensory, progressive limb and gait ataxia, impaired ambulation after 15-20 years from the initial onset.

Heart disease plays a vital role in disability and early death. The most common symptoms of heart disease are shortness of breath in 40% of the patients and palpitation in 11% of FRDA patients. 10-25% of FRDA patients are more susceptible to develop diabetes mellitus. 30% of FRDA patients develop optic atrophy and 20% suffer from hearing loss (Boyer *et al.* 1962; Harding 1981; Scrimgeour *et al.* 1996; Cossee *et al.* 2000; Delatycki *et al.* 2000; Pandolfo 2003).

In recent years, technological advances in the medical field have raised the standard of the clinical evaluation of several complicated diseases such as FRDA, consequently improving the routine diagnostic procedure of the disorder. Molecular genetic tests for FRDA are available as a primary step for the diagnosis, followed by other clinical assessments such as, magnetic resonance imaging (MRI) to assess the degeneration in the brainstem, spinal cord and cerebellum (Pandolfo 2003; Della Nave *et al.* 2008a; Della Nave *et al.* 2008b). Magnetic resonance spectroscopy (MRS) is also used in the clinical assessment to measure very low quantities of metabolites *in vivo* in skeletal muscle and heart (Pandolfo 2003).

1.2.3 Pathology

FRDA affects the central nervous system (CNS), heart, muscles and pancreas in the human body (Figure 1.1) (Brice 1998; Taroni and DiDonato 2004). The remarkable and first pathological changes occur in the dorsal root ganglia (DRG) (Figure 1.2) when the large sensory neurons degenerate. Following this, loss of axons in the posterior columns, spinocerebellar and pyramidal tracts of the spinal cord occur (Harding 1984; Cossee *et al.* 2000; Simon *et al.* 2004; De Biase *et al.* 2007b). In addition, atrophy of the Clarke's column, and the dentate nucleus of the

cerebellum takes place (Delatycki *et al.* 2000; Pandolfo 2003; Seznec *et al.* 2004). The large myelinated sensory fibres in peripheral nerves also degenerate (Pandolfo 2003; De Biase *et al.* 2007b). In a recent study, Della Nave and colleagues showed that there is a significant loss of the white matter and grey matter in FRDA patients, and these structural changes relate to the interval and the severity of the disease (Della Nave *et al.* 2008a).

FRDA patients commonly develop heart disease; the most common cardiac defect is hypertrophy (Delatycki *et al.* 2000). Hypertrophy is more common in young and early onset patients and is milder in adult or late-onset patients (Seznec *et al.* 2004). Five percent of the patients are affected with hypertrophic cardiomyopathy for 2-3 years before they show any neurological symptoms (Harding 1981). The main clinicopathological symptoms of FRDA patients are mitochondrial dysfunction and iron deposits in specific myocardial cells (Pandolfo 1998).

The full explanation of organ specificity of pathology in FRDA is still inconclusive, but it can be clarified by the alignment of different patterns of frataxin expression in different tissues. In addition, different requirements for different tissues and frataxin in dealing with the iron accumulation and oxidative stress in the mitochondria (Delatycki *et al.* 2000).

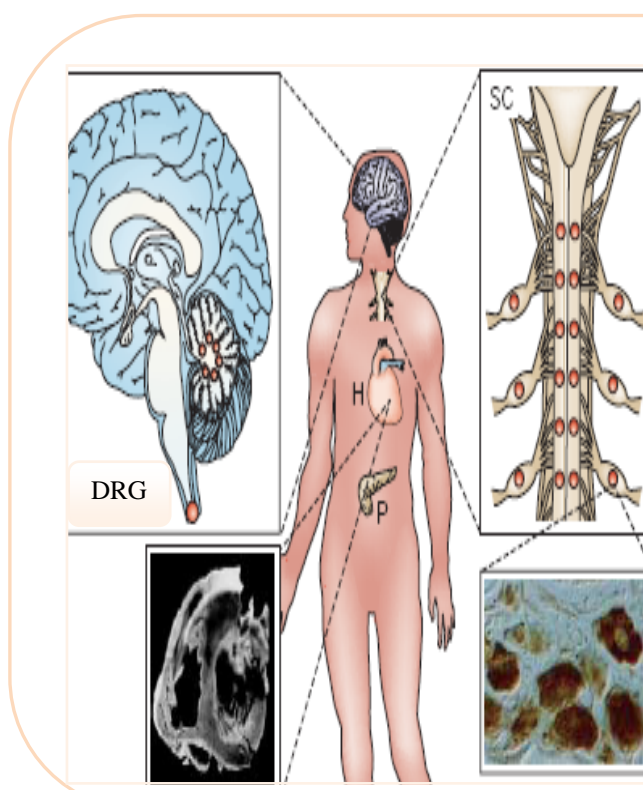


Figure 1.1:
Overview of the main sites of neuronal loss and organ dysfunction in Friedreich ataxia. Prominent frataxin expression in the large primary sensory neurons of dorsal root ganglia. Pathological features are shown for the brain, spinal cord (SC), heart (H) presenting as cardiac hypertrophy and pancreas (P) presenting as diabetes. Large dots indicate more severe neuronal loss. Adapted from (Taroni and DiDonato 2004).

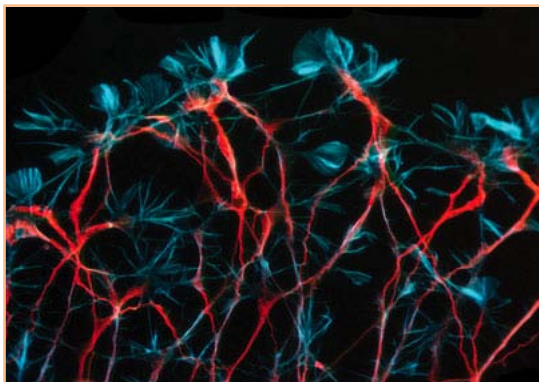


Figure 1.2:
Dorsal root ganglion neurons of an embryonic rat (100X) (Paves 2003).

1.2.4 Epidemiology and prevalence

FRDA has a prevalence of 1 in 50,000 in the Caucasian population (Lopez-Arlandis *et al.* 1995). In addition, FRDA is found in North Africa, the Middle East and India, although the incidence of the disease in the Far East, sub-Saharan Africa and Native America is very low (Pandolfo 2003).

According to a study conducted by Scrimgeour and colleagues in 1996, the prevalence of FRDA in the Middle East, specifically in Saudi Arabia is higher due to the high rate of consanguinity (Scrimgeour *et al.* 1996).

1.2.5 Genetic background

1.2.5.1 Inheritance pattern

Neurodegenerative FRDA is an autosomal recessive trinucleotide repeat disease (Pelletier *et al.* 2003; Taroni and DiDonato 2004; Wells *et al.* 2005; Hebert 2007; Hebert and Whittom 2007), which is caused by a pathological trinucleotide repeat expansion. Between 96-98 % of FRDA patients are homozygous for a non-Mendelian mutation, which is a pathological $(GAA)_n \cdot (TTC)_n$ expansion, in the first intron of the frataxin (*FXN*) gene (previously known as *FRDA* or *X25*). This pathological expansion contributes to reduce the expression level of frataxin protein

by inhibiting the transcription of its corresponding gene (Pelletier *et al.* 2003; Seznec *et al.* 2004; Taroni and DiDonato 2004; Al-Mahdawi *et al.* 2006).

2 to 4% of patients are compound heterozygotes, having an expanded repeat in the first allele and a point mutation (missense or splice site mutation) or a premature stop codon (non-sense mutation) in the second allele. All missense mutations are in the C terminus, which is encoded by exon 4 and 5a (Section 1.2.5.5 page 26). These types of mutations will affect protein function or its interactions with other molecules, stability (Section 1.2.5.6 page 28) or expression. Homozygous point mutations will cause a lethal phenotype (Bidichandani *et al.* 1997; Cossee *et al.* 2000; Taroni and DiDonato 2004; Correia *et al.* 2006; Gottesfeld 2007; Hebert 2007).

1.2.5.2 FXN Gene mapping

In 1988, the Friedreich ataxia gene was mapped to Chromosome 9, then localized in the long arm 9q13-21.1 by fine mapping and subsequent linkage studies (Figure 1.3) (Pandolfo 2003; Seznec *et al.* 2004; Correia *et al.* 2006).

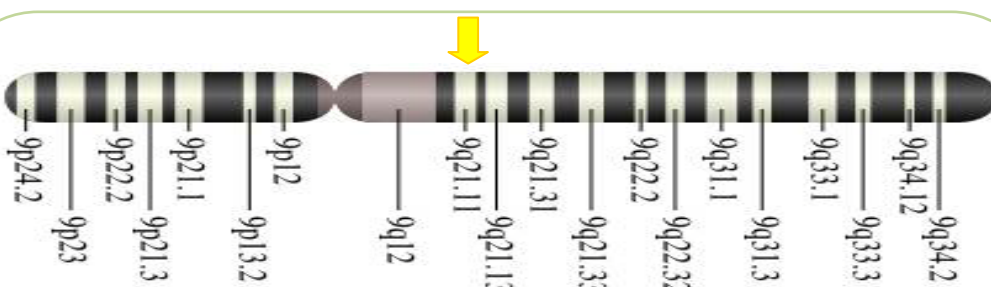


Figure 1.3:

Ideogram of the human chromosome 9. Cytogenetic Location of frataxin gene: 9q21.1 (Yellow arrow). Molecular Location: base pairs 70,840,163 to 70,878,771 from *pter* (Mysid 2007).

1.2.5.3 *FXN* Gene structure

The *FXN* gene encodes for the frataxin mitochondrial protein which is composed of 210 amino acids (Campuzano *et al.* 1996; Cossee *et al.* 2000; Taroni and DiDonato 2004). The *FXN* gene consists of seven exons spread over 95 kilobases (kb) of genomic DNA. Six exons (1,2,3,4,5a,5b) are coding regions and one exon (exon 6) is non-coding. The gene is transcribed in centromere → telomere direction, the most common transcript is from the first five exons (1-5a) and it is 103 kb in size (Pandolfo 1998; Pandolfo 2003; Gomez-Sebastian *et al.* 2007). By alternate splicing, another transcript, which is less common, from exon 1-5b can be generated to give a theoretical 171 amino acid protein (Figure 1.4) (Pandolfo 1998; Delatycki *et al.* 2000).

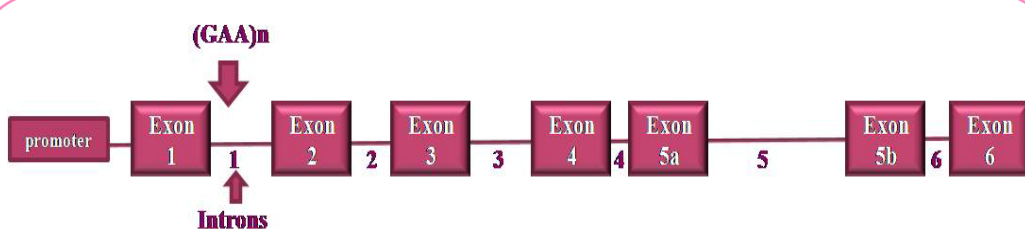


Figure 1.4:

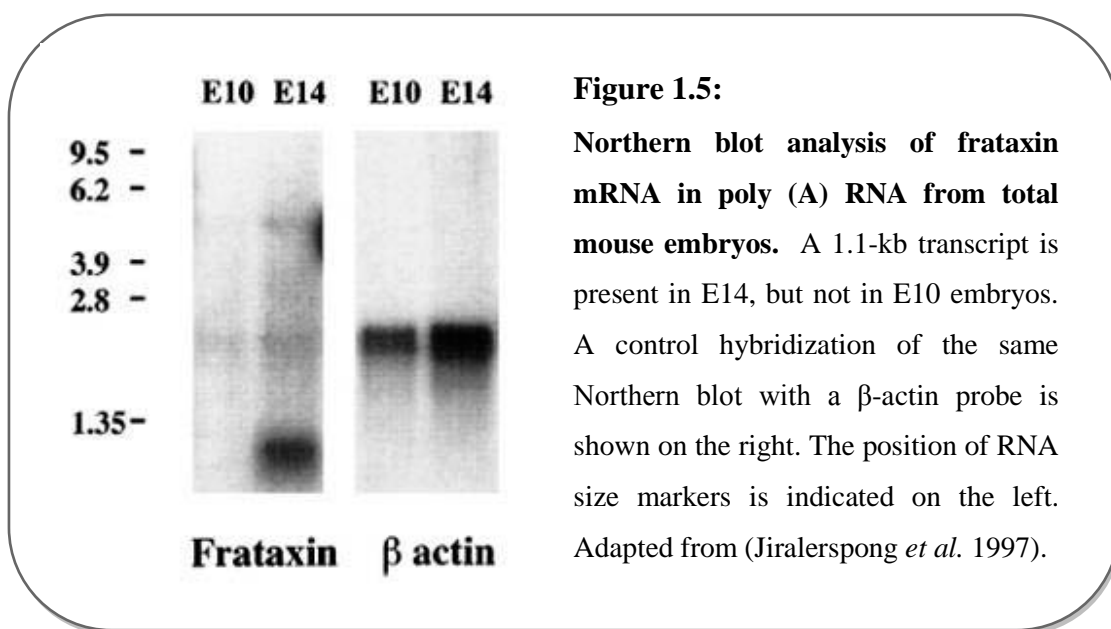
***FXN* gene structure** including exons, intron and the promoter region. In addition to the GAA repeat location.

1.2.5.4 *FXN* gene expression

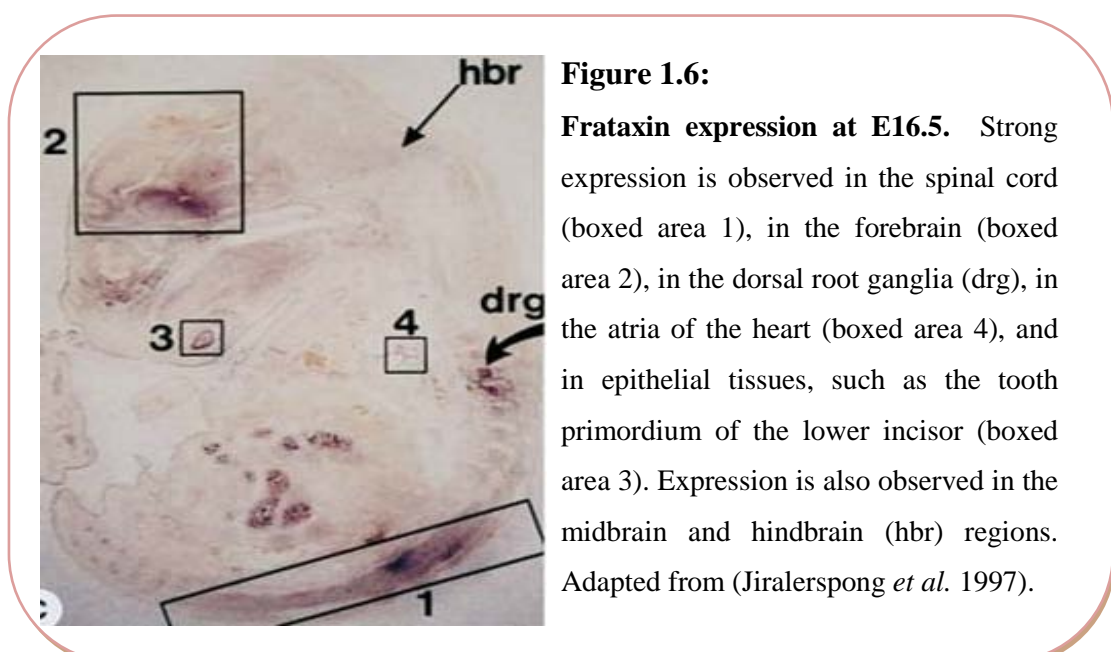
The *FXN* gene is expressed in all cells (Pandolfo 2003), but it also shows tissue specific differences in expression and it is developmentally regulated. Tissues having the highest level of frataxin expression during development are the atrophied tissues in FRDA patients (Jiralerpong *et al.* 1997; Pandolfo 1998).

In the adult human, frataxin expression is very high in heart, with intermediate level in the liver, skeletal muscle, and pancreas. The highest expression in CNS tissues occurs in the spinal cord, there is less expression in the cerebellum and is further reduced in the cerebral cortex (Pandolfo 2003).

In mice, the developing brain is highly loaded with frataxin mRNA, while the mRNA level is less in the adult mouse brain (Pandolfo 2003). The frataxin developmental expression has been tested by using Northen blot analysis and RNA *in situ* hybridization. In the neuroepithelium, a very faint expression was detected at embryonic day (E) 10.5, weak but detectable expression at E12.5 in the developing central nervous system (Jiralerspong *et al.* 1997; Koutnikova *et al.* 1997), while at E14.5 and post-natal time higher and constant expression was detected (Figure 1.5).



At E14.5–E16.5 high frataxin expression was detected in the central nervous system (CNS), mainly in the spinal cord, forebrain and DRG (Figure 1.6).



The highest level of frataxin expression was observed in spinal cord and large neuronal cells of the dorsal root ganglia (Figure 1.7a) (Jiralerpong *et al.* 1997; Koutnikova *et al.* 1997; Delatycki *et al.* 2000). A high level of frataxin was observed in proliferating cells in the cortical plates, in the heart, in the axial skeleton (Figure 1.7b), in thymus, in some epithelial (skin, teeth) and in fat brown tissues (Figure 1.6) (Delatycki *et al.* 2000; Pandolfo 2003). The presence of frataxin expression in the axial skeleton of the mouse embryo may be related to scoliosis, which is seen in most FRDA patients as a main clinical feature (Jiralerpong *et al.* 1997). However, differences in the frataxin expression system between human and mouse are considered likely.

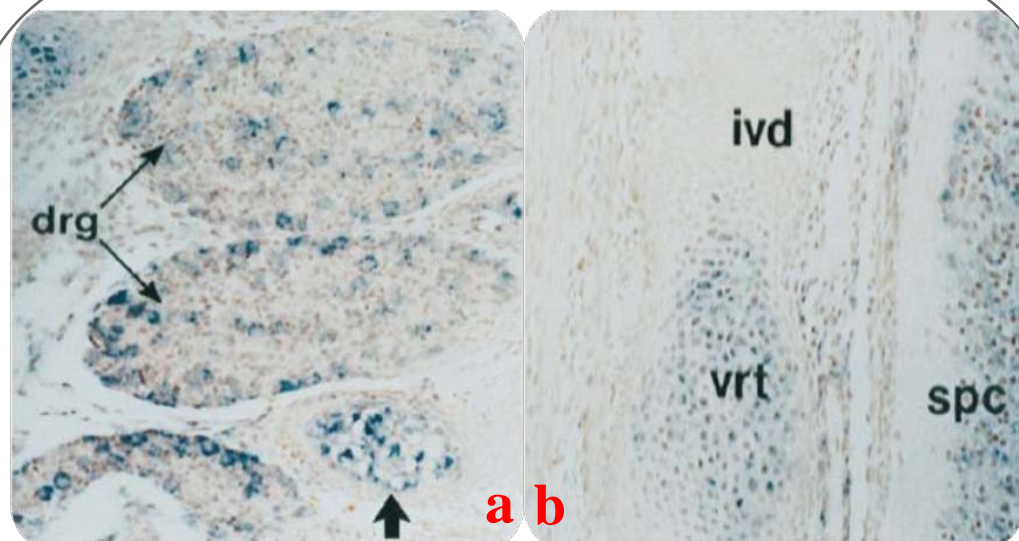


Figure 1.7:

Frataxin expression in developing dorsal root ganglia.

Hybridization of a frataxin antisense riboprobe to sagittal sections through the lower thoracic dorsal root ganglia of an E14.5 embryo. **A,** Strong expression is detected in large round cells in the dorsal root ganglia (drg) and in elements of the axial skeletons, including the cartilage primordia of ribs and vertebral bodies (arrow). **B,** Frataxin expression is strong in the cartilage primordia of vertebral bodies (vrt), but is absent in intervertebral discs (ivd). Notice also expression in the spinal cord (spc). Adapted from (Jiralerpong *et al.* 1997).

Generally, the frataxin mRNA level is higher in mitochondria-rich cells, such as neurons and cardiomyocytes (Koutnikova *et al.* 1997; Pandolfo 2003). The reduced level of mRNA causes the inhibition of the gene transcription process, and not at the post-transcriptional RNA stage.

In addition, when the protein level was tested by western blot, the results showed a high frataxin level present in human and mouse brain and cerebellum (Pandolfo 2003). In FRDA patients the protein level was very low in cerebral cortex, skeletal muscle, and lymphoblasts (Cossee *et al.* 2000; Delatycki *et al.* 2000). However, the presence of the frataxin protein at a very low level is important to allow the viability of the FRDA patients and the slowly progressive nature of the human disease (Cossee *et al.* 2000).

Individuals who are heterozygous for the (GAA)n·(TTC)n expansion have around 50% of normal *FXN* mRNA and frataxin protein level (Herman *et al.* 2006). FRDA patients express 5-35% of the normal level of frataxin, emphasizing the relationship between the frataxin level, disease phenotype and the size of the (GAA)n·(TTC)n repeats (Pook *et al.* 2001; Coppola *et al.* 2006). Also an earlier study demonstrated the inverse correlation between the length of the (GAA)n·(TTC)n repeats and the amount of RNA *in vivo* and *in vitro* (Delatycki *et al.* 2000; Sakamoto *et al.* 2001).

Frataxin is an essential protein for survival, it is found in living organisms starting from purple bacteria to human (Musco *et al.* 2000). This protein has an important role during embryonic development. In FRDA patients, with lower levels of frataxin than normal, only those cells that are dependent on frataxin at some stage of their development are affected (Pandolfo 2001). While the complete absence of frataxin causes early stage embryo cell death. Cossee and colleagues observed this during the experimental stage of generation of a mouse model for the disease. The group stated that the homozygous frataxin knock-out mice die at E7.5 (Cossee *et al.* 2000; Pandolfo 2001). The lethality problem was solved when Dr. Mark Pook and his group, succeeded in generating a rescued transgenic mouse with the normal human *FXN* gene (Pook *et al.* 2001). More details about this mouse and other FRDA mice models are covered in the “Animal Model” section (1.4).

1.2.5.5 Frataxin structure

In recent years, many researchers have dedicated their time and effort to build up the knowledge about frataxin protein structure based on biochemical experiments. This knowledge will lead to a clearer understanding of the protein, function and, more importantly, the role of frataxin deficiency in causing the clinical symptoms of the disease, eventually hoping to develop an effective therapy for Friedreich ataxia.

Human frataxin is a nuclear encoded mitochondrial protein (Delatycki *et al.* 2000) expressed in the cytoplasm. Before its entry to the mitochondria it is processed by an enzyme known as mitochondrial processing peptidase (MPP). Firstly, MPP cleaves the protein to intermediate form of, ~17kDa, which contains (56-210 amino acids). Secondly, the intermediate form has self-cleavage function that results in the mature frataxin protein (75 to 81-210 amino acids), ~14kDa in size that approximately equals 130 amino acids of protein. The latter is found in the mitochondria matrix (Branda *et al.* 1999; Dhe-Paganon *et al.* 2000; Musco *et al.* 2000; Babady *et al.* 2007).

The mature frataxin sequence contains: N-terminal and C-terminal sequences. The N-terminal region is an unstructured and non-conserved region that contains the mitochondrial import sequence. This region does not affect the folding stability of the C-terminal. The C-terminal domain is the conserved region that can independently fold in to a compact α - β sandwich and has no grooves or cavities.

The α - β sandwich composed of an N-terminal α helix, middle β sheet that contains seven β strands and a C-terminal α helix. The axis of the two helices are parallel to each other and to the β sheet (Figure 1.8) (Gordon *et al.* 1999; Dhe-Paganon *et al.* 2000; Musco *et al.* 2000; Pandolfo 2001).

Hydrophobic amino acids are gathered (hydrophobic core) at the edge of β sheet and on the side of two helices contributing to form a stable folded protein by creating a significant charge dipole. The 12-amino acids residues form an anionic surface on the protein. Frataxin is a monomeric protein in solution (Dhe-Paganon *et al.* 2000; Musco *et al.* 2000).

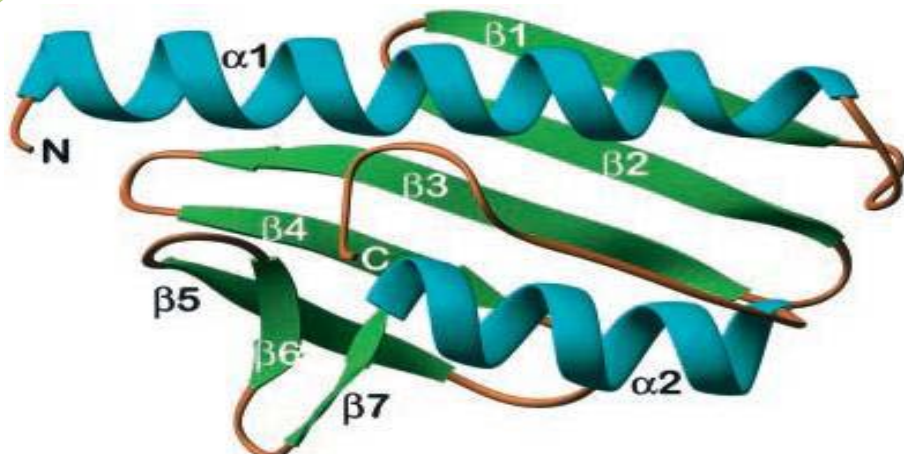


Figure 1.8:

Structure of frataxin. Ribbon diagrams showing the fold of frataxin, a compact α β sandwich, with helices colored *turquoise* and β strands in *green*. Strands β 1– β 5 form a flat antiparallel β sheet that interacts with the two helices, α 1 and α 2. The two helices are nearly parallel to each other and to the plane of the large β sheet. A second, smaller β sheet is formed by the C terminus of β 5 and strands β 6 and β 7. Adapted from (Dhe-Paganon *et al.* 2000).

Although it had been confirmed by many research studies that frataxin is involved in iron metabolism in the mitochondria, because of the iron accumulation in the mitochondria in case of frataxin deficiency in cells (Babady *et al.* 2007; Bencze *et al.* 2007; Hebert 2007), the monomer structure of frataxin does not have any cavity or pocket to hold the iron molecule. In addition, the presence of high affinity iron-binding sites in the frataxin structure has not been proved experimentally.

Therefore, the presence of the conserved negatively charged side on the protein surface can be a possible site for positively charged iron to bind (Musco *et al.* 2000; Pandolfo 2001).

1.2.5.6 Frataxin function

Research to date has not provided a clear understanding of frataxin function. However, numerous studies have reported and hypothesized that frataxin is a vital mitochondrial protein (Pandolfo 1998; Delatycki *et al.* 2000; Miranda *et al.* 2002; Simon *et al.* 2004; Al-Mahdawi *et al.* 2006; Hebert 2007) playing an important role in: mitochondrial iron homeostasis (Foury and Cazzalini 1997), iron storage (Gakh *et al.* 2006), iron transport, anti-oxidant activity (Karthikeyan *et al.* 2003), and biosynthesis of heme and iron sulphur (Fe-S) clusters (ISCs) (Huynen *et al.* 2001; Lesuisse *et al.* 2003; Pandolfo 2006; Babady *et al.* 2007). It had been reported that frataxin's function cannot be perceived by its amino acid sequence (Pandolfo 1998)

Twenty years ago, iron deposits in myocardial cells from FRDA patients and iron accumulation in the dentate nucleus in the CNS had been reported (Lamarche *et al.* 1980; Waldvogel *et al.* 1999; Pandolfo 2003). Another observation confirmed a reasonable increase in iron concentration in the mitochondria from FRDA fibroblast cells (Delatycki *et al.* 1999; Pandolfo 2001). Oxidative stress was also observed in FRDA patients by measuring the increased concentration of lipid peroxidation, dihydroxybenzoic acid, and malondialdehyde in the plasma and 8-hydroxy-2-deoxyguanosine level in the urine. FRDA fibroblasts showed higher sensitivity to low doses of hydrogen peroxide (H_2O_2) than normal cells. It induced cell shrinking, nuclear condensation, and cell death (Delatycki *et al.* 2000; Simon *et al.* 2004; Pandolfo 2006).

It is well known that the primary information about frataxin function was obtained from the knockout yeast frataxin homolog gene ($\Delta YFH1$) model. This model was developed, in 1997, to study genes involved in cellular iron metabolism (Foury and Cazzalini 1997; Koutnikova *et al.* 1997; Delatycki *et al.* 2000; Seznec *et al.* 2004). $\Delta YFH1$ as the model helped researchers to prove the occurrence of mitochondrial dysfunction *in vivo* in FRDA patients (Rotig *et al.* 1997; Pandolfo 2003). Relative to that, there is much evidence suggesting that FRDA is a result of mitochondrial iron accumulation causing cell death by the production of free radicals which are toxic to the cell (Figure 1.9). This is called the Fenton reaction:



This reaction produces a hydroxyl radical OH^\cdot that will become toxic by reacting with many intracellular component such as, protein, DNA, carbohydrate, and membrane lipids (Delatycki *et al.* 2000; Puccio and Koenig 2002).

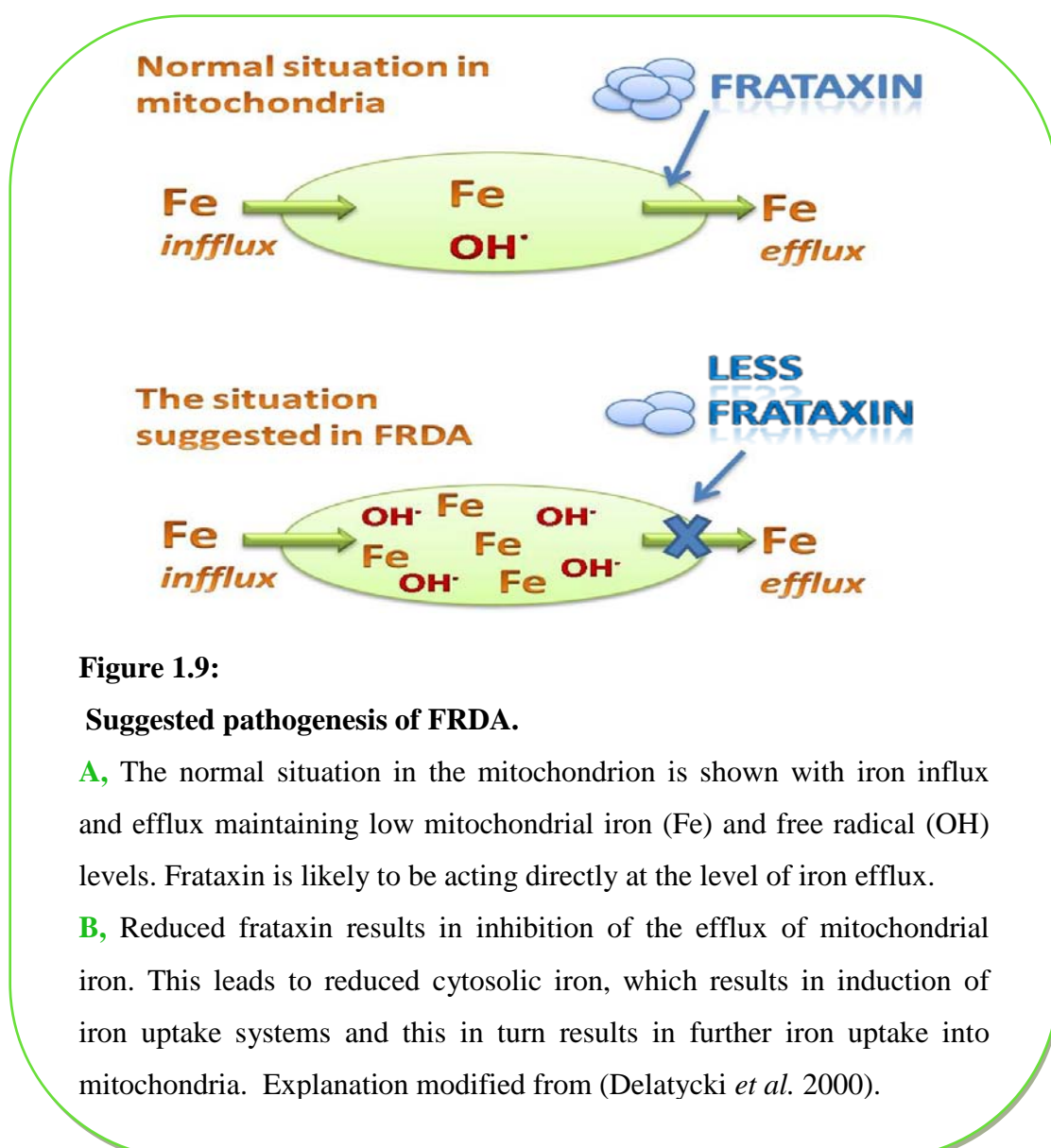


Figure 1.9:
Suggested pathogenesis of FRDA.

A, The normal situation in the mitochondrion is shown with iron influx and efflux maintaining low mitochondrial iron (Fe) and free radical (OH^\cdot) levels. Frataxin is likely to be acting directly at the level of iron efflux.

B, Reduced frataxin results in inhibition of the efflux of mitochondrial iron. This leads to reduced cytosolic iron, which results in induction of iron uptake systems and this in turn results in further iron uptake into mitochondria. Explanation modified from (Delatycki *et al.* 2000).

In 2003, Pandolfo proposed a similar pathogenic pathway (Figure 1.10). When less frataxin is available in the mitochondria, it directly affects the iron-sulphur clusters (ISC) synthesis, which causes the inhibition of iron export and,

as a result, iron accumulation. Accumulated iron generates free radicals that cause extra damage to ISC_s and decrease the enzyme activities of ISC-containing proteins (ISPs) such as aconitase. As a consequence, the activities of the respiratory complexes and Krebs cycle enzymes are decreased. This is followed by a further increase in the free radical production (Pandolfo 2003; Pandolfo 2006) that ultimately leads to impaired oxidative phosphorylation (Kulkarni and Wilson 2008).

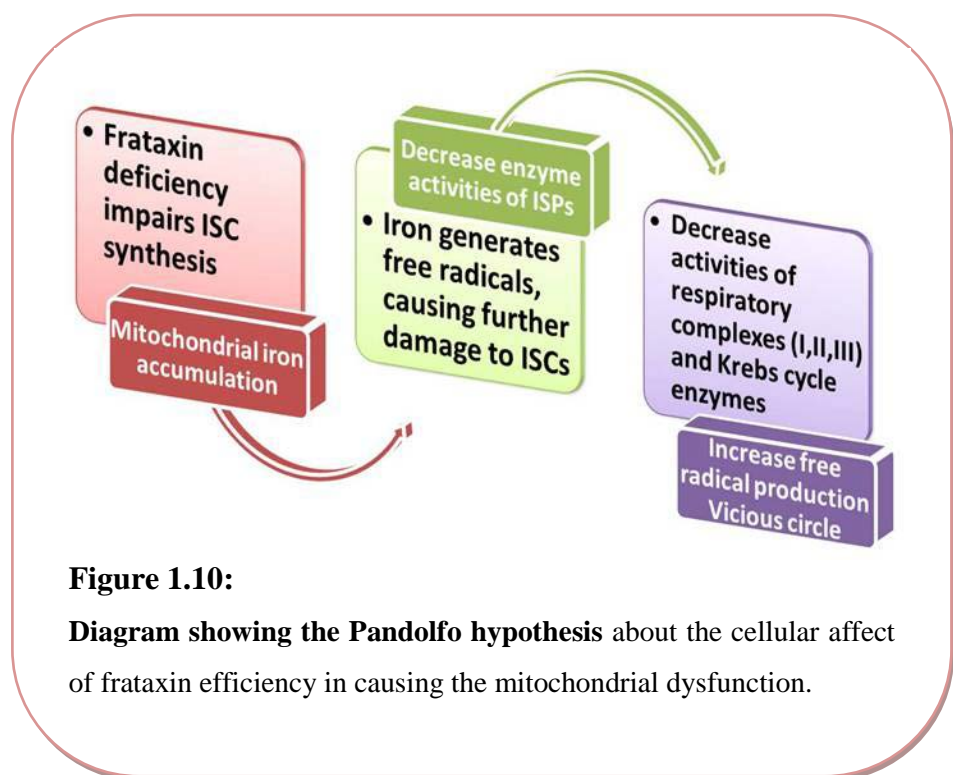


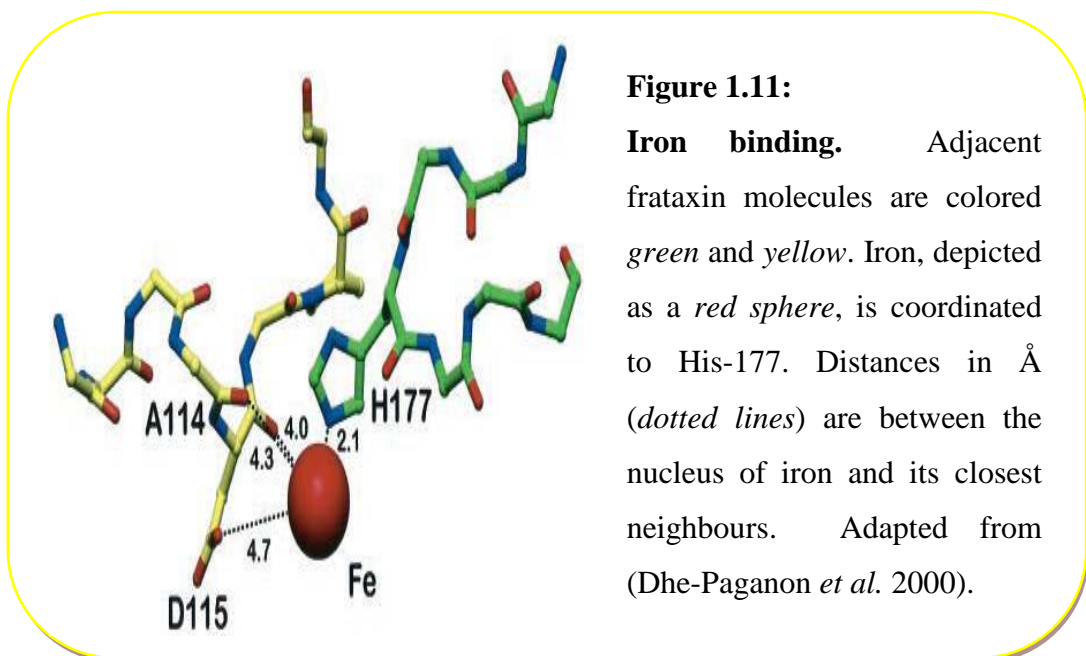
Figure 1.10:

Diagram showing the Pandolfo hypothesis about the cellular affect of frataxin efficiency in causing the mitochondrial dysfunction.

The way that frataxin deficiency controls iron homeostasis and ISC synthesis is still debatable. Some studies showed that frataxin directly influences the iron efflux. Other studies revealed indirect ways, as frataxin can either function as a carrier of antioxidant, a chaperone or an adapter of protein import processing (Rotig *et al.* 1997; Musco *et al.* 2000). It is well known that frataxin function is involved in a multi-step cycle process in the mitochondria. Some studies have indicated that frataxin may act indirectly as a tumour suppressor gene (Hebert and Whittom 2007).

In 2000, Dhe-Paganon and colleagues performed a crystal structure study; the study reveals that frataxin monomer has a novel folding profile, and it is binding non-specifically to the iron. In addition, results show that one iron atom binds to a

frataxin molecule at His -177. His-177 is a non conserved and a solvent exposed side chain, for these reasons, the iron binds to it loosely (Figure 1.11). In conclusion, frataxin binds to iron to utilize the acidic patch on its surface (Dhe-Paganon *et al.* 2000). Another study showed that the binding capacity for a subunit of frataxin is ten iron atoms (Taroni and DiDonato 2004), while Nair and colleagues claimed that a frataxin molecule can bind to six or seven iron atoms (Nair *et al.* 2004).



Recent research experiments confirmed the binding of the frataxin to the mitochondrial iron scaffold protein IscU2 to deliver the iron to the IscU2, and this is an initial step in ISC clusters synthesis. Equally, frataxin binds to ferrochelatase, an enzyme needed to process last step in the heme synthesis. These results were only observed in the presence of the iron atom (Napoli *et al.* 2006; Babady *et al.* 2007; Bencze *et al.* 2007).

Recently, microarray analysis of FRDA cells revealed a decrease in the expression of many genes involved in sulphur amino acid and ISC pathways. While another group of genes that related to apoptosis were up-regulated (Seznec *et al.* 2004; Taroni and DiDonato 2004; Babady *et al.* 2007).

It is important to mention that the frataxin level is altered by the $(GAA)_n \cdot (TTC)_n$ repeat expansion, while the frataxin function is directly affected by the

heterozygous point mutations. Point mutations affect the fold stability, by reducing the thermodynamic stability and refolding ability of the protein molecule. As a result there is less functional frataxin in the mitochondria and more degradation of the mature frataxin (Figure 1.12) (Musco *et al.* 2000; Correia *et al.* 2006). An alteration of the surface charge and eventually protein polarity has also been suggested (Dhe-Paganon *et al.* 2000).

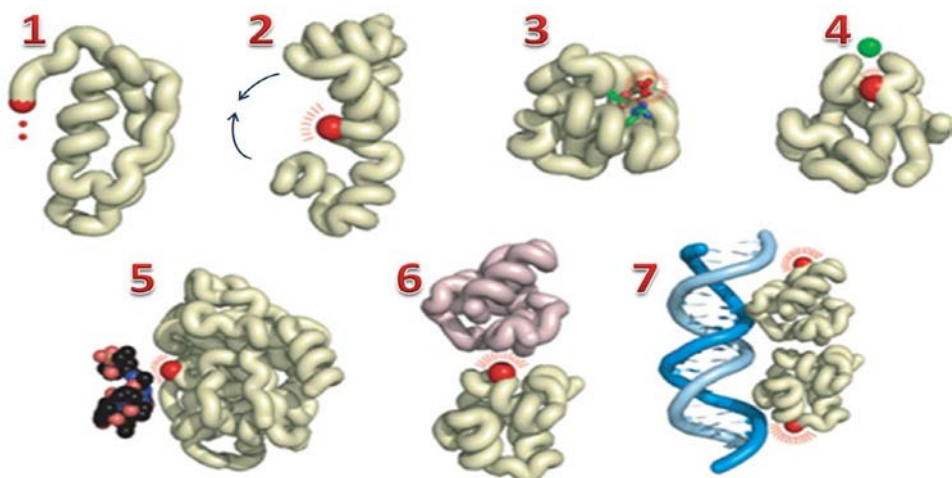


Figure 1.12:

Diagram showing some of the ways that an amino-acid mutation can disrupt a protein's structure or function. The protein chains are depicted as curvy green tubes with the location of the mutation indicated by a red beacon. **1**, A mutation that introduces a stop codon into the protein-coding region results in a truncation of the sequence, which might prevent it from folding or cause it to lose one or more of its functional domains. **2**, A mutation to a residue in the protein's core, or one that disrupts either a region of secondary structure or a disulphide bond, can also prevent the protein folding, possibly leading to aggregation. **3**, One of the protein's catalytic residues is altered, disrupting its function. **4-7**, Mutations that disrupt the protein's interactions with other molecules: metal binding (**4**), binding to ligand (**5**), disruption of dimerization (**6**), and binding to, or specific recognition of, DNA (**7**). Adapted from (Laskowski and Thornton 2008).

In summary, to improve a rational therapy for FRDA patients it is necessary to focus on specific research on a cellular level, which will help to fully understand human frataxin structure and function in the mitochondria.

1.2.5.7 The Pathogenic (GAA)n·(TTC)n repeats

The polymorphic (GAA)n·(TTC)n trinucleotide repeats occur within an Alu sequence in the first intron (1.4 kb after exon 1) of the *FXN* gene. These trinucleotide repeats are present in normal individual alleles, but if these repeats go above certain threshold they will become pathogenic. Normal alleles have (GAA)n·(TTC)n repeats ranging from 6 up to 36 repeats, while FRDA alleles have expanded repeats ranging from approximately 66 to more than 1700 repeats. The longer the repeat is, the more severe the disease (Delatycki *et al.* 2000; Pandolfo 2003; Taroni and DiDonato 2004; Al-Mahdawi *et al.* 2006; Herman *et al.* 2006; Gottesfeld 2007). Alleles that have repeats larger than those in normal alleles and smaller than those in FRDA alleles (larger than 36-and less than 66), are called premutation alleles or borderline alleles. Premutation alleles, present in around 1 % of chromosomes, tend to have a large expansion in one generation, but in most cases they are not pathogenic because the second allele inherited from the other parent is expected to be normal (Friedreich 1876; Delatycki *et al.* 1998).

The triplet (GAA)n·(TTC)n repeats in normal alleles can be categorized into two classes of alleles. First, short normal alleles, which comprise about 80-85% of chromosomes in Caucasians, and contain (GAA)n·(TTC)n repeats ranging from 6 to 12 repeats. Second, large normal alleles, about 15% of chromosomes in Caucasians, and contain uninterrupted (GAA)n·(TTC)n repeats ranging from 12 to 36 repeats. The mechanism of the sudden expansion of the repeats from small normal alleles to large normal alleles is ambiguous, but it is been strongly suggested that the expanded FRDA alleles are raised from large normal alleles. Large normal alleles had been observed to hyper-expand to hundreds repeats in one generation. Few large normal alleles, which are interrupted by hexanulceotide repeat (GAGGAA), are stable from generation to generation (Delatycki *et al.* 2000; Pandolfo 2003). From a population

genetics view it has been noticed that in Japan and China there is no (GAA)n·(TTC)n repeat expansion, no large normal alleles, and consequently no FRDA disorder (Pandolfo 1998).

Recently, it has been found that (GAA)n·(TTC)n repeat is correlated with a transcriptionally silent chromatin and DNA replication, also it is contributing to mediate position effect variegation (PEV) (Saveliev *et al.* 2003; Baralle *et al.* 2008).

1.2.5.8 The (GAA)n·(TTC)n repeat expansion and instability

The expansion and the instability of the repeat have a significant role in the progression process of the disease. (GAA)n·(TTC)n repeat is an unstable mutation when it is transmitted from parent to child. When the repeat is transmitted paternally, it tends to contract by ~ 20 to 30% (Pollard *et al.* 2008). FRDA male carriers have smaller (GAA)n·(TTC)n repeats in spermatazoa than (GAA)n·(TTC)n repeats in lymphocytes. In the case of maternal transmission, the (GAA)n·(TTC)n repeat is equally as likely to contract or expand. The size of the contraction is bigger when it is transmitted to a homozygote than when it is transmitted to a carrier. In addition, the sperm of a premutation carrier has been shown to contain a smaller (GAA)n·(TTC)n repeats than that within his leucocytes, and his son's smaller allele contains even less (Delatycki *et al.* 2000; Sharma *et al.* 2002; Pandolfo 2003).

From previous findings, it was concluded that when the expansion occurs it leads to instability (Pianese *et al.* 1997; Pandolfo 2001). The instability of the (GAA)n·(TTC)n repeats is meiotic and mitotic, and it is pre or postzygotic. The mitotic instability of the expanded (GAA)n·(TTC)n repeats causes somatic mosaicism for expansion sizes noted in the fibroblasts, leukocytes, and brain of FRDA patients. This somatic mosaicism is the possible reason for the variability in the phenotype between different individuals with the same diagnosis (Delatycki *et al.* 2000; Sharma *et al.* 2002; Pandolfo 2003; De Biase *et al.* 2007a; De Biase *et al.* 2007b; Mirkin 2007; Pollard *et al.* 2008).

Sharma and colleagues have conducted a further study on a significant number of FRDA patients investigating the (GAA) n ·(TTC) n triplet repeat instability *in vivo*. They have shown a high level of somatic instability in the FRDA peripheral leukocytes, with a threshold length for somatic instability ranging from 26 to 44 uninterrupted (GAA) n ·(TTC) n repeats *in vivo*. A proportional relationship between the somatic instability and the (GAA) n ·(TTC) n repeat length has been demonstrated; the longer the allele is, the more variable it is. Two other remarkable findings were that large expanded (GAA) n ·(TTC) n alleles, which contain more than 500 repeats, have a high affinity to contract largely, whereas shorter alleles, which contain less than 500 repeats, illustrated the affinity to expand. The large expanded alleles rarely can regress to the normal or premutation size range, as observed in peripheral blood cells and sperm. However, these results were not seen when the study was continued to investigate the somatic instability in lymphoblastoid cell lines (Baldi *et al.* 1999; Sharma *et al.* 2002; De Biase *et al.* 2007a; Pollard *et al.* 2008).

In the dorsal root ganglia, the most affected tissue; there is a high tendency for a large expansion. However, all other human tissues show a contraction bias (De Biase *et al.* 2007a; Pollard *et al.* 2008). In addition, a recent study indicates that the somatic instability is age-dependent and tissue specific in cerebellum and DRG in transgenic mouse (Clark *et al.* 2007). DRG shows a very high tendency to expand and a low tendency to contract. The progressive accumulation of (GAA) n ·(TTC) n expansions together with a low frequency of a large contraction, especially in DRG of FRDA patients, is due to the somatic instability (De Biase *et al.* 2007a). Furthermore, somatic instability mostly takes place after early embryonic development and progresses throughout life (De Biase *et al.* 2007b). As a result, progressive somatic instability is contributing to the pathogenesis and progression of the disorder.

Studies have shown that several *cis*-elements and *trans*-acting DNA metabolic proteins, including the orientation and the position of the repeats in relation to the replication origins, cooperate in influencing the instability of the (GAA) n ·(TTC) n repeats (Baldi *et al.* 1999; Krasilnikova and Mirkin 2004; Napierala *et al.* 2005; Pearson *et al.* 2005; Mirkin 2007; Pollard *et al.* 2008). An example of a

cis-element that may affect the instability is DNA methylation. DNA methylation can alter DNA structure, protein binding, differentiation, and cellular activity (Pearson *et al.* 2005).

Further substantial investigations on the instability mechanisms have been conducted by different laboratories and many evidences confirm the involvement of the non B-DNA structures and triplexes in the genetic instability behaviour and DNA repair-recombination function. The results revealed that the conformation of the non B-DNA structures *in vivo*, which are localized in the repeat tracts and in the flanking sequence, is responsible for the genetic instability behaviour. In addition, these structures enhance the slippage of the DNA complementary strands. Furthermore, slipped DNA and unusual DNA structures act as targeted substrates to be recognized by repair proteins such as MSH2 and enzymes (more details are covered in section 1.2.5.9) (Wells *et al.* 2005; Wells 2008). Further specific studies, for better understanding of these phenomena, are essential to precedent to a better treatment approach.

1.2.5.9 (GAA)_n·(TTC)_n repeat expansion molecular mechanism and DNA replication, repair, and recombination

During the last few years, evidence has indicated that the (GAA)_n·(TTC)_n repeat expansion is mediated by DNA replication, followed by the contribution of several enzymes involved in DNA repair, double-strand breaks (DSBs) and the influence of recombination processes. In addition, it had been recognized that simple repeating sequences have the tendency to adapt triplexes, slipped structures and other unusual conformations (non-B DNA), which are involved in the expansion mechanism (Wells *et al.* 2005). Mismatch repair (MMR), nucleotide excision repair (NER), DNA binding repair and DNA polymerases are considered factors that are involved in the expansion mechanism (Sinden *et al.* 2002).

During transcription and replication processes, the DNA duplex unwinds, thus the chance for the single strand DNA (which contains the repeat sequence) to

fold back in an alternative way and form different non-B DNA structures is high. As a result expansion takes place because of the stability of the misaligned intermediates (Wells *et al.* 2005).

Extensive studies have proposed molecular models of how expansions arise, for example, Kunkel proposed the first model in 1993. This model was based on DNA strand slippage during replication (Kunkel 1993). The denaturation and renaturation processes of expanded repeat, which contains double stranded DNA fragments, promote the ‘Slipped-stranded’ DNA formation. Slipped DNA has a different stability and different degree of flexibility. In some studies, it had been shown that the binding of a slipped DNA structure to certain repair proteins such as MSH2 and other recombination repair proteins can lead to DSBs. Later, the concept of an unusual DNA structure formation, from all expandable repeats, was recognized (Figure 1.13, A-E) (Baldi *et al.* 1999; Wells *et al.* 2005; Mirkin 2007).

(GAA)_n·(TTC)_n repeats have the ability to form both inter- and intra-molecular triplets. The homopurine-homopyrimidine repeat can form an intramolecular triplet called H-DNA under the influence of negative super-coiling, the presence of Mg²⁺ and neutral pH. Furthermore, another structure that can be formed with longer forms of this repeat which is called sticky DNA form (Figure 1.13, D) (Gacy *et al.* 1998; Sinden *et al.* 2002; Mirkin 2007; Wells 2008).

The sticky DNA structure was discovered in 1999. It is a self-associated complex that is formed by the combination of two long (GAA)_n·(TTC)_n repeats in the RR·Y triplet construction. The pyrimidine strands in the two·RY triplet constructions are exchanging with each other to form an extremely stable unusual structure. The formation of the sticky DNA structure required the same conditions that influence the triplets structure formation. Sticky DNA structure of the (GAA)_n·(TTC)_n repeats is involved in inhibiting DNA replication, transcription and regulating gene expression and DNA metabolism (Sakamoto *et al.* 2001; Wells *et al.* 2005; Baralle *et al.* 2008).

In addition, It has been suggested that the formation of unusual DNA structures *in vitro* can cause DNA polymerisation blockage. This blockage assists

misalignment between newly synthesized and template DNA strands, which leads the repeat to expand (Pelletier *et al.* 2003; Mirkin 2007). Furthermore, mutations that affect DNA repair increase the probability of the repeat expansion.

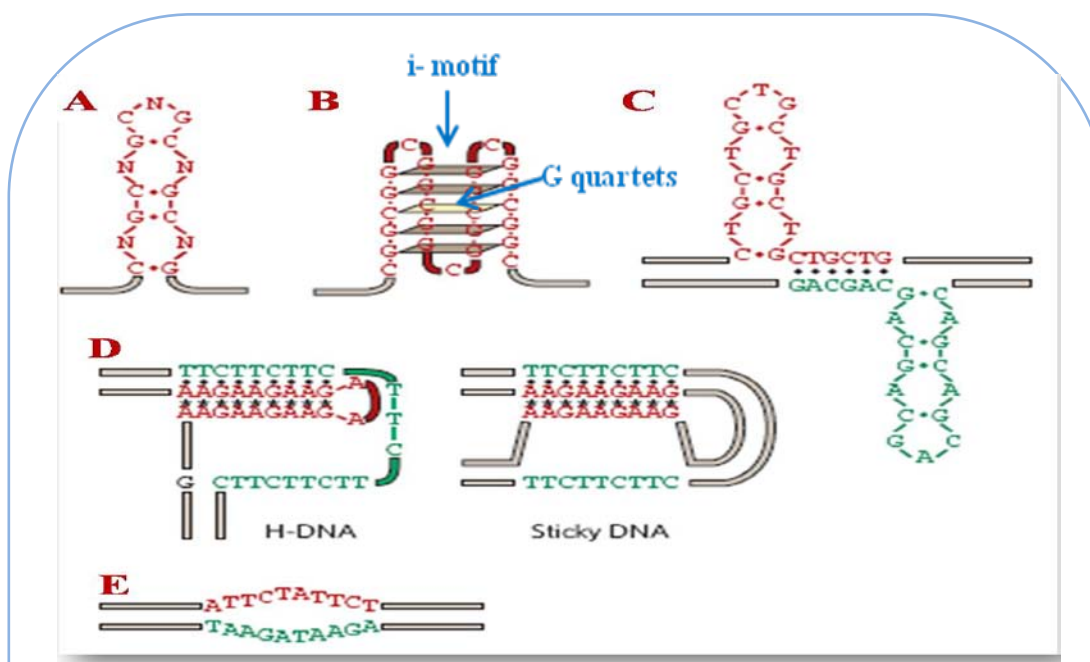


Figure 1.13:

Unusual DNA structures formed by all expandable repeats.

The structure-prone strand of the repetitive run is shown in red, its complementary strand in green, and flanking DNA in beige. Different expandable repeats have the ability to form unusual DNA structures. **A**, (CNG)_n repeats (in red) form an imperfect hairpin structure. **B**, (CGG)_n repeats form a quadruplexlike structure. **C**, (CTG)_n•(CAG)_n repeat form a slipped-stranded structure (in red) and the complementary (in green). **D**, (GAA)_n•(TTC)_n repeats form H-DNA and sticky DNA structures where the homopurine strand formed triplex structure. Black asterisks indicate Reverse Hoogsteen pairing. **E**, (ATTCT)_n•(AGAAT)_n repeats form a DNA-unwinding element (Mirkin 2007).

Negative super-coiling density is an important factor in the expansion mechanism; the higher the level of the negative super-coil density, the more stable the non-B DNA structure is, and the greater the probability of the expansion to occur. A significant study demonstrated the role of the negative super-coiling density on the instability of triplet repeats *in vivo*. An increase in the negative super-coiling density stimulates the triplet repeats instability by accelerating the formation of stable non-B DNA structures (Napierala *et al.* 2005; Wells 2008).

For a relatively short single strand of $(GAA \cdot TTC)_{9-23}$ repeats, the formation of intramolecular triplex structure takes place and its instability increases with the increase of the super-coiling density. Moreover the $(GAA \cdot TTC)_{42}$ repeats can form a very stable bi-triplex structure (Sinden *et al.* 2002; Potaman *et al.* 2004; Napierala *et al.* 2005; Wells *et al.* 2005).

Investigating the mechanisms of the trinucleotide repeat expansion led to the recognition of DNA replication, recombination and repair processes contribution in the repeat instability mechanism (Napierala *et al.* 2005). Figure 1.14 shows a model of how all these processes can contribute to influence the instability and finally causing the disease (Figure 1.14).

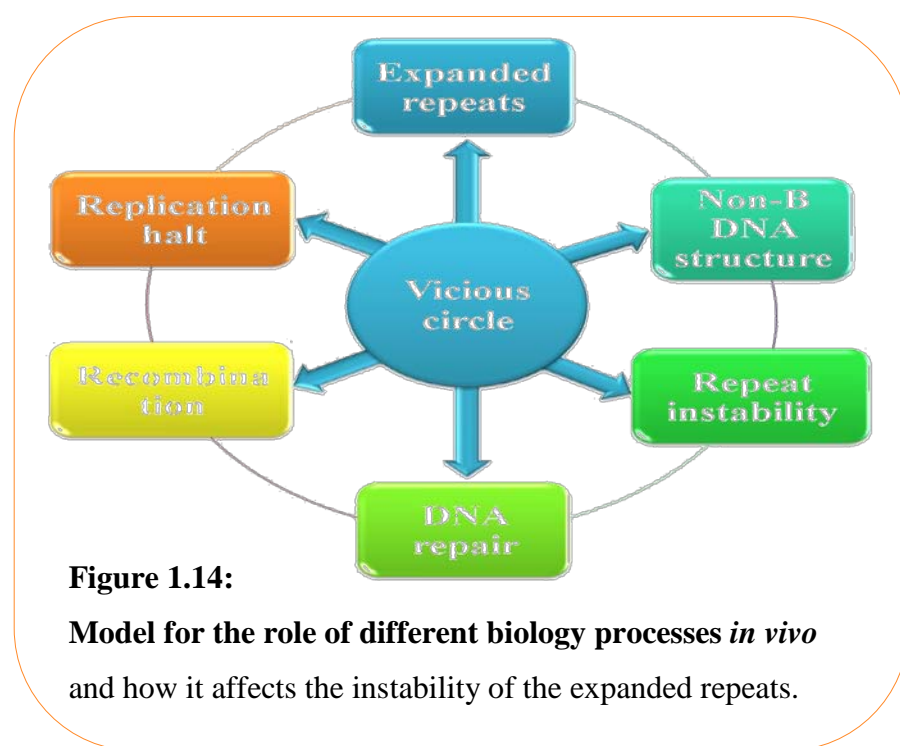


Figure 1.14:
Model for the role of different biology processes *in vivo*
and how it affects the instability of the expanded repeats.

1.2.5.9.1 DNA replication

Many studies suggest that the repeat expansion arises during the DNA replication process for two main reasons. Firstly, there is a rapid accumulation of repetitive DNA because of substantial amount of DNA synthesis. Secondly, the fork replication progression part of the lagging strand template tends to be single stranded, and this facilitates the formation of DNA unusual secondary structures (Mirkin 2007). These secondary structures cause DNA polymerase to halt causing the collapse of replication fork to occur; and finally the involvement of DNA repair and recombination processes to help restart the replication process (Wells *et al.* 2005). Following what has been mentioned previously, the super-coiling dependent non-B DNA structure formation can stop the replication fork progression; which can lead to nicks or double strand break formation and slippage events. In addition, the unusual structures that exist on the leading or lagging strand during DNA replication, can be avoided by DNA polymerases causing repeat instability (Napierala *et al.* 2005; Pearson *et al.* 2005; Gakh *et al.* 2006).

To demonstrate the effect of triplet repeat on replication fork progression a direct study was carried out *in vivo*, in a eukaryotic system (Pelletier *et al.* 2003). In 2004, an experimental study demonstrated that the expanded (GAA) n ·(TTC) n repeats attenuate the replication fork progression *in vivo*, considering the length, the distance from the origin of replication and the orientation of the (GAA) n ·(TTC) n repeats. The effect of the (GAA) n ·(TTC) n repeats is orientation dependent when the homopurine strand of the repeats is in the lagging strand template for the replication process. Furthermore, it had been proven that the replication blockage does not depend on the transcription status *in vitro*. In addition, it had been assumed that the (GAA) n ·(TTC) n expansion, which arises after replication stalling, is positioning in the leading and lagging strands template (Krasilnikova and Mirkin 2004; Mirkin 2007; Pollard *et al.* 2008).

Three hypotheses have been introduced by Mirkin and others to link the repeat expansion steps with the orientation and the position of this repeat through the replication process (Mirkin 2007). The first hypothesis, “ori switch” it suggests that the inactivation of the replication origin on one side of the repeat is associated with

the activation of a cryptic origin on the other side; thus triggering the repeat expansion by placing the structure prone strand of the repetitive run as the lagging strand (Figure 1.15a). The second “ori shift” hypothesis assumes that the repeat expansion depends on the position of the repeat within the Okazaki initiation zone (OIZ), which is always single stranded, so changing the distance between the repeat and the replication origin could enhance the expansion to occur (Figure 1.15b). The third hypothesis, is the “fork shift” model; this hypothesis presumes that changing the mode of the replication fork, by epigenetic event in the region of the repeat, could change the position of the repeat within the OIZ; as a result expansion takes place (Figure 1.15c) (Mirkin 2007).

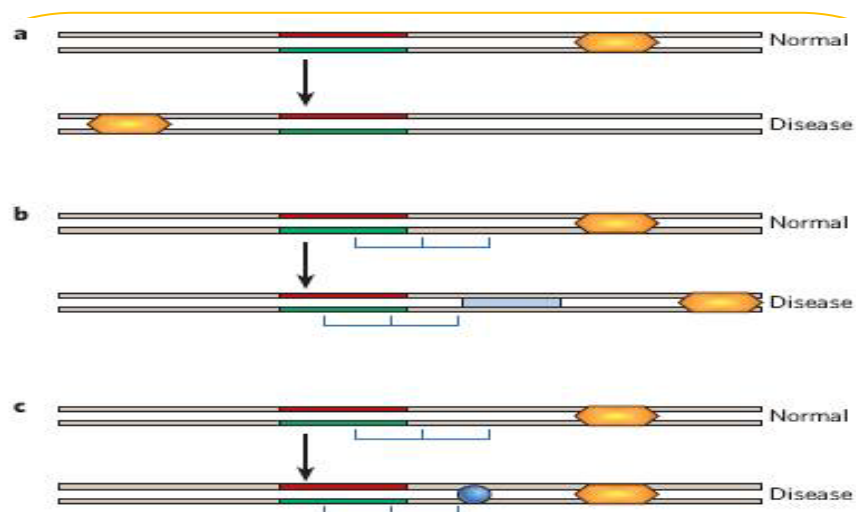


Figure 1.15:

Three hypotheses to explain early events in repeat expansions.

The structure-prone strand of the repetitive run is shown in red, its complementary strand in green, and flanking DNA in beige. **a**, In the ori-switch model, the replication origin (shown in orange) in the repetitive region is reversed to be on the other side. That will cause the inactivation of the replication origin on one side and the recognition of the repetitive run as the lagging-strand template. **b**, In the ori shift model, changing the position of the repetitive run within the OIZ (shown as blue brackets) is leading to change its location in respect to the replication origin because of a mobile element insertion (blue rectangle). This will help to evoke the repeat expansion process. **c**, The fork-shift model arises when an epigenetic event within the repeat (blue oval) occurs. This event will cause in changing the repeat position in the OIZ region and result in the repeat expansion. (Mirkin 2007).

In addition, Krasilnikova and Mirkin explained one of the anticipated mechanisms, during the DNA replication. A part of the single lagging strand template, which contains an expanded $(GAA)_n \cdot (TTC)_n$ repeats, folds back and forms a stable triplex structure along with the remaining double stranded part and this causes DNA polymerase to halt and dissociate (Figure 1.16) (Krasilnikova and Mirkin 2004). Other replication protein molecules may contribute to the repeat expansion process together with DNA repair enzymes such as DNA polymerases or ligases to repair mutant tracts (Pearson *et al.* 2005). Realistically, further substantial research is required to increase the known knowledge in this area.

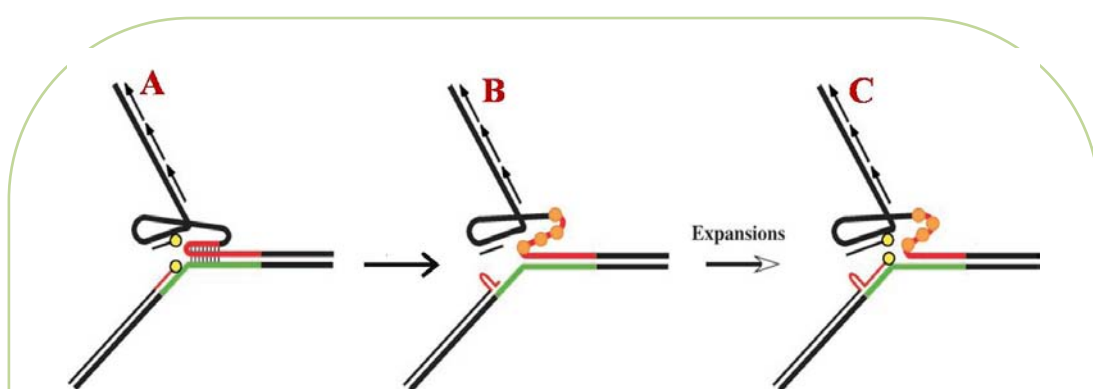


Figure 1.16:

A model for replication blockage by $(GAA)_n \cdot (TTC)_n$ repeats leading to their expansion. Red line, homopurine strand; green line, homopyrimidine strand; black line, flanking DNA. Arrows depict Okazaki fragments. Yellow circles represent leading and lagging DNA polymerases. Orange circles symbolize genome guardians, such as DNA helicases, SSB proteins. **A**, Part of the lagging DNA strand template containing $(GAA)_n$ run forming a stable triplex structure by folding, this folding stalls the DNA polymerase on the leading strand. **B**, the formation of this triplex structure is associated with the polymerase dissociation and misalignment of the newly synthesized and template DNA strands. **C**, The continuation of the DNA synthesis after the demolish of the triplex structure is leading to repeat expansion. Adapted from (Krasilnikova and Mirkin 2004).

1.2.5.9.2 DNA repair

Although the genetic link between the defect in DNA repair pathways and neurological diseases has been established, many substantial studies have been conducted to give a conclusive proof of the DNA repair contribution in the repeat expansion mechanisms (Wells *et al.* 2005; Kulkarni and Wilson 2008).

The DNA repair pathways are meant to be a protective process for the genomic material against different types of mutations and any irregularity in these pathways causes the propagation of genomic instability. In non-replicating differentiated cells such as neurons, the loss of genomic integrity leads to cell death followed by tissue degeneration. Moreover, in these non-dividing cells the replication-dependent recombination repair process is not plausible; consequently cells utilize DSBs, MMR and NER as a viable repair mechanisms to maintain the genomic integrity in the cell (Kulkarni and Wilson 2008). Subsequently, if there are any repetitive DNA intermediates left unrepaired after the replication fork passes on; the expansion of these intermediates takes place (Mirkin 2007).

Some experiments have showed that in aging non-dividing cells, such as human and mouse brain and skeletal muscle cells, the repeat expansion takes place during DNA repair process of DNA nicks or gaps which is created by oxygen radicals (Figure 1.17, page 44) (Mirkin 2007).

Repair of (DSBs), which are induced by replication pause, has a contribution to the repeat instability through gene conversion and single strand annealing (Pearson *et al.* 2005).

The effect of the DSB repair on the (GAA)_n·(TTC)_n repeat somatic instability considering its location to the repeat tracts has been investigated by a recent study in mammalian cells (Pollard *et al.* 2008). Pollard and colleagues revealed that when the DSB repair is within (in the center or off-center) the (GAA)_n·(TTC)_n repeat tract, the frequency of the instability (deletion of nearly half of the repeat tract) increases significantly. Whereas, when the DSB repair is immediately outside the repeat tract the frequency of the instability is not affected.

From these results, it was concluded that the DSB repair process is dependent on the physical properties of the repeat tract.

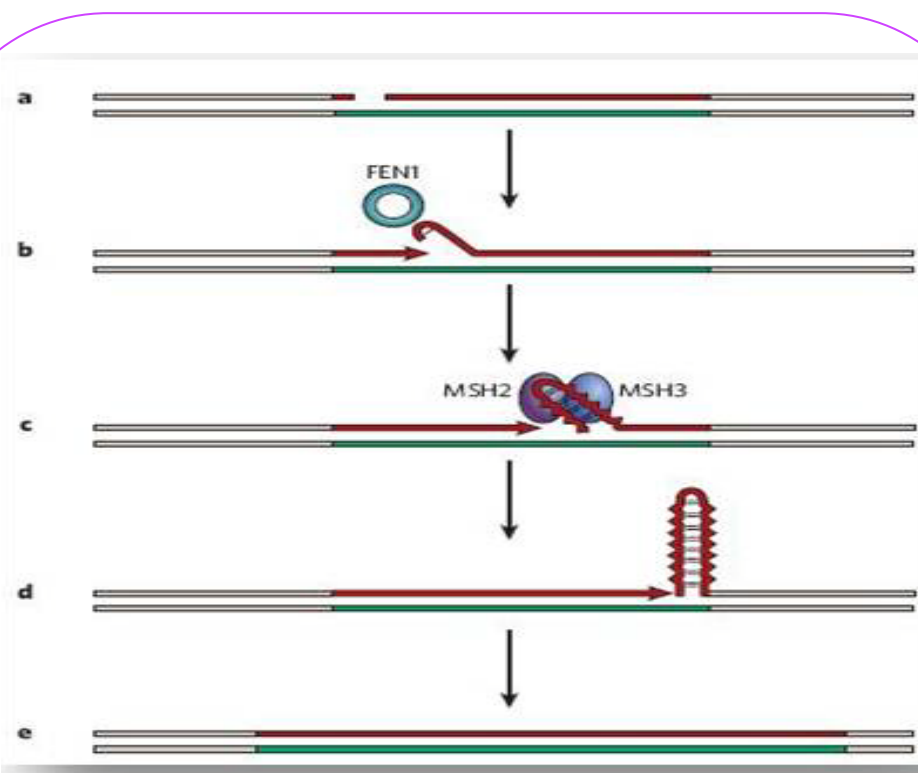


Figure 1.17:

Gap repair model for repeat expansions in non-dividing cells.

The structure-prone strand of the repetitive run is shown in red, its complementary strand in green, and flanking DNA in beige.
a, In the repetitive run a small gap is generated by an oxidizing radicals.
b, Hairpin structure is formed at a repetitive flap and impaired the binding of the flap endonuclease-1 (FEN1) molecule during DNA-repair process. **c**, The repetitive hairpin is stabilized by the binding of MSH2-MSH3 molecule, which resulting in preventing flap removal. **d**, The formation of a stable slipped stranded DNA intermediate is occurred by the time of repair process is completed. **e**, The slipped stranded DNA intermediate is converted into an expansion by a fault in the repair pathway. Adapted from (Mirkin 2007).

The Mismatch repair (MMR) role in normal cells is to remove mismatches and small insertion or deletions that arise during replication or recombination. The role of MMR in repeat instability was firstly identified and widely studied using transgenic mouse models for Huntington's disease and Myotonic dystrophy. The possible hypothesis was that MSH2 and MSH6 have the affinity to bind to the hairpin structures and this binding causes the sequester repair proteins stabilize these structure instead of repairing them (Kovtun and McMurray 2001; Mirkin 2007).

Other experiments demonstrate mixed effects of mismatch repair on instability. MMR repair takes place and MMR proteins, including MutS α [MSH2 and MSH6] and MutS β [MSH2-MSH3] heterodimer, bind to looped-out secondary structure when these DNA unusual structures formed and result in the mismatching of bases within the structure or in the flanking region (Genschel *et al.* 1998; Wells *et al.* 2005; Kulkarni and Wilson 2008). The hypothesis was that mismatch repair has a key role in instabilities mainly through MSH2 or other downstream proteins (Wells *et al.* 2005).

However, some studies showed there is no increase in the instability with human cell lines with mutations in MMR proteins at Myotonic dystrophy (DM1) and Fragile-X (FRAXA) loci, furthermore none of the MMR proteins have a conclusive link to the neurodegenerative disease to date (Kramer *et al.* 1996; Kulkarni and Wilson 2008).

Nucleotide excision repair (NER) is a repair process specific for DNA helical alterations. In some cells, the recognition for the helical alterations includes the recognition and the removing of DNA loops which are part of the secondary or non B-DNA structures. This causes a DNA gap which requires repair process and consequently the repeat instability takes place (Parniewski *et al.* 1999; Wells *et al.* 2005). Previously, some studies had been conducted on bacterial models to clarify the NER role in the repeat instability. The results indicate that NER either preventing or enhancing large contraction for (CTG) n -(CAG) n repeat sequence. In conclusion, NER contribution to repeat instability is dependent on the repeat tract and the transcription replication direction (Pearson *et al.* 2005; Wells *et al.* 2005). Furthermore, extra significant work is required to clarify this area; specially with

(GAA)_n·(TTC)_n repeat tract. Moreover, it is necessary to contemplate other proposed mechanisms from different research studies related with different neurological disorders. A co-excision mechanism had been proposed in 2000 by Rolfsmeier and colleagues, from a yeast study explaining the loss of stabilizing interruption within expandable repeats (Figure 1.18) which is a possible mechanism for the repeat expansion in FRDA ataxia disorder (Rolfsmeier *et al.* 2000; Mirkin 2007). In addition, DNA repair proteins might be considered as a factor contributing to the repeat instability mechanism. For example, MMR proteins interfere with NER process (Pearson *et al.* 2005). Future studies are still required to decipher these biological processes roles in the body and their contribution to the disease.

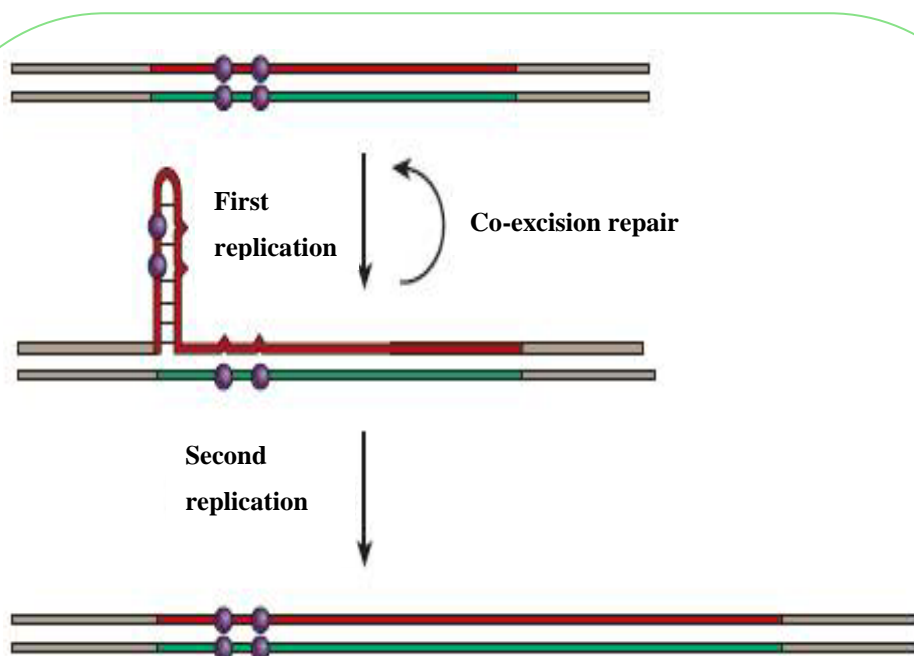


Figure 1.18:

Loss of stabilizing interruptions within expandable repeats.

The structure-prone strand of the repetitive run is shown in red, its complementary strand in green, and flanking DNA in beige. During the first DNA replication process a misalignment of nascent and template DNA strands in long-normal alleles can occur and this creates mismatches in both the hairpin and duplex part of the slipped-stranded structure. Failure to repair them by co-excision repair leads to the generating of the non-interrupted expansion at the 3' end of the repetitive run. Adapted from (Mirkin 2007).

1.2.5.9.3 DNA recombination

DNA recombination also has a limited contribution to the repeat expansion mechanism. One of the possible models, which was explained by Mirkin, suggests that as a result of DNA synthesis-dependent strand annealing; a mitotic, unequal crossing over (intrachromosomal strand annealing) occur between the repetitive tracts on homologous chromosomes causing expansion or contraction (Figure 1.19) (Warren 1997; Pearson *et al.* 2005; Mirkin 2007).

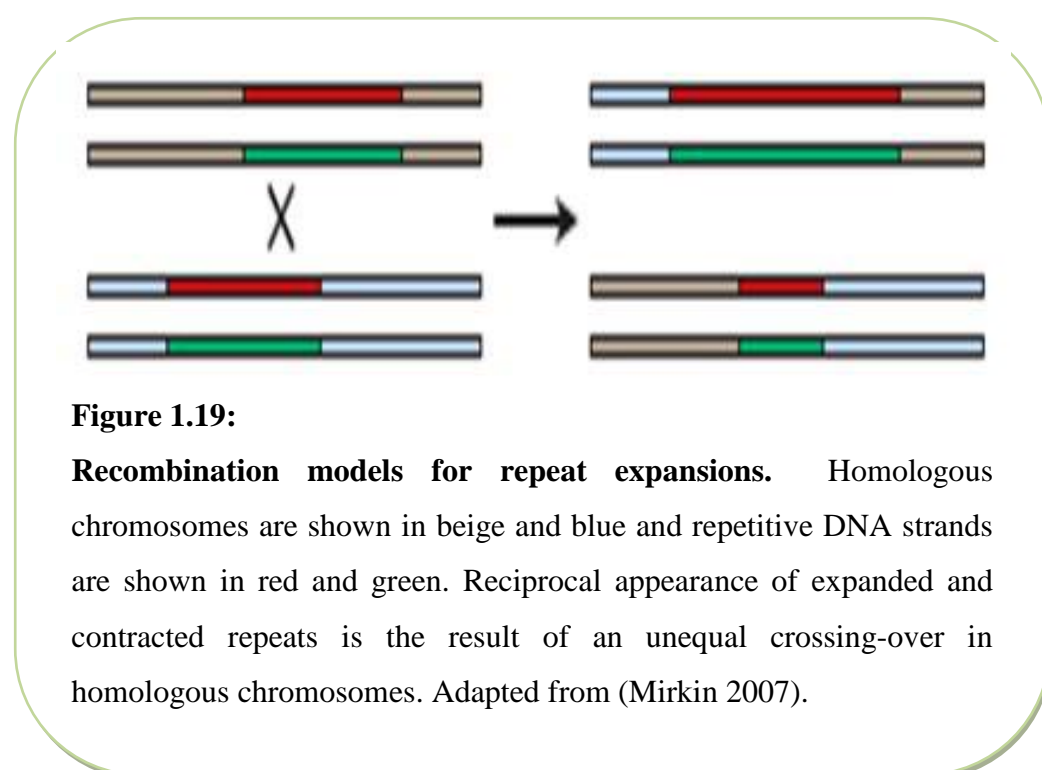


Figure 1.19:

Recombination models for repeat expansions. Homologous chromosomes are shown in beige and blue and repetitive DNA strands are shown in red and green. Reciprocal appearance of expanded and contracted repeats is the result of an unequal crossing-over in homologous chromosomes. Adapted from (Mirkin 2007).

In addition, it been assumed that the stimulation of the recombination is dependent on the repeat orientation within the replicon. Thus, after the pausing of the replication fork, the single stranded DNA fragment is generated. This strand has the ability to infest the sister chromatid then the expansion takes place (Figure 1.20) (Mirkin 2007). A positive correlation between increasing the length of the $(GAA)_n \cdot (TTC)_n$ repeat tracts and decreasing the frequency of the intramolecular recombination was discovered (Wells 2008).

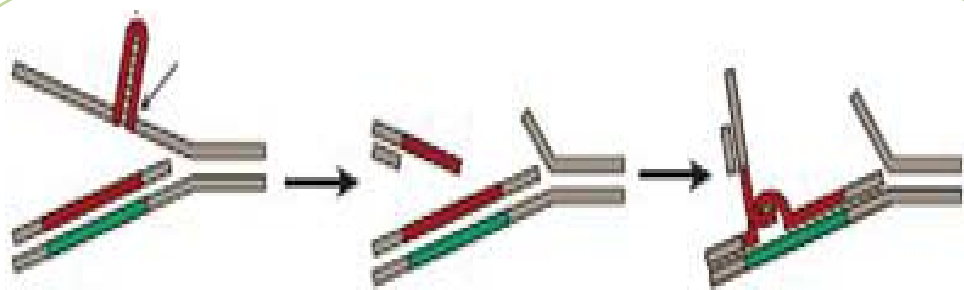


Figure 1.20:

Cleavage of a stable DNA structure on the lagging-strand template

The structure-prone strand of the repetitive run is shown in red, its complementary strand in green, and flanking DNA in beige. Small arrows show potential cleavage sites. (left), during DNA replication, the cleavage of a stable DNA on the lagging-strand generates a single-stranded 3' repetitive extension (centre) the single-stranded DNA invade a sister chromatid (right) as a result a repeat expansion or contraction may occur. Adapted from (Mirkin 2007).

At the end, it is difficult to determine the exact role of recombination in instability because of the difficulty of detecting the recombination events that have break points within the repeat (Pearson *et al.* 2005).

In conclusion, understanding the molecular basis of the expansion instabilities mechanism is essential to know the origin and the progression of the disease. Then, different creative approaches for treatment can be raised to control the progressive instability in some tissues in FRDA patients.

1.2.5.10 The expanded (GAA)_n·(TTC)_n repeats and its role in reducing FXN gene transcription

Knowing the exact mechanism of how the expanded (GAA)_n·(TTC)_n repeats reduce the gene transcription is as important as knowing the (GAA)_n·(TTC)_n expansion mechanism; since both will lead to a better concept of successful therapy.

It is well known, that the transcription process starts with the binding of pre-initiation complex at the gene promoter, then RNA synthesis begins followed by the elongation stage. The transcription is usually regulated at the stage of the RNA polymerase (Pol II) recruitment to the promoter region, which is essential for gene activation (Muse *et al.* 2007; Tamkun 2007; Zeitlinger *et al.* 2007). Relating to this fact, many suggested mechanisms had been proposed to explain the way the expanded (GAA)_n·(TTC)_n repeats modify gene transcription process.

In 1998, the inhibitory effect of the expanded (GAA)_n·(TTC)_n repeats was investigated *in vivo* and the results showed a very low level of mature mRNA with no accumulation of the primary transcript in the plasmids with long (GAA)_n·(TTC)_n repeats (Ohshima *et al.* 1998; Baralle *et al.* 2008; Wells 2008). In addition, a lot of evidences prove that the expanded (GAA)_n·(TTC)_n repeats have an inherited ability to form a non B-DNA structures such as triplex, hairpin, parallel DNA and a triple-helical (H-DNA) or sticky DNA (see previous section 1.2.5.9 and Figures 1.13, 1.14). A specific and persistent inhibitory d(TTC)_n·r(GAA)_n hybrid and a heterochromatin mediated gene silencing effect had been reported. Such intermediates have been shown to interfere with the gene transcription *in vivo* and *in vitro* and contribute to the aetiology of FRDA (Sakamoto *et al.* 2001; Al-Mahdawi *et al.* 2004; Krasilnikova and Mirkin 2004; Hebert and Whittom 2007; Baralle *et al.* 2008; Wells 2008).

It has been demonstrated that the sticky DNA structure has an essential function, *in vivo*, by interacting with proteins or interfering in metabolic pathways. Sticky DNA has an inhibitory effect, *in vivo* and *in vitro*, on the transcription process of the *FXN* gene, by inhibiting the synthesis of RNA. Sakamoto and colleagues have explained the way the sticky DNA is involved in the RNA polymerase sequestration step. They suggested that RNA polymerase is paused within sticky DNA structure during RNA synthesis and less free RNA polymerases are available for further transcription. Another suggestion was that the sticky DNA structure has the ability to bind to an inactive RNA polymerase without transcription (Sakamoto *et al.* 2001; Baralle *et al.* 2008; Wells 2008).

Two mechanisms have been proposed to explain the role of the triplex structure in affecting transcription. First, the triplex structure may physically block the transcription elongation process. Second, the triplex structure may interfere with the binding of transcription factors (*trans*-acting factors) that control the transcription (Giovannangeli *et al.* 1996; Kovacs *et al.* 1996; Sakamoto *et al.* 2001; Saveliev *et al.* 2003). Wells and his colleagues have demonstrated that an expanded (GAA)_n·(TTC)_n repeats can form a DNA:RNA triplex that reduces transcription (Ohshima *et al.* 1996).

Another well-explained (*in vitro*) experiment, which was conducted by Grabczyk and Usdin, showed how the RNA polymerase molecule is trapped in an R·R·Y triplex when it enters in an expanded (GAA)_n·(TTC)_n repeats area and produce negative super-coiling and that leads to form an intramolecular triplex structure. As a result RNA polymerase stalls (Grabczyk and Usdin 2000; Hebert and Whittom 2007). It is important to mention that RNA polymerase II stalling has a key regulatory role for gene transcription in the development stage (Muse *et al.* 2007; Zeitlinger *et al.* 2007)

In 2007, Grabczyk and colleagues proposed another model, with the same principle, explaining the transcription coupled RNA·DNA hybrid formation in an expanded (GAA)_n·(TTC)_n repeat area. The template DNA strand d(TTC)_n forms a stable RNA·DNA hybrid with a moderate length, then the DNA triplex is dislodged, in the presence of the transcription complex, to give longer RNA·DNA hybrid. The formation of the stable RNA·DNA hybrid and DNA triplex creates a pause site at the expanded (GAA)_n·(TTC)_n repeat area (Figure 1.21, page 51) (Grabczyk *et al.* 2007; Wells 2008).

At this stage, it is important to note that triplexes or sticky DNA have no obligatory role in the aetiology of FRDA, thus further investigations are required to clarify the direct relation between these unusual DNA structures and the transcription inhibition effect (Wells 2008).

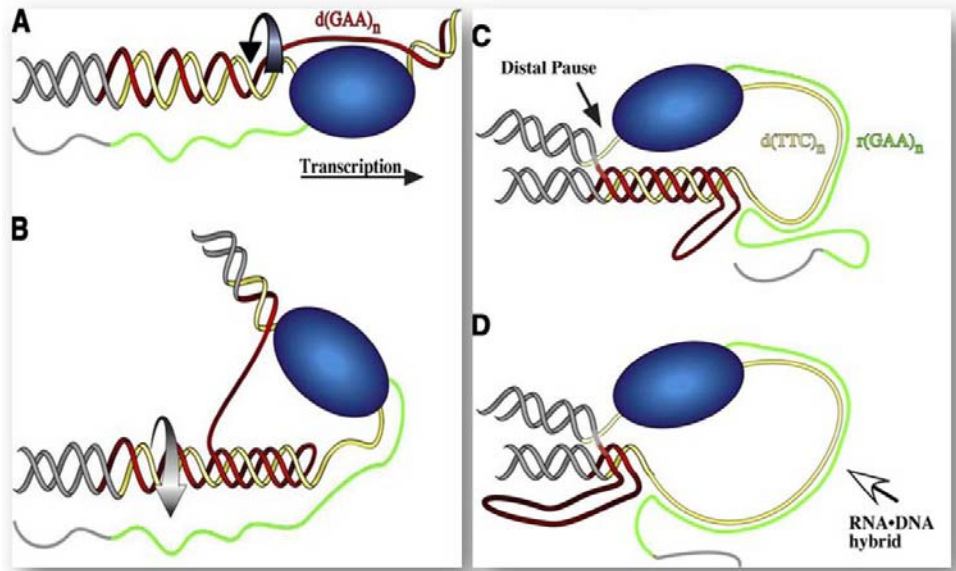


Figure 1.21:

Transcription-coupled RNA·DNA hybrid formation in a $(GAA)_n\cdot(TTC)_n$ repeat. Model for transient transcription dependent triplex formation leading to an RNA polymerase pause and RNA·DNA hybrid formation. The purine (GAA or R) strand of the repeat is red, the pyrimidine (TTC or Y) strand is yellow, and the flanking DNA is gray.

A, A standing wave of negative super-coiling follows RNA polymerase. At the transcription bubble, the non-template (GAA) strand is available to fold back in an R·R·Y interaction; the template strand is covered by RNA polymerase. **B,** Rotation of the helix (curved arrow) as it winds in the third strand relaxes the negative super-coils caused by transcription and leaves a length of the template single-stranded. **C,** RNAP is impeded at the distal template-triplex junction and the nascent transcript (green) can anneal to the single-stranded stretch of template. **D,** The RNA·DNA hybrid displaces the much less stable triplex structure.

Adapted from (Grabczyk *et al.* 2007).

However, a recent study using a hybrid minigene system explained the composite affect of the transcribed (GAA)_n repeat, that can form an intronic sticky RNA structure, affecting the normal intronic pre-mRNA processing. This sticky RNA sequence can act as an exonic splicing enhancer (Baralle *et al.* 2008).

In this study, the results showed that in the mammalian reporter gene, (GAA-TTC)₁₀₀ and (GAA-TTC)₂₁₇ repeats affect neither the polymerase II transcriptional elongation step, nor pre-mRNA transcription abundance. Nevertheless, this pathogenic repeat results in a complex defect in pre-mRNA process by inhibiting the splicing efficiency. Furthermore, the insertion of the GAA repeat at different locations (upstream and downstream) from the reporter exons has different effects on the splice site selection. These repeats have the ability to bind to different *trans*-acting splicing factors, as a result enhancing the accumulation of an up-stream pre-mRNA splicing intermediates and stop the pre-mRNA from turning over to a mature form (mRNA), thus the degradation of the RNA molecules and lower level of mRNA. Furthermore, the number of the repeat affects the severity of the splicing pattern, consistent with variable phenotypic expression of the disease. The affect of the GAA repeat depend on position and context manner.

Insertion of the (GAA)_n-(TTC) repeat in the first intron of a frataxin minigene model has also been conducted. The results revealed that the repeat did not block the transcription but it affected the splicing efficiency of the first *frataxin* intron. In addition, the repeat presence in its original context is not affecting the quality of the final transcript (Figure 1.22) (Baralle *et al.* 2008).

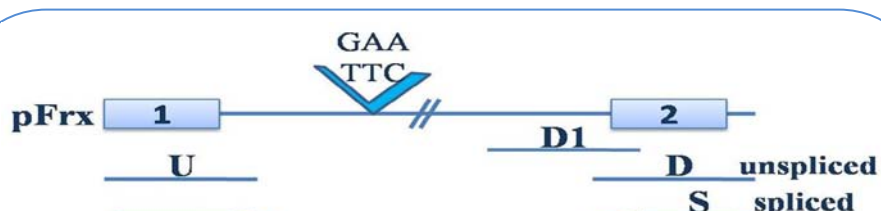


Figure 1.22:
Schematic representation of the frataxin minigene.

It contains the GAA or TTC ($n = 100$) repeats and showing the un-spliced (U, D, and D1) and spliced (S) amplification products. Modified from (Baralle *et al.* 2008).

In addition to the DNA structure, DNA recombination, and DNA repair; epigenetic modifications may contribute to affect *FXN* gene transcription and contribute to the pathogenesis of FRDA (Pollard *et al.* 2008).

1.3 Epigenetics

In the last decade, because researchers have given considerable attention to the field of epigenetics, the amount of information about epigenetics and its implication in the aetiology of some human diseases has increased dramatically. The main contribution to this knowledge has come from the development of molecular genetics approaches, for instance the use of the chromatin immunoprecipitation (ChIP) technique with genome-wide scan and mapping techniques, high-throughput DNA microarray and sequencing, serial analysis of gene expression (SAGE), and serial analysis of chromatin occupancy (SACO) (Bock and Lengauer 2008; Schones and Zhao 2008).

1.3.1 The definition of epigenetics

Epigenetic regulations have been implicated in normal development and human illness. They are vital regulations for the normal functioning of genomes, for example, segregation of chromosomes in mitosis and regulation of gene activity. If any misregulation takes place, then epigenetic regulations will be highly relevant to various complex non-Mendelian disorders (Jaenisch and Bird 2003; Feinberg 2007).

In the 1940s, Conrad Waddington proposed the first theoretical concept about the term “epigenetics”. That is ‘the interaction of genes with their environment, and how genotypes give rise to phenotypes during development’ (Waddington 1942; Murrell *et al.* 2005; Bird 2007; Crews 2008). Later, in the 1970s the modern era of epigenetics, Robin Holliday used modern genetic methods to present a molecular model for inheritability of the gene activation and inactivation during development by DNA methylation and demethylation (Holliday and Pugh 1975; Holliday 1987; Crews 2008).

Epigenetic modifications are involved in aging and long term memory process such as, DNA methylation (Bird 2007; Santos-Reboucas and Pimentel 2007; Crews 2008). The increase of the epigenetic modifications with age have helped to explain the late age of onset in some complex diseases (Stuffrein-Roberts *et al.* 2008).

Then Arthur Riggs and colleagues defined epigenetics as ‘the study of all meiotically and mitotically heritable changes in gene expression that are not coded in the DNA sequence itself’ (Egger *et al.* 2004; Bird 2007; Bock and Lengauer 2008). Since then epigenetics is used in molecular and developmental genetics studies of gene function that is not attribute to the change in DNA sequence, so nowadays epigenetics refers to ‘the transmission of genetics information, other than that stored in the DNA sequence, from a cell to its daughter cells, and from an organism to its offspring’ (Laskowski and Thornton 2008).

Epigenetic modifications are heritable, reversible, gradual and dynamic process that contribute to modify gene expression in the cell (Egger *et al.* 2004; Santos-Reboucas and Pimentel 2007; Crews 2008; Schones and Zhao 2008). In more detail, in certain developmental stages or in some diseases; some cells undergo a major reprogramming step. This step involves the removal or the modulation of their epigenetic markers. Otherwise, in normal cases, these epigenetic markers are fixed after cell differentiation or existence in the cell cycle (Bock and Lengauer 2008; Nafee *et al.* 2008; Ptak and Petronis 2008). Therefore, for each cell, there is a unique gene expression profile, which will determine its identity; this profile will be remembered and passed on to a daughter cell. This is known as “Epigenetic inheritance” (Nafee *et al.* 2008; Schones and Zhao 2008).

Epigenetic inheritance occur between generations of cells, which is mitotic inheritance, and between generations of species, which is meiotic inheritance. Mitotic inheritance is involved in cellular differentiation. That is to say, the differentiated cells of the gremline reprogram epigenetic information in a parent-specific way, before it is passed on to the daughter cells as sperm or egg.

While the meiotic inheritance is considered the result of the incomplete reprogramming in the early embryo stage that produces an epigenetic information from the parent to the offspring; that is to say across the germline generations (Bock and Lengauer 2008; Ptak and Petronis 2008).

The advanced approaches have been used by international collaborations to identify epigenetic changes on a genome-wide scale, here the term “Epigenomics”. The epigenome covers two different areas: chromatin structure and DNA methylation. Therefore, the epigenome can vary from cell to cell, can change over time, and depends on the tissue type and developmental stage. Thus complex organisms, such as humans have a multiple epigenomes (Murrell *et al.* 2005; D'Alessio and Szyf 2006; Schones and Zhao 2008; Stuffrein-Roberts *et al.* 2008).

1.3.2 Molar and Molecular epigenetics

In both animal and human inheritance systems, epigenetic modifications take place at two different levels: the physiological and morphological level, which is **molar epigenetics**, and at the normal patterns of gene expression, which is **molecular epigenetics**. These changes cause functional differences in brain and behaviour; thus, different genotypes arise. As a result, individual response to their environment is changing and the modifications will be on a higher level of biological organization. Figure 1.23 shows the interaction between different epigenetic factors at different levels (Figure 1.23) (Holliday 2006; Crews 2008; Stuffrein-Roberts *et al.* 2008).

Molar epigenetics is the study of how the environment stimuli affect the genome of the individual during its development followed by the observations of the individual's interaction with its physical environment after birth (Gottlieb 2007; Crews 2008). Numerous environmental factors can stimulate epigenetic modifications. For example, nutrition, maternal behaviour, internal factors (hormones) and some drug treatments can influence gene expression by altering DNA methylation status.

A previous experiment explains the case of monozygotic twins (MZ) that showing a significant difference in the phenotypic outcomes, which comes from different level of genes expressions of the diseases causing genes due to the differences in epigenetic modifications, Although they are genetically identical (Fraga *et al.* 2005; Ptak and Petronis 2008; Stuffrein-Roberts *et al.* 2008).

Molecular epigenetics is the study of heritable gene regulations during embryogenesis without involving the changes occur in DNA sequence (Crews 2008; Keverne and Curley 2008).

In this research, our investigation concern only about the molecular epigenetic modifications and their involvements in the FRDA pathology, so any epigenetic modifications will be discussed later are referred to the epigenetic modifications at the molecular level.

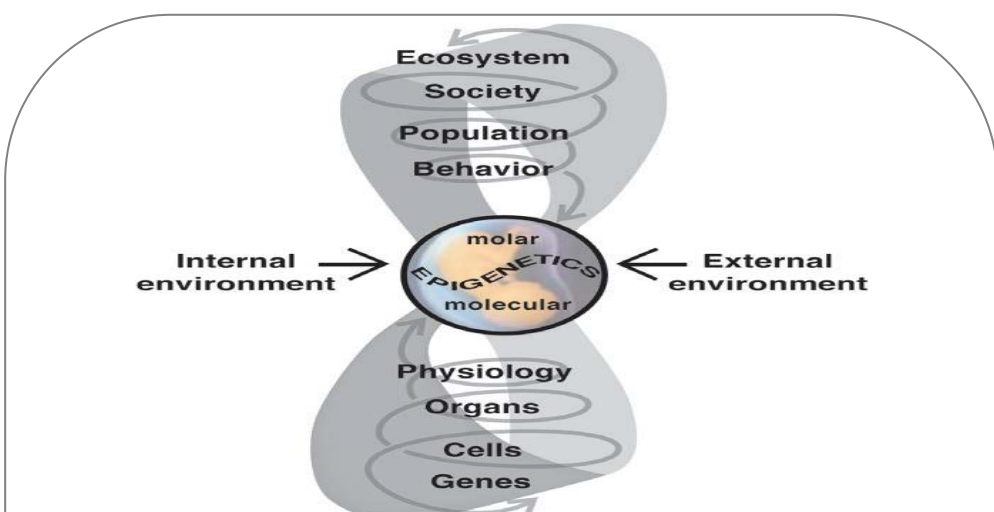


Figure 1.23:

The external environment interacts with the internal environment to influence fetal development with both immediate and life-long consequences. Such environmentally-induced changes can occur at all levels of biological organization, from the molecular to the organism's behaviour, and tend to be amplified in their consequences as they ascend through these levels. Ultimately, these influences may be epigenetic in nature, inducing heritable alterations in gene expression without changing the DNA. Adapted from (Crews 2008).

1.3.3 Mechanisms of molecular epigenetic regulations

In recent years, the availability of the advanced databases for genome-wide DNA and RNA sequences, protein (3D) structures, DNA methylation patterns, ChIP-sequence techniques and others, has helped to bring new insights of the epigenetic modification mechanisms that are associated with some human complex diseases; thus, a new era of research has arisen. Studies that consider chromatin structures and nucleosome arrangement including the DNA molecule and its way of interaction with histone proteins have a great impact in elucidating the epigenetic mechanisms in affecting the transcriptional process in the cell. However, more sophisticated studies are still needed in the next few years for a new expanded direction in the therapeutic and pharmacological fields.

In eukaryotic cells, DNA is packaged in the form of chromatin. Chromatin is composed from DNA, octamers of core histone proteins (H2A, H2B, H3, and H4) and non-histone proteins, which facilitate the DNA packing to form a higher order structure ‘nucleosome’. Each histone has a flexible domain, which remains outside the nucleosome called histone tails (Figure 1.24). These tails can encode epigenetic information and store different distinct epigenetic information patterns, which are called histone code (More details about histone code definition are covered in section 1.3.3.1, page 60) (Laskowski and Thornton 2008; Nafee *et al.* 2008; Ptak and Petronis 2008; Stuffrein-Roberts *et al.* 2008).

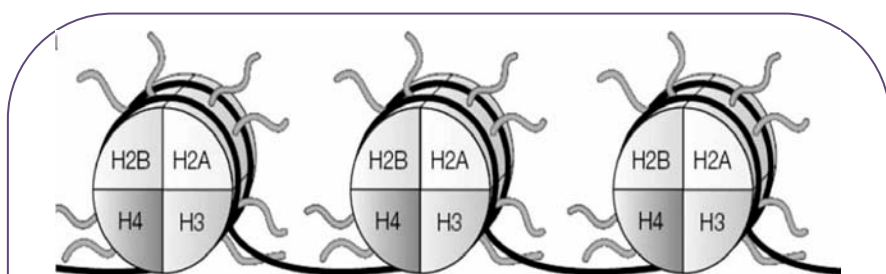
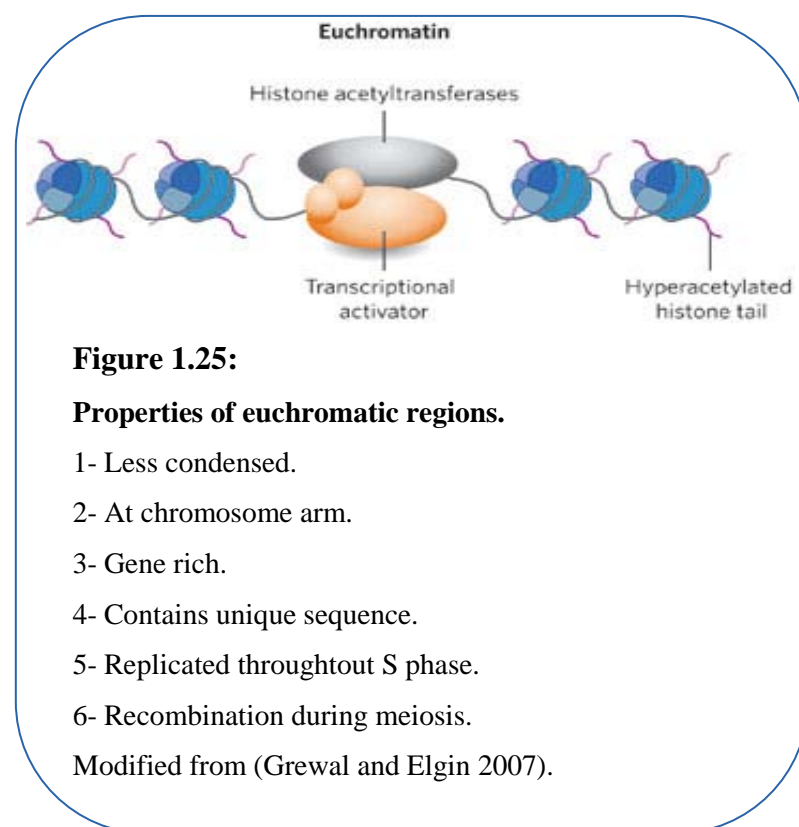


Figure 1.24:

Nucleosome structure. Each nucleosome consists of two copies each of H2A, H2B, H3 and H4 (core histones) forming an octamer around which the DNA is wrapped. The amino-terminal tails of core histones are exposed on the outside of the nucleosomes. Adapted from (Stuffrein-Roberts *et al.* 2008).

There are two forms of chromatin: euchromatin, which is loose and accessible for the transcription factors to be recruited at the promoter regions, then transcription process is initiated (Figure 1.25). It has been reported that the enhancers are more competitive in binding to the silencing factors than the promoters are, and that they maintain the euchromatin structure. The heterochromatin form, which is more condensed, compact, stable (maintained through mitosis and meiosis) and inaccessible for the transcription factors to bind and function; as a result the inhibition of the transcription process takes place (Figure 1.26) (Grewal and Elgin 2007; Stuifrecht-Roberts *et al.* 2008). The relationship between the heterochromatin formation and gene silencing has been derived from the loss of gene expression correlated with condensed packaging in position effect variegation (PEV). PEV occurs when a gene, which is normally euchromatic, is abnormally close to heterochromatin that is characterized by the presence of H3K9me3 and histone tails hypoacetylation, during rearrangement; resulting in variegating phenotype indicated that the gene has been silenced in a proportion of the cells in which it is normally active (Saveliev *et al.* 2003; Gottesfeld 2007).



In contrast, a genomic DNA microarrays study showed that compact chromatin fibres contain some active genes in addition to the heterochromatin (D'Alessio and Szyf 2006).

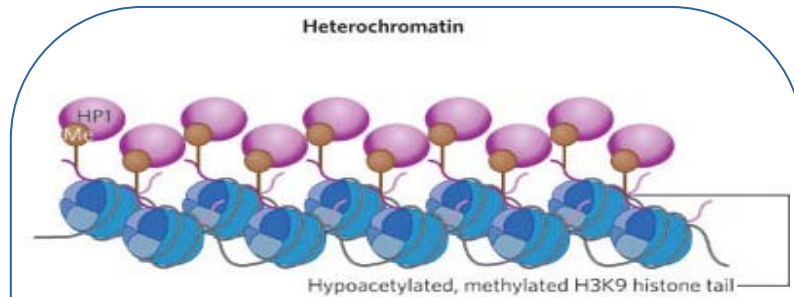


Figure 1.26:
Properties of heterochromatic regions.

- 1- Highly condensed.
- 2- At centromeres and telomeres.
- 3- Gene poor.
- 4- Contains repetitious.
- 5- Replicated in late S phase.
- 6- No meiotic recombination.

Modified from (Grewal and Elgin 2007).

Epigenetic mechanisms can have two different affects on the gene transcription process: activation (open chromatin; euchromatin) and that occurs when the histone acetylation signal such as, H3k9ac and H3K14ac is high. Inactivation (condense chromatin; heterochromatin) occurs when the signal of the histone hypermethylation signal is high for example, H3K9me3 (Bock and Lengauer 2008).

Histone modifications, DNA methylation, RNA-associated silencing, binding of non-histone proteins (such as, polycomb and trithorax group complexes) and action of methylation dependent sensitive insulators are the suggested mechanisms that initiate the heritable epigenetic silence (Egger *et al.* 2004; Bock and Lengauer 2008).

1.3.3.1 Chromatin remodelling through histone modifications

Chromatin remodelling plays an important role in regulating gene expression by controlling the recruitment of transcriptional and regulatory factors to the underlying DNA (Nafee *et al.* 2008; Ptak and Petronis 2008; Stuffrein-Roberts *et al.* 2008).

Over the past view years, post-translational histone modifications have been studied substantially. In embryonic stem cells (ES) there are some regions termed ‘bivalent domains’. These domains contain both of these histone modifications, which are essential in ES cell differentiation and development by providing the potential for transcriptional activation or inhibition (Berger 2007; Spivakov and Fisher 2007; Schones and Zhao 2008).

These modifications, which occur at various amino acid molecules on the histones N-terminal tail domains, include histone acetylation (lysine), phosphorylation (serine and threonine), methylation (lysine and arginine), ubiquitination (lysine), sumoylation and ADP-ribosylation. These chemical modifications can alter the structure of the chromatin fibre, its degree of condensation, and then the interaction and the accessibility of the transcriptional proteins to the DNA within (Egger *et al.* 2004; Santos-Reboucas and Pimentel 2007; Bock and Lengauer 2008; Nafee *et al.* 2008; Ptak and Petronis 2008).

Three models have been presented to explain the post-translational histone modifications (Schones and Zhao 2008). First, **histone code** which is defined as ‘multiple histone modifications occurring in the same region to generate a unique chromatin structure, which is compatible with specific level of gene expression’. These modifications function combinatorially to regulate downstream functions (Egger *et al.* 2004; Santos-Reboucas and Pimentel 2007; Nafee *et al.* 2008; Schones and Zhao 2008). In addition, the histone code functions as epigenetic signals from the DNA to the cellular machinery including, gene regulation, DNA repair, and chromosome condensation (Stuffrein-Roberts *et al.* 2008). Second, in more general aspect histone modifications can serve as **signalling pathway** to accelerate binding of enzymes for their function on the chromatin. This model is providing specificity,

redundancy and combination through feedback loop. Third, certain histone modifications such as, acetylating and phosphorylation initiate **charge neutralization** of the chromatin. For example, acetylation of histones neutralize positive charge on DNA and phosphorylation adds negative charge, and this leads to a general decondensation of the chromatin fibre (Schones and Zhao 2008).

Predominantly, the *acetylation* of the histone tail, such as H3K9, is related to an uncondensed chromatin structure and active transcriptionally regions, whereas hypoacetylation is related to inactive euchromatic or heterochromatic regions. The balance between these two processes is controlled by an opposite activity of histone deacetylases (HDACs) and histone acetyltransferases (HATs) enzymes (Egger *et al.* 2004; Santos-Reboucas and Pimentel 2007). HAT enzyme acetylates the lysine residues on the N-terminal tail of the histone and neutralizes the positive charge of the protein, causing the formation of an open chromatin structure (euchromatin) that is accessible to the transcription regulatory factors. Whereas, HDAC enzyme deacetylates the lysine residues, causes a chromatin condensation (heterochromatin) and inaccessible DNA for the transcription machinery (Ptak and Petronis 2008).

Histone *phosphorylation*, is the addition of the negatively charged phosphate group to the histone tails, and the neutralization of the basic charge, which leads to reduce the histone affinity to the DNA. It is seen in cell cycle progression during mitosis and meiosis. For example, the phosphorylation of serine 10 in histone H3 was related with gene activation in mammalian cells. In addition, the phosphorylation of the H2A, which occur after the activation of DNA-damage signalling step, will allow the chromatin to open and facilitate the DNA repair process (Santos-Reboucas and Pimentel 2007; Nafee *et al.* 2008).

Histone *methylation* is a mark for both active and inactive regions of the chromatin, and different degrees of methylation are related with different levels of gene silencing. Histone methylation of lysine residues can be monomeric, dimeric or trimeric. These variations give rise to multiple combinations of different modifications ‘histone code’. In addition, it was shown that histone methylation is reversible by histone demethylases as an oxidative process. For instance, the trimethylation of the lysine residue 9 on the N terminus of histone 3 (H3-K9) is a

DNA silent mark and associated with constitutive heterochromatin. This modification is spreading throughout certain heterochromatic regions such as telomeres and centromeres, while mono and dimethylation of the same position is associated with facultative heterochromatin. On the other hand, the methylation of the lysine residue 4 on the N terminus of histone 3 (H3-K4) is an active mark at the promoter regions of active genes. The suggested explanation for this variety is the specific binding of the heterochromatin protein 1 (HP1), which mediates H3K9 methylation specifically but not H3K4 (Egger *et al.* 2004; Santos-Reboucas and Pimentel 2007; Nafee *et al.* 2008; Schones and Zhao 2008).

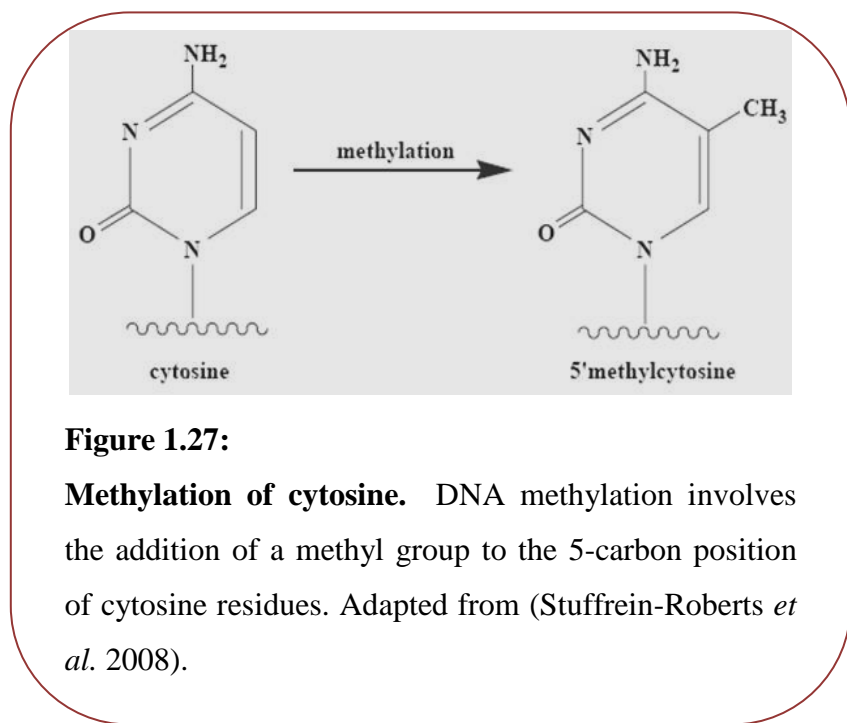
Recent studies, which were performed on human and mouse, indicate that the histone methylation of H3 lysine 9 H3K9, H3K27, H3K4 and H4K20 are implicated in heterochromatin formation and transcription inhibition. The monomethylations signals of H3K4, H3K27, H3K9, and H4K20 found to be significantly high in the enhancers and transcribed regions, and correlated positively with the transcriptional activation, while the trimethylation of H3K27me3, H3K9me3 and H3K4me3 signals are inversely correlated with active promoters. In addition, the localized distribution patterns of these histones were observed; H3K4me3 and H3K27me3 are spreading over large regions, while H3K9me3 and H4K20me3 are present near the boundaries of large heterochromatin domains (Heintzman *et al.* 2007; Santos-Reboucas and Pimentel 2007; Schones and Zhao 2008).

1.3.3.2 DNA methylation

In recent years, strong evidence has proven that DNA methylation is one of the major epigenetic modifications, which contributes to regulate many biological processes in the cell such as, chromatin structure, genomic imprinting, X chromosome inactivation, gene transcription and embryonic development. In normal cells, it is vital for the mammalian development and for normal organism functioning for the adult to have established and maintained DNA methylation patterns. Moreover, the loss of the normal DNA methylation patterns in somatic cells leads to the loss of growth control (Robertson 2005; Schones and Zhao 2008). Repetitive

genomic regions are considered as preferable areas for the methylation process to occur. Around 3% of the cytosines in human DNA are methylated (Robertson 2005; Nafee *et al.* 2008).

DNA methylation is the only epigenetic change that affects the DNA directly; it is the replacement of the hydrogen atom of the cytosine base by a methyl group (Figure 1.27), which is established by the functional DNA methyltransferases (DNMTs) enzymes (Ptak and Petronis 2008; Schones and Zhao 2008; Stuifrein-Roberts *et al.* 2008)



DNA methyltransferases enzymes are responsible for establishing and maintaining DNA methylation. In addition, its contribution to the chromatin remodelling processes by establishing the binding site of HP1 through methylating H3K9. Dnmt1 is responsible for maintaining the previous heritable methylated pattern of CpG of hemi-methylated DNA. It requires chromatin deacetylation before it can methylate DNA molecule, while the *de novo* Dnmt3a and Dnmt3b methyltransferases, which are highly expressed in embryonic cells, are responsible for starting DNA methylation during early embryonic development and establishing

the methylation pattern at previously unmethylated CpG sites (Saveliev *et al.* 2003; Robertson 2005; Santos-Reboucas and Pimentel 2007; Ptak and Petronis 2008).

The methylated CpG expanded islands, which are hundred bases in size, are located in the promoter regions of 40% of mammalian genes and have the ability to generate a heritable transcriptional silencing (Egger *et al.* 2004; Nafee *et al.* 2008).

Methyl-CpG binding proteins (MBPs) are involved in reading the methylation patterns and control the suppression process of the methylated islands, by recruiting chromatin remodelling factors, such as HDACs, as gene expression regulators. Moreover, the right dosage of methylCpG binding protein 2 (MeCP2) in the CNS is vital for neuronal function. For example, a slight over-expression of MeCP2 in neurons cause a severe symptom of motor dysfunction and seizures (Robertson 2005; Santos-Reboucas and Pimentel 2007).

The methylation of the C⁵ position of cytosine residues within dinucleotides (CpG) has a fundamental importance as an epigenetic silencing mechanism by stimulating the formation of the heterochromatin structure which affects transcription factors binding. The level of the DNA methylation is related with the level of the gene silencing. The methylation pattern of a gene can be detected by sodium bisulphite sequencing or high performance liquid chromatography methodologies (Bock and Lengauer 2008; Nafee *et al.* 2008; Ptak and Petronis 2008).

DNA methylation pattern is a balance of methylation and demethylation reactions (D'Alessio and Szyf 2006). Aberrant DNA methylation patterns in cells have been considered as a major element contributing to a wide range of human complex disorders such as, trinucleotide repeat (TNRs) diseases. Many studies of repeat instability disorders demonstrate that only some of the TNRs have a higher susceptibility to be targeted for methylation process then the silencing mechanism. However, other studies showed that TNRs are targeted for silencing mechanism regardless what their sequence is. For example, in FRDA the expanded (GAA)n·(TTC)n repeats adapt a heterochromatin structure. Therefore, TNRs might be targeted for silencing at the chromatin level and then other factors may or may not stimulate the DNA methylation process (Robertson 2005; Ptak and Petronis 2008).

Interestingly, a recent study demonstrates that DNA methylation patterns can be mediated by the CCCTC-binding factor (CTCF) in addition to its primarily role, which is read the DNA methylation marks and ensures the allele specific gene expression. CTCF is an 11-zinc factor protein that is ubiquitously expressed and it acts as a regulator of imprinted gene expression. This protein can protect certain regions from DNA methylation and has a boundary element function by blocking the spread of heterochromatin (Robertson 2005). Furthermore, DNA methylation patterns can also be mediated by H3K27 methyltransferase enzyme by the direct physical interaction with the DNA methyltransferase in human cell line (Schones and Zhao 2008).

1.3.3.3 RNA-associated silencing

Many studies showed that RNA is involved closely in regulating the gene expression process in FRDA and other human complex disorders; thus, many recent research areas are considering expanding the knowledge and the understanding of this mechanism is important.

RNA, which can lead to the heritable transcriptional silencing due to the formation of heterochromatin, is present in three forms: non-coding RNAs, antisense transcript RNAs and RNA interference (RNAi), (Hebert and Whittom 2007).

The non-coding RNAs, regulate the binding of the HP1 protein to the chromatin and it involve in initiating X inactivation by DNA methylation and chromatin condensation. Furthermore, the involvement of the antisense transcript RNAs in different silencing mechanisms has been observed. A previous study showed that the antisense transcript has effect on the DNA methylation and silencing the intact HBA2 α -globin gene in a α -thalassaemia case (Egger *et al.* 2004; Santos-Reboucas and Pimentel 2007; Schones and Zhao 2008).

Whereas, RNAi is a highly conserved silencing machinery that regulates gene expression by the homology dependent degradation of the target mRNAs by using small double-stranded RNA (dsRNA) molecules as triggers, as a result the inhibition

of mRNA transcription (Robertson 2005; Kim and Rossi 2008). In trinucleotide repeat diseases with the repeat instability, the large repeats are targeted for methylation and the formation of hairpin RNA, which might be cleaved to a short hairpin RNA (shRNA) and recruit the RNAi silencing mechanism. To date there are few clinical trials using RNAi as a treatment strategy for wide range of diseases, including neurodegenerative diseases (Santos-Reboucas and Pimentel 2007; Kim and Rossi 2008).

1.3.3.4 Non-histone proteins

Non-histone proteins have an influence on the chromatin remodelling. ATP-dependent chromatin remodelling complexes can directly move or displace nucleosomes along the DNA, allowing the access of the transcription factors to bind within the chromatin and activating the transcription (Bird 2007; Bock and Lengauer 2008).

Furthermore, Heterochromatin protein (HP1), Polycomb group (PcG) and Trithorax complexes (TrxG) are chromatin modifier proteins, which are part of a cellular memory system responsible for controlling chromatin accessibility and maintaining transcription in the first stages of embryonic life and throughout development. PcG function as a stable repressor, while TrxG promote maintenance of gene activity. They can bind to the DNA or to specifically modified histone tails and catalyze other histone modification or DNA methylation, as a result causing a gene silencing. For instance, polycomb protein catalyzes repressive histone methylation and recruit DNA methylation while it is interacting with DNA methyltransferases (Santos-Reboucas and Pimentel 2007; Bock and Lengauer 2008; Laskowski and Thornton 2008).

In summary, histone modifications as a cellular mechanism are getting a significant attention in the genetic field, thus there are many ongoing studies using the advanced technologies to accumulate the knowledge about this area of research. In addition, according to the significant importance of the DNA methylation

mechanism more knowledge is still needed to fully describe its role in the disease aetiology. Finally, additional studies are needed to fully understand the fundamental role of RNA molecule and the non-histone protein in silencing *FXN* expression in FRDA and other diseases. All will lead to a new and wide applicable treatment approach in the future.

1.3.4 The relationship between the different mechanisms of epigenetic regulations

DNA methylation, histone modificationas, RNAs and DNA binding proteins are not independent elements. They function together to organize chromatin structure and they influence each other during dynamic regulations of cellular differentiation or pathological conditions (Figure 1.28) (Schones and Zhao 2008).

An epigenetic study suggested that RNA could be the trigger for DNA and histone methylation modifications, resulting in stable and a heritable silencing. However, the exact sequence of DNA methylation, histone modifications and RNA in the concept of which initiates the recruitment of different epigenetic modifiers is currently unknown (Figure 1.29) (Egger *et al.* 2004).

The correlation between DNA methylation and chromatin remodelling had been established long time ago. A hypermethylated DNA profile is correlated with hypoacetylated, inactive chromatin. Whereas, a hypomethylated DNA profile is correlated with active acetylated chromatin. In addition, DNA methylation is related to the gene transcription directly or indirectly through chromatin remodelling. As a conclusion a recent study suggests that the relation between these two epigenetic mechanisms is a bidirectional relationship (D'Alessio and Szyf 2006).

In conclusion, having a comprehensive knowledge about the connection between different epigenetic mechanisms is vital to establish a valid research toward a more specific treatment for epigenetic complex diseases such as, trinucleotide repeat disorders.

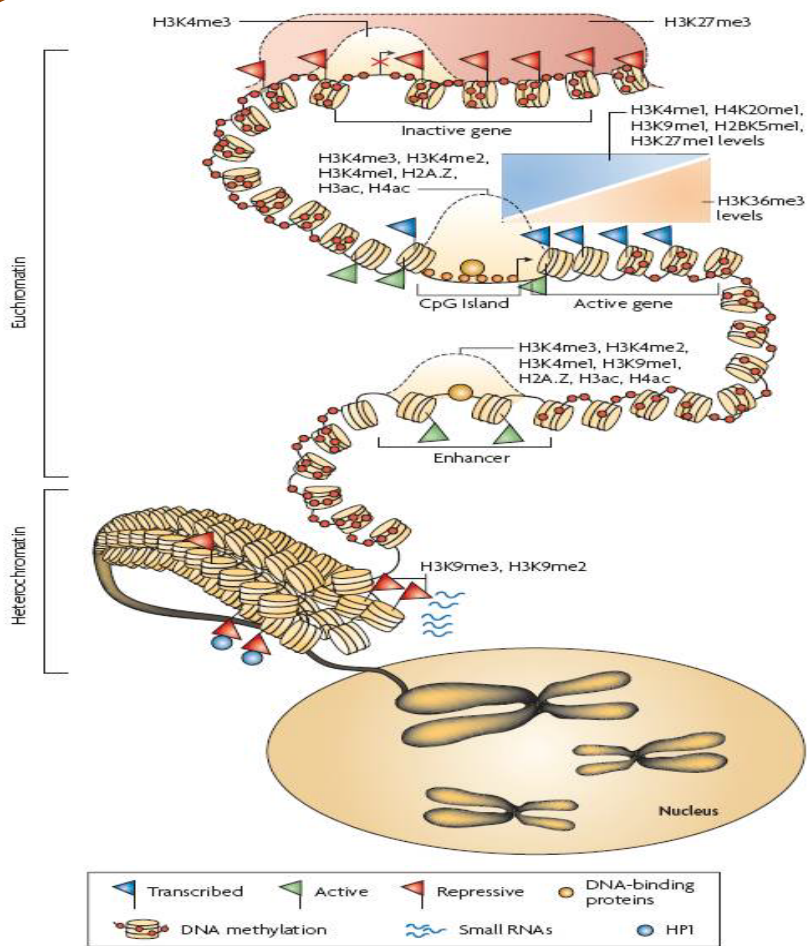


Figure 1.28:
The interaction of DNA methylation, histone modification and other factors such as small RNAs contribute to an overall regulation of the gene expression and allows cells to remember their identity.
Heterochromatic regions are marked with H3K9me2 and H3K9me3, which serve as a platform for HP1 binding. Small RNAs have been implicated in the maintenance of heterochromatin. DNA methylation is persistent throughout genomes, and is missing only in regions such as CpG islands, promoters and possibly enhancers. The H3K27me3 modification is present in broad domains that encompass inactive genes. Histone modifications including H3K4me3, H3K4me2, H3K4me1 as well as histone acetylation and histone variant H2A.Z mark the transcription start site regions of active genes. The monomethylations of H3K4, H3K9, H3K27, H4K20 and H2BK5 mark actively transcribed regions, peaking near the 5' end of genes. The trimethylation of H3K36 also marks actively transcribed regions, but peaks near the 3' end of genes. Modified from (Schones and Zhao 2008).

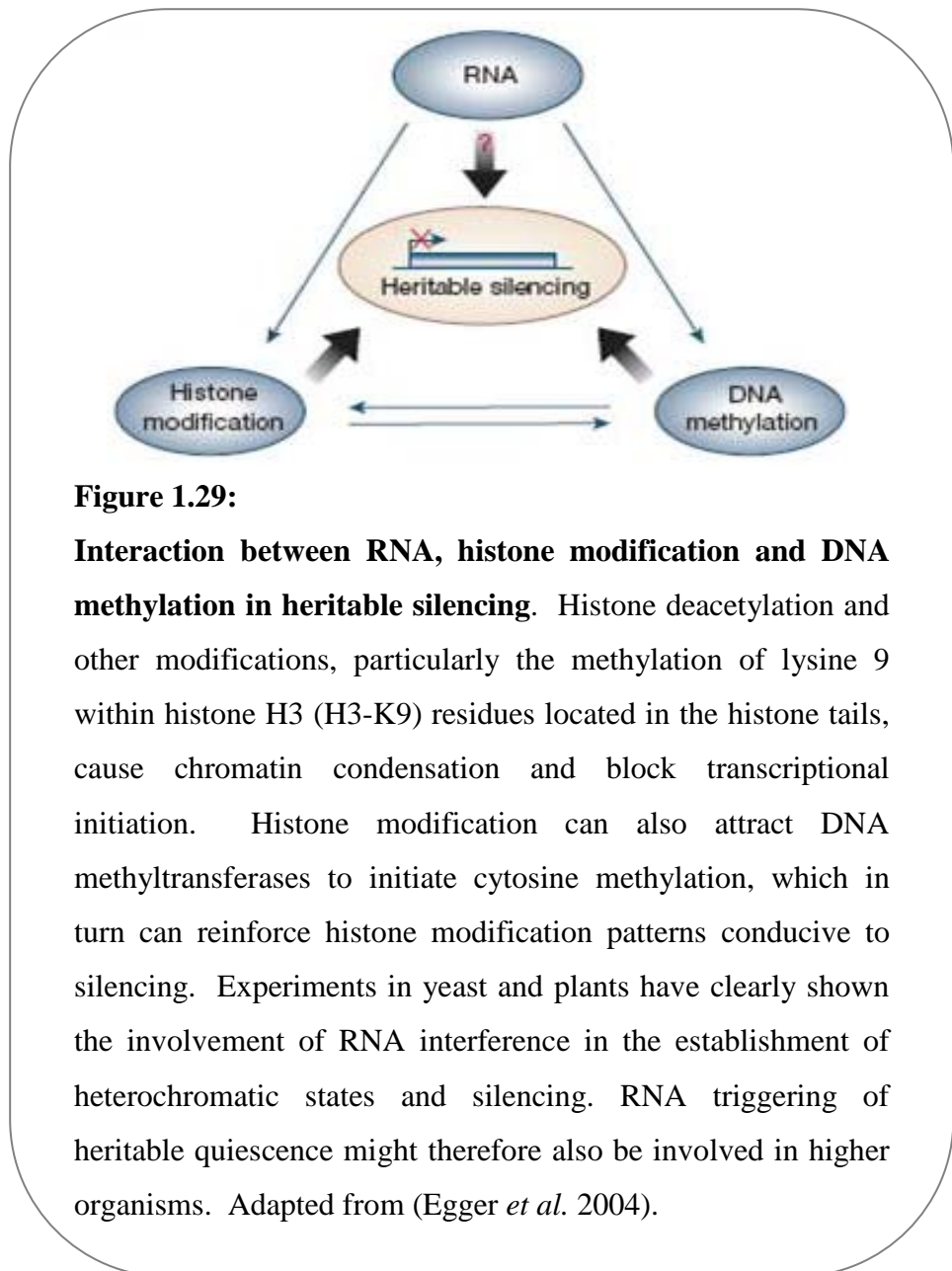


Figure 1.29:

Interaction between RNA, histone modification and DNA methylation in heritable silencing. Histone deacetylation and other modifications, particularly the methylation of lysine 9 within histone H3 (H3-K9) residues located in the histone tails, cause chromatin condensation and block transcriptional initiation. Histone modification can also attract DNA methyltransferases to initiate cytosine methylation, which in turn can reinforce histone modification patterns conducive to silencing. Experiments in yeast and plants have clearly shown the involvement of RNA interference in the establishment of heterochromatic states and silencing. RNA triggering of heritable quiescence might therefore also be involved in higher organisms. Adapted from (Egger *et al.* 2004).

1.3.5 Molecular epigenetic mechanisms in Friedreich ataxia (FRDA)

FRDA is one of the most thoroughly studied hereditary neurological disorders and it now has well-defined genetic and biochemical pathways. As a result, this disorder is a full resource model to study the epigenetic mechanisms that are involved in the progression of the disease in more depth (Wells 2008).

DNA methylation and histone modification are the main mechanisms, which have been studied and related to FRDA. Therefore, only these two mechanisms will be discussed in this section.

1.3.5.1 DNA methylation and its contribution to *FXN* gene transcription

Considering that DNA methylation is an important epigenetic mechanism, an epigenetic study showed that the DNA methylation pattern of specific CpG sites upstream of the GAA repeat in intron 1 was more extensive by 50% in FRDA patient lymphoblastoid cell lines than it was in the control cell lines. Three CpG residues (termed 3, 6, and 13) were always methylated in FRDA cells by 75 to 100% of alleles; whereas, they were methylation free in the control cells. One of these residues (residue 13) was located within the E-box in intron 1, which might be the binding site for certain transcription factors that contribute to gene's promoter activity. Consequently the methylation of these residues in intron 1 might affect transcription factors binding and lead to a reduction in frataxin expression (Gottesfeld 2007; Greene *et al.* 2007; Hebert and Whittom 2007; Al-Mahdawi *et al.* 2008; Wells 2008). This study also suggested that the increased methylation of residue 13 may be a secondary effect of a compact chromatin structure that blocks binding factors (Figure 1.30) (Greene *et al.* 2007).

Another recent experiment using bisulfite sequence analysis had investigated the DNA methylation pattern in three occurrences in *FXN* gene: *FXN* promoter, upstream GAA and downstream GAA. Results have demonstrated an altered DNA methylation pattern in FRDA brain and heart tissues, moving from hypomethylation

in the downstream GAA toward hypermethylation in the upstream GAA region (Al-Mahdawi *et al.* 2008).

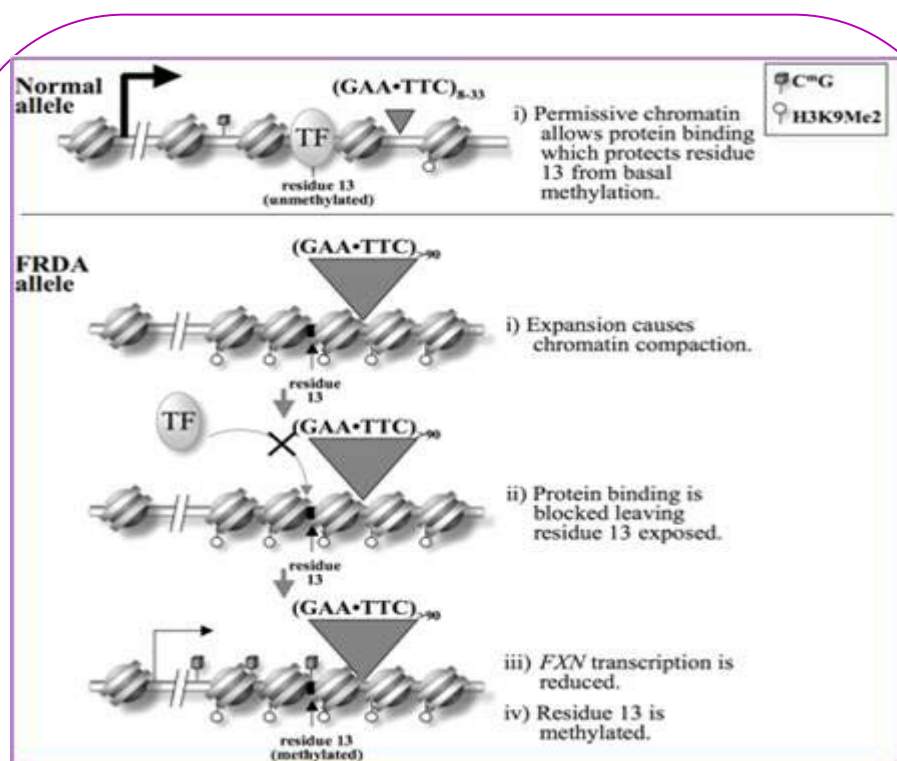


Figure1.30:
Model for chromatin organization in the region containing residue 13 in normal and FRDA alleles. Adapted from (Greene *et al.* 2007).

Up to date many substantial studies are continuing in order to have a better understanding about DNA methylation mechanism and its contribution to FRDA disorder.

1.3.5.2 Chromatin remodelling (histone modifications) and its contribution to *FXN* gene transcription

Heterochromatin-mediated silencing mechanisms regulate the level of gene silencing; hence the clinical severity in the triplet repeat diseases (Saveliev *et al.* 2003). The expanded (GAA)_n(TTC) repeats correlates with heterochromatin formation at the promoter regions of the gene; thus mediating gene silencing. In addition, heterochromatin structure has been observed in the surrounding regions of the expanded repeats in cells from FRDA patients (Saveliev *et al.* 2003; Wells 2008).

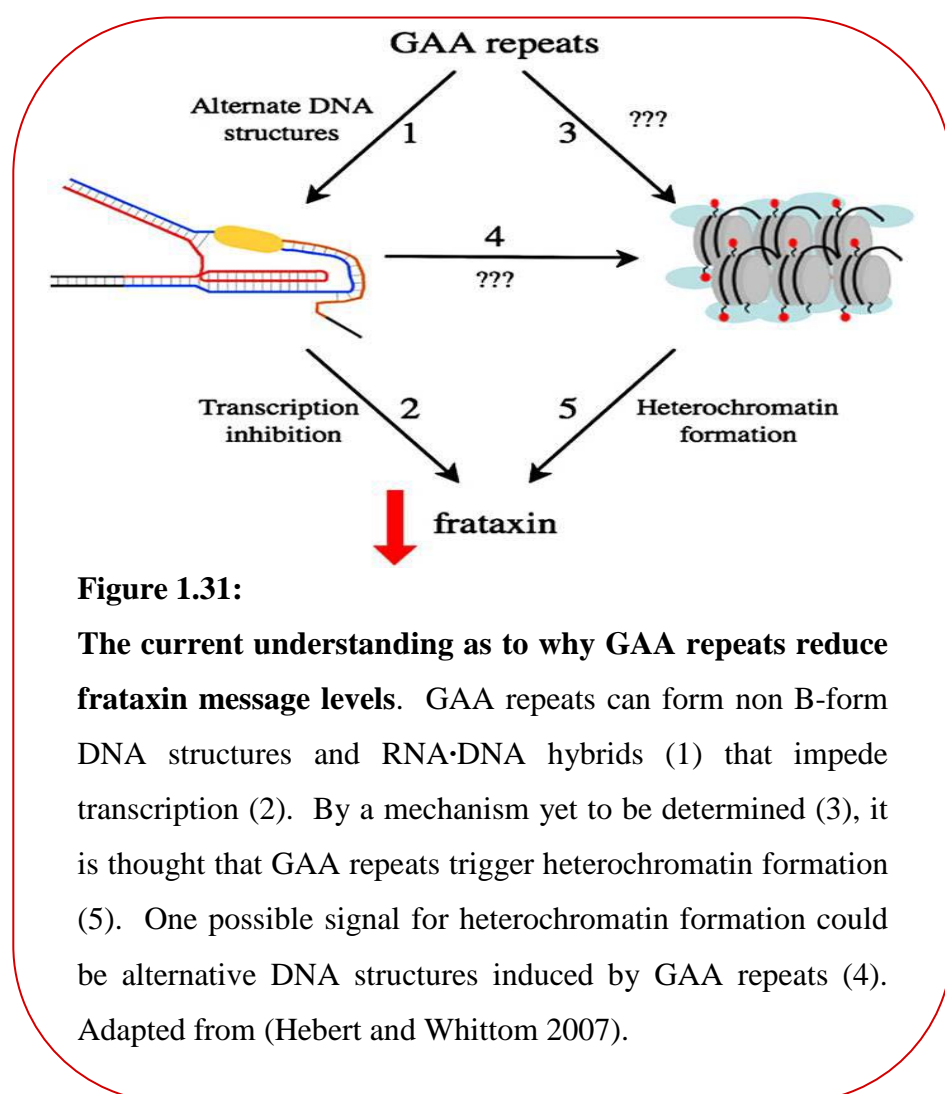
A well structured experiment, which was conducted by Festenstein and colleagues, revealed that (GAA)_n(TTC) repeats induced positive effect varigation (PEV) in euchromatic and heterochromatic regions, resulting in gene silencing by stimulating the overexpression of HP1 to methylate H3K9 (Saveliev *et al.* 2003; Hebert and Whittom 2007).

Another previous study showed a high level of H3K9me2 in FRDA cells with more repressive chromatin structure and low level of *FXN* mRNA level (10 to 30 %). A significant hypoacetylation of H3K9, H3K14, H4K5, H4K8, H4K12 and H4K16 in FRDA cells upstream and downstream of the (GAA)_n(TTC) repeats were observed. No significant changes in histone acetylation of the promoter region were found between FRDA and control cells (Gottesfeld 2007; Hebert and Whittom 2007; Wells 2008).

The transcriptional inhibition seen on *FXN* is consistent with a high level of trimethylation of H3K9 and low level of methylation of H3K4 at the surrounding regions of the expanded (GAA)_n(TTC) repeats (Herman *et al.* 2006).

It has also been experimentally approved that the presence of the hypoacetylated histones at the expanded (GAA)_n(TTC) repeats can facilitate the accessibility to the chromatin remodelling protein molecules that leads to the heterochromatin formation and stimulates the GAA-GAA-TTC triplex formation (Wells 2008).

In summary, understanding the mechanisms of how the expanded (GAA) n ·(TTC) repeats inhibit *FXN* gene expression either through forming unusual DNA or heterochromatin structures still to be investigated in more specific aspects (Figure 1.31). This will support the researchers in the genetic field with a vital knowledge to further proceed with the therapeutic field research toward the right direction to help FRDA patients to have a better-adjusted life.



1.4 Therapeutic approaches

Friedreich ataxia is considered as a single gene disorder and that makes it a good candidate for experimental therapeutic research (Wells 2008). Any therapy that can result in increased frataxin expression would be considered as useful.

1.4.1 Antioxidant and iron chelation-based approaches

Antioxidant drugs were developed to reduce the load of free radicals, protect the mitochondria from oxidative damage and slow the progress of the disease (Delatycki *et al.* 2000). This type of drugs may benefit FRDA patients by treating later symptoms rather than directly increase frataxin expression (Gottesfeld 2007). Iron chelator, chelating iron from extracellular fluid and cytosol but not from the mitochondria (Pandolfo 2008).

1.4.2 Gene based approach

1.4.2.1 DNA interacting binding compounds

Small molecules designed to recognize a predetermined DNA sequence such as, polyamides. They have the specific ability to permeate cells and localize in the nucleus and downregulate target genes in the cell. Such molecules may inhibit the protein-DNA interaction such as, HP1 thereby resulting in having an open chromatin structure. They could also target the expanded (GAA)n(TTC) n tract directly and disrupt or reverse the sticky DNA formation and increase the *FXN* transcription in FRDA cells. Polyamides do not bind to single strand or duplex regions of RNA so no effect on RNA processing or translation of frataxin mRNA (Gottesfeld 2007; Hebert and Whittom 2007; Wells 2008).

1.4.2.2 Epigenetic drugs

Histone deacetylase inhibitors (HDACi) have a positive and a negative effect on gene transcription on epigenetic level. Various HDACis target various HDAC enzymes and regulate the level of acetylation of histone and non-histone chromosomal protein (Herman *et al.* 2006). It has been suggested that HDACi has effect on pre-mRNA splicing rather than effect the transcription (Baralle *et al.* 2008).

Many studies showed the effect of HDACi on *FXN* activity as treatment and its ability to reverse heterochromatin structure to an active form and restore the normal function of the gene (Gottesfeld 2007). Herman and colleagues used different classes of HDACi and showed a significant increase in frataxin level and partial reverse of the silencing with an increase in the acetylation of H3K14, H4K5, H4K12 in the FRDA lymphocytes (Herman *et al.* 2006; Hebert and Whittom 2007).

Another recent study indicates an increase in the acetylation of H3K14, H4K5, H4K8 and H4K16 of the homozygous knock-out (KIKI) mice brain, cerebellum and heart tissues; thus restoring the normal level of frataxin expression after HDACi treatment for three consecutive days (Rai *et al.* 2008).

DNA demethylating agents, there are many DNA methylation inhibitors one of these agents is 5-aza-2'-deoxycytidine which is a powerful inhibitor of DNA methylation, it induces gene expression and differentiation in cultural cells in S-phase only (Egger *et al.* 2004). It targets replicating DNA in place of cytosine and traps DNA methyltransferases (Santos-Reboucas and Pimentel 2007). This compound had been used for fragile-X disorder and it showed an increase in the frataxin protein in fragile-X lymphoblasts in low doses because it has a cytotoxic effect (Chiurazzi *et al.* 1998; Hebert 2008). For therapy that is more effective the combination between HDACi and DNA demethylating agents were used. This suggestion was used as treatment for fragile-X lymphoblast. The experiment demonstrated that the level of transcription was increased and it has been suggested to be used for FRDA (Chiurazzi *et al.* 1999; Hebert 2008).

1.4.3 Molecules that increase frataxin mRNA or protein

There are several molecules have been reported to increase the frataxin expression such as, sodium butyrate, hemin, cisplatin and recombinant human erythropoietin (rhuEPO). rhuEPO shows an increase in the frataxin expression in FRDA cells by increasing the translation, without any effect on mRNA expression (Sturm *et al.* 2005; Babady *et al.* 2007). The molecular basic of this observation still not clear but there are clinical trials currently in progress (Gottesfeld 2007).

1.4.4 Gene therapy approach

Viral gene based approach, is a valid theoretic approach but it has its own technological limitations to apply it clinically. Adeno-associated viral and vector expressing frataxin cDNA shown a decrease in the sensitivity to the oxidative stress in FRDA primary fibroblast. Another promising approach for nervous system gene therapy (TOOL) was reported, herpes simplex virus type 1 (HSV-1) amplicon vector can express either the entire *FXN* genomic locus or frataxin cDNA and it can successfully restore the normal phenotype (Gomez-Sebastian *et al.* 2007; Lim *et al.* 2007; Hebert 2008).

1.5 *In vitro* and *in vivo* models

To facilitate having a comprehensive understanding of the frataxin deficiency and its contribution to FRDA disease pathology and progression there is a need for *in vitro* (cell lines) and *in vivo* (mouse) models as tools for several talented groups have given the intention to evolve these models as reliable resources for FRDA researchers.

1.5.1 *In vitro* models

Recently, the Hebert group investigated a stable HeLa cell lines. These cell lines hold part of the first inton of *FXN*, which contains (GAA·TTC)₁₅ or (GAA·TTC)₁₄₈ repeats, fused to the coding sequence for the enhanced green fluorescent protein (EGFP) gene. Results demonstrated reduced levels of GFP expression in the (GAA·TTC)₁₄₈ cell line compared with the (GAA·TTC)₁₅ cell line (Grant *et al.* 2006). In addition, a collection of established lymphoblast and fibroblast cell lines obtained from FRDA patients, their parents and siblings with different repeat numbers is available. These cell lines are considered a useful resources to study *FXN* gene in its native chromosomal context (Gottesfeld 2007).

1.5.2 *In vivo* models

In order to study the FRDA disorder at all levels, mouse models are considered the most appropriate approach for the *in vivo* experiments. The homologous mouse gene (*Frda*) has 73% similarity to the human frataxin and it shows a very high identity in exons 3 to 5 and less conservation in first two exons (Cossee *et al.* 2000).

In 2000, Cossee and colleagues generated the first mouse model, the ‘*Fxn* knockout mouse’, by homologous recombination to delete exon 4 (98bp), leading to a framshift of the exon 5 coding sequence and resulting in severe truncation in

frataxin. The homozygous mouse (-/-) for the deleted $\text{Frda}^{\text{del4}}$ alleles showed an early embryonic lethality as early as E6.5 and morphological abnormalities, which indicates that frataxin is a vital protein for embryonic development. However, the heterozygous mouse (+/-) for the deleted $\text{Frda}^{\text{del4}}$ was morphologically normal, viable and has a normal life span (Cossee *et al.* 2000).

To solve the embryonic lethality of the homozygous Frda knockout mouse Pook and colleagues have generated a human transgenic mouse, which contains the whole *FRDA* locus in a 370 kb human yeast artificial chromosome (YAC), to rescue the knockout mouse. Results indicated that human frataxin showed an expression at a comparable level to the endogenous mouse gene, a successful functional replacement for it, a right posttranslational modification, and the right localization in the mitochondria. In addition, the *FXN* human transgenic mouse (Y47) contains (GAA·TTC)₉ repeats and two copies of the gene, thus manifests a normal phenotype. Furthermore, to generate the transgenic rescued mice ($\text{Y47}^+/\text{Frda}^{-/-}$), a two step strategy was used. The strategy is well explained in Figure 1.32 (Figure 1.32) (Pook *et al.* 2001).

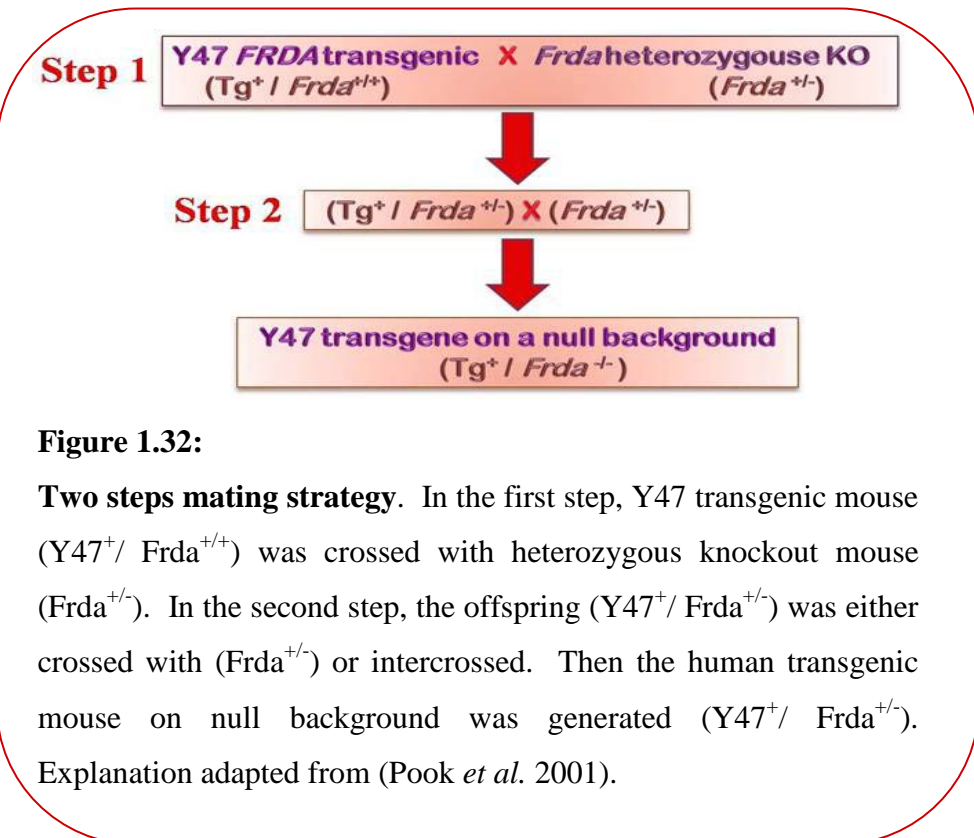


Figure 1.32:

Two steps mating strategy. In the first step, Y47 transgenic mouse ($\text{Y47}^+/\text{Frda}^{+/-}$) was crossed with heterozygous knockout mouse ($\text{Frda}^{+/-}$). In the second step, the offspring ($\text{Y47}^+/\text{Frda}^{+/-}$) was either crossed with ($\text{Frda}^{+/-}$) or intercrossed. Then the human transgenic mouse on null background was generated ($\text{Y47}^+/\text{Frda}^{-/-}$). Explanation adapted from (Pook *et al.* 2001).

A valid step ahead after generating the human wild-type *FXN* transgenic rescued mouse was to generate a mouse model with an expanded (GAA)n·(TTC)n repeat into the YAC clones. In 2004, Pook and his group generated 2 lines of the human *FXN* transgenic mice models, YG8 and YG22, containing (GAA·TTC)₁₉₀₊₉₀ and (GAA·TTC)₁₉₀ repeat expansions. Then these mice were cross bred with the heterozygous knockout mouse (*Frda*^{+/−}) and the offspring showed a reduced level of frataxin mRNA and protein expression. In addition, these mice manifest the neurodegenerative and cardiac pathological phenotype. In this model, it had been proven that YG22 have a single copy of the FRDA gene, while YG8 have two copies of the gene. This model has showed a (GAA)n·(TTC)n repeat age related somatic instability and repeat instability in the cerebellum. Therefore, this model is considered an excellent model to further investigate epigenetic modifications and potential therapeutic approaches (Al-Mahdawi *et al.* 2004; Al-Mahdawi *et al.* 2006; Babady *et al.* 2007). Within this thesis, *FXN* expression levels, histone modification and epigenetic changes were investigated within the brain, heart and liver tissues from this mouse model.

Other mouse models were generated by different research groups, For instance, Miranda and colleges generated the knock-in mouse in order to have a mouse model with a reduced frataxin level. This mouse model was generated by the insertion of (GAA·TTC)₂₃₀ repeats within the mouse frataxin gene. The homozygous knock-in mouse (KIKI) is showing a reduced level of frataxin by 64-75% only from the normal level and it is not associated with any obvious pathological phenotype. Then these mice were crossed with the frataxin knockout mice to produce a knock-in/knockout model (KIKO) with more reduced level of frataxin expression, by 25% decrease (Miranda *et al.* 2002; Baralle *et al.* 2008).

Furthermore, another mouse model, which was developed by Sarsero and colleagues using a 180kb modified bacterial artificial chromosome (BAC), containing an in frame fusion of the human *FXN* gene and EGFP reporter system. Although, these mice show a low level of frataxin, they do not develop any phenotype. This model does not contain (GAA·TTC)n repeats (Sarsero *et al.* 2005; Babady *et al.* 2007; Gottesfeld 2007).

Up to date, there is no mouse model that effectively parallels the progressive human neurological disease; therefore research is ongoing to develop further FRDA mouse models. Using a different approach, a new conditional knockout mouse model was generated by the complete deletion for the mouse frataxin in specific tissues such as, heart, skeletal muscle and neurons. This model demonstrates the accumulation of damaged mitochondria, degenerative mechanism in the DRG and the involvement of the frataxin in iron metabolism in the mitochondria. This model is a very useful tool to study the mechanism of late-onset and slowly progressive neurodegeneration of the disease (Simon *et al.* 2004; Coppola *et al.* 2006; Babady *et al.* 2007). The availability of these mice models is a great help and support toward a deep understanding of the FRDA disorder at all levels.

1.6 Aim of the study

Friedreich ataxia (FRDA) is an autosomal recessive neurodegenerative disorder. It is most often caused by homozygous expanded (GA)_nC repeats within intron 1 of the *FXN* gene, as a consequence severely reduced level of frataxin protein. Many studies have suggested that the expanded repeat may have the ability to induce epigenetic modifications that cause the *FXN* transcription inhibition to occur.

In the past few years, epigenetic modifications have given a considerable attention as an important mechanism that is contributing to the aetiology of FRDA disorder. Therefore, the aim of this project is to investigate the effect of the epigenetic changes such as, histone modifications including histone acetylation and methylation of H3 and H4 in three different regions: the *FXN* promoter, upstream GAA and downstream GAA within the *FXN* gene on the *FXN* mRNA transcription level. In addition, investigate the effect of HDACi, which is an epigenetic promising treatment, on the *FXN* mRNA transcription level and histone acetylation in YG8 and YG22 transgenic mice brain, heart and liver tissues.

Chapter 2

Material and Methods

2.1 Genotyping of mice

2.1.1 DNA extraction

Genomic DNA was extracted from mouse-tails as described by Wang and Storm, 2006 (Wang and Storm 2006). Tails 5 mm in length were collected in 1.5 ml tubes (Eppendorf). Each tail sample was digested in 400 µl of digestion buffer (100 mM Tris-HCl pH= 8.0 [Tris-hydroxymethylaminomethane], 5 mM EDTA [ethylene diamine tria acetic acid], 200 mM NaCl [sodium chlride], and 0.2% SDS [sodium dodecyl sulfate], [Sigma,UK]) + 10 µl of 50 mg/ml proteinase K (BDH), then incubated in a 55 °C waterbath overnight. The incubated sample was then vortexed (Whirlimixer) for 15 seconds (s) and centrifuged (Eppendorf Micro Centrifuge Model 5415 R) at 13,000 rpm (16110 g) for 5 minutes (min) at room temperature (RT). The supernatant was collected into a clean, labelled tube; 1 ml of absolute ethanol (Hayman,UK) was added, mixed and placed at -80 °C for 10-15 min. The tube was centrifuged at 13,000 rpm for 30 min at 4 °C and the supernatant was discarded. The pellet was washed with 1 ml of 70% (v/v) ethanol and centrifuged at 13,000 rpm for 20 min at 4 °C; the ethanol was discarded. The pellet was left to air-dry for 10-15 min and then suspended in 50-100 µl T.E. (10 mM Tris, 1mM EDTA, pH= 8.0) buffer and stored at 4 °C.

2.1.2 (GAA) PCR

A polymerase chain reaction (PCR) was performed on mouse genomic DNA samples to detect the genotype (Campuzano *et al.* 1996). The following primers were used:

GAA-F: 5'-GGGATTGGTTGCCAGTGCTTAAAAGTTAG-3' (Sigma GENOSYS)

GAA-R: 5'-GATCTAAGGACCATCATGGCCACACTTGCC-3' (Sigma GENOSYS)

For each sample, the following reaction was set up in a 0.2 ml tube:

Reagents	Concentration	Quantity in μ l
Kapa Master mix (KapaBiosystem,UK)	2X	12.5
GAA-F primer	50 mM	0.25
GAA-R primer	50mM	0.25
dH₂O	-	11
Sub-total	-	24
DNA	-	1
Total	-	25

Controls were included every time the PCR was performed and are described below:

1- Positive control 2- Negative control 3- Blank (water) control

The amplification conditions were as follows:

Steps	Temperature	Duration	Cycles
Denaturation	94 °C	2 mins	1
Denaturation	94 °C	10 s	
Annealing	60 °C	30 s	10
Elongation	68 °C	45 s	
Denaturation	94 °C	10 s	20
Annealing	60 °C	30 s	
Elongation	68 °C	1 min ← With 20 s increments	
Extension	68 °C	10 mins	1

Amplification was performed using a PTC-225 Peltier Thermal Cycler (MJ Research). After amplification, 5-10 µl of PCR product was loaded on a 1 % (w/v) agarose mini-gel (1 g agarose [Invitrogen, UK] in 100ml 1X TBE [89 mM tris-borate, 2 mM EDTA] buffer) (Sigma, UK), stained with 1.3µl of 10mg/ml ethidium bromide (EtBr) with 5 µl of 1 kb plus DNA ladder [Invitrogen, UK] at 80 volts for 30-45 min in a Flowgen mini-gel electrophoresis tank. The photograph of the gel was taken and evaluated using an Alphaimage 2200, INNOTECH system.

2.1.3 (FXN) knockout PCR

This PCR was performed (Cossee *et al.* 2000) to identify the wild-type or knockout *Fxn* alleles. The following primers were used:

WJ5: 5'-CTGTTACCATGGCTGAGATCTC-3'

WN39: 5'-CCAAGGATATAACAGACACCATT-3'

WC76: 5'-CGCCTCCCCTACCCGGTAGAATTC-3'

For each sample, the following reaction was set up:

Reagents	Concentration	Quantity in µl
Kapa Master mix	2X	12.5
<u>WJ5</u> primer	50 mM	0.5
<u>WN39</u> primer	50mM	0.5
<u>WC76</u> primer	50mM	0.1
dH₂O	-	10.4
Sub-total	-	24
DNA	-	1
Total	-	25

Controls were included every time this PCR was performed. They are as follows:

1- Wild-type control

2- Heterozygous control

3- Rescue control

4- Blank (water) control

The amplification conditions were as follows:

Steps	Temperature	Duration	Cycles
Denaturation	94 °C	20 s	
Annealing	54 °C	20 s	30
Elongation	72 °C	20 s	
Extension	72 °C	6 mins	1

After amplification, 10µl of PCR product was loaded on a 2% (w/v) agarose mini-gel (2g agarose in 100ml 1X TBE buffer) stained with 1.3 µl of 10 mg/ml (EtBr) along with 5µl of the 1kb plus DNA ladder at 80 volts for 30-45 minutes in a Flowgen mini-gel electrophoresis tank. The photograph of the gel was taken and evaluated using AlphaImager2200, INNOTECH system.

2.2 RNA extraction using TRIZOL® Reagent

RNA was isolated from brain, heart and liver mouse tissues that were between 50 -100 mg in weight (Chomczynski and Sacchi 1987). The various tissues were collected and weighed in 1.5 ml RNase-free eppendorf tubes. All steps were performed on dry ice until the TRIZOL® Reagent (Invitrogen) was added. Dr.Al-Mahdawi (Brunel University, UK) had previously prepared the RNA and cDNA samples from the first group of mouse tissues (Heart, Brain, and Liver) and the human (heart and brain) tissues.

2.2.1 Tissue homogenisation

A) For brain and liver tissue

A small piece of tissue was cut and weighed in a 1.5 ml tube. 250 µl of TRIZOL was added to the tissue and homogenised with an RNase-free plastic

pastille. In this step, the solution was homogenised until no big pieces remained. A further 250 µl of TRIZOL was added and the tissue was again homogenised with the pastille. Finally, 500 µl of TRIZOL was added and again the solution was homogenised.

B) For heart tissue

Frozen tissue was ground into a powder consistency with a pestle and mortar, TRIZOL was added, or TRIZOL was added to the tissue in a bijou tube and homogenised with an electric homogeniser.

2.2.2 Phase separation

The homogenised tissue sample was incubated in a 30 °C water bath for 5 min. After incubation, it was mixed gently and firmly by inversion 4-5 times. 200 µl of chloroform (CHCl_3) (Sigma,UK) was added, the tube was mixed vigorously by hand for 15 s. The tube was incubated in a 30 °C water bath for 15 min. The sample was centrifuged at 13,000 rpm for 15 min at 4 °C. 5 µl of the upper aqueous phase was transferred to a fresh-labelled tube to run in a 1% agarose mini-gel along with 1 kb plus DNA ladder at 80 volts for 25-30 min. The photograph of the gel was taken and evaluated.

2.2.3 RNA precipitation and wash

The aqueous phase (upper layer, with approximately 60 % of TRIZOL volume added) was transferred to a fresh-labelled 1.5 ml tube. It should be noted that it is very important not to disturb the bottom phase. RNA was precipitated by adding and mixing 500 µl of isopropyl alcohol to the aqueous phase, followed by incubation at 30 °C in a water bath for 10 min. The sample was then centrifuged at 13,000 rpm for 10 min at 4 °C, where a small white pellet can be observed after stage. The isopropyl alcohol was discarded and 1 ml of 75% (v/v) ethanol was added

to wash the RNA pellet. The sample was vortexed and centrifuged at 13,000 rpm for 5 min at 4 °C, and the supernatant was discarded. The pellet was left to air-dry for 10-15 min and then suspended in 50-100 µl of pre-heated elution buffer to 60°C. Finally, the sample was incubated in a 60 °C hot block for 10 min. 5µl of RNA sample was used to check the quality of the extracted RNA. After incubation, the RNA sample can be used immediately for cDNA synthesis or stored at -80 °C for future use. The tube containing the bottom phase was stored at - 20° C for DNA extraction in the future.

2.2.4 RNA quality check

The quality of each RNA sample was checked by running 5 µl on a 1 % agarose mini-gel along with 1 kb plus DNA ladder at 80 volts for 25-30 min. The photograph of the gel was taken and evaluated.

In addition, the optical density (OD) of each RNA sample was measured at a wavelength of 260 nm. The concentration of each sample was calculated, together with the ratio of absorbance at 260nm/280nm.

2.3 cDNA synthesis

RNA was synthesised into cDNA using the Cloned AMV First-Strand cDNA Synthesis Kit, (Invitrogen).

2.3.1 cDNA synthesis

The first mix was prepared for each sample in a 1.5 ml tube on ice as follows:

Reagents	Concentration	Quantity in µl
Oligo (dT ₂₀) primers	50 pmoles	1
dNTPs	10 mM	2
DEPC-treated water	-	7.5
RNA	-	1.5
Total	-	12

The sample was incubated in a 65 °C water bath for 5 min, and placed directly on ice. The second mix was prepared on ice for each sample in order to be added to the previous mix in a 1.5ml tube on ice as follows:

Reagents	Concentration	Quantity in μ l
cDNA synthesis buffer	5X	4
DTT	0.1 M	1
RNaseOUT	40 U/ μ l	1
DEPC-treated water	-	1
Cloned AMV RT	15 units/ μ l	1
Total		8
Master mix 1		+12
Final Volume		20

8 μ l of the second mix was added to each tube placed on ice and the sample was incubated in a 50 °C water bath for 60 min. The reaction was stopped by transferring the tube to a 85 °C hot block for 5 min. The sample was then used immediately for PCR or stored at -20 °C for future use.

2.3.2 cDNA quality check

Further PCR amplification was carried out in order to check the quality of the newly-synthesised cDNA sample, using different sets of primers depending on the expression profile to be tested and the sample type used. The following sets of primers were used:

FxnRT-m-F 5'-CAGAGGAAACGCTGGACTCT-3'
FxnRT-m-R 5'-AGCCAGATTGCTTGTGTC-3' } *Human*
Gapdh-m-F 5'-ACCCAGAAGACTGTGGATGG-3'
Gapdh-m-R 5'-GGATGCAGGGATGATGTTCT -3' } *Mouse*

Gapdh-h-F 5'- GAAGGTGAAGGTCGGAGT -3'
 Gapdh-h-R 5'- GAAGATGGTGATGGGATTTC-3' } *Human*
 FRTIb-F 5'- TTGAAGACCTYGCAGACAAG -3'
 RRTII-R 5'- CCAAACAAGCAAATCTGGCT -3' } *Mouse and Human*
 Y= C or T

For each sample the PCR reaction mix was prepared in a 1.5 ml tube on ice as follows:

Reagents	Concentration	Quantity in μ l
Kapa Master Mix	2X	12.5
FW primer	5 mM	1
RV primer	5 mM	1
dH₂O		9.5
DNA	-	1
Total	-	25

Controls were included every time this PCR was performed. They are as follows:

1- Human Placenta cDNA

2- Blank (water) control

The amplification conditions were as follows:

Steps	Temperature	Duration	Cycles
Denaturation	94 °C	1 min	1
Denaturation	94 °C	20 s	
Annealing	60 °C	20 s	35
Elongation	72 °C	30 s	
Extension	72 °C	10 mins	1

10 μ l of PCR product was resolved on a 2% (w/v) agarose gel, which was photographed and evaluated. The cDNA sample was stored at -20°C to be used for quantitative Real-Time PCR.

2.4 Chromatin immuno-precipitation assay (ChIP)

Histone modifications at three regions of *FXN* gene were detected by chromatin immune-precipitation assay (ChIP) (Al-Mahdawi *et al.* 2008). Human and mouse brain tissues were included and were between 30-40 mg in weight. They were collected and weighed in a 1.5 ml Eppendorf tube. All steps were performed on dry ice until the 1X PBS (phosphate buffered saline, Sigma,UK) was added. Dr.Al-Mahdawi (Brunel University, UK) had previously prepared the first set of Brain ChIP samples (mouse and human) with different antibodies.

2.4.1 Tissue homogenisation

A) For brain

A small piece of tissue was cut and weighed in a 1.5 ml tube. 250 µl of 1X PBS was added to the tissue and homogenised with a plastic pastille. In this step, the solution should be homogenised until there are no large pieces remaining in the solution.

2.4.2 DNA and protein cross-linking

A further 722.9 µl of 1X PBS and 27.1 µl of 35% formaldehyde (Sigma,UK) were added to the sample , which was then left at RT on a shaker (Grant Boekel BFR25) for 20 min. The cross-linking reaction was stopped by adding 62.5 µl of glycine (Sigma,UK) and the tube was mixed again on the shaker at RT for 5 min. The sample was then centrifuged at 5000 rpm for 2 min at RT, and the supernatant was subsequently discarded. A small white pellet can be observed at this stage. The pellet was washed twice with 500 µl of 1X cold PBS and then centrifuged at 5000 rpm for 2 min at RT. The PBS was discarded each time.

The pellet was resuspended in 250 µl of cell lysis buffer (10 mM HEPES [N-2-hydroxyethylpiperazine-N'-2-ethanesulfonic Acid], 85 mM KCl [potassium chloride], and 0.5 % NP-40 [Nonidet P-40], [Sigma,UK]) and 10 µl of 25X ROCHE protease Inhibitor (RPI) and then the tube was incubated on ice for 10 min. The tube was centrifuged at 5000 rpm for 5 min at 4° C and the supernatant was discarded. The pellet was resuspended 100 µl of nuclei lysis buffer (1 % SDS, 10 mM EDTA, and 50 mM Tris [Sigma,UK]) + 5 µl of 25 X ROCHE protease Inhibitor (RPI) and the tube was incubated on ice for 10 minutes. As an optional step in this method, the sample can be homogenised again at this stage.

5 µl of the sample was transferred to a fresh 1.5 ml tube labelled as “before sonication”, and kept on ice to be evaluated on a 1 % agarose gel in order to check the DNA sample before the sonication step.

2.4.3 DNA shearing

The DNA sample was sheared by sonication (Soniprep 150, MSE) three times for 12 s, each time at 18 amplitude. After each sonication, the sample was kept on ice for 1-2 min to cool. The sample was centrifuged at 13,000 rpm for 10 min at 4° C. The supernatant was collected in to a fresh labelled 1.5ml tube to be used in the DNA immuno-precipitaion step. 5 µl of the sample was transferred to a fresh 1.5 ml tube labelled as “after sonication” and kept on ice to be evaluated on a 1% agarose gel, this is to check the DNA sample after the sonication step. The two samples, before and after sonication, were run on a 1% agarose gel, which was photographed and evaluated.

2.4.4 DNA immuno-precipitation

DNA was immuno-precipitated with anti-acetylated histone H3 and H4 antibodies: H3K9ac, H3K14ac, H4K5ac, H4K8ac, H4K12ac, H4K16ac, and H3K9me2 (Upstate, cell signalling solution, UK) and H3K9me3 (Diegenode).

Protein-A-agarose beads (Upstate, cell signalling solution, UK) were used and prepared for this step. 40 µl of the bead suspension was washed twice with 1 ml of 1X PBS in a fresh 1.5ml tube, and then centrifuged at 5000 rpm for 2 min at RT. The PBS was discarded each time. The supernatant from Section 2.4.3 was added to the beads and mixed gently by tapping without creating any bubbles. The tube was incubated on the shaker for two hours at 4 °C and then centrifuged at 5000 rpm for 5 min at 4 °C.

The supernatant was transferred to a fresh labelled 1.5 ml tube; 10 µl of this supernatant was transferred to a new 1.5 ml tube labelled as “INPUT” and stored immediately at – 80 °C. 1.5 ml of dilution buffer (1 % triton, 150 mM NaCl [sodium chloride], 2 mM EDTA, and 20 mM Tris) + 60 µl of 25X of RPI was added to the supernatant, and mixed. The mixture was divided into three 1.5 ml tubes, each containing approximately 550 µl. One of the tubes was labelled as “minus antibody” containing only the mixture, and the other two tubes contained the mixture and 5 µl of each studied antibody. Tubes were incubated on the shaker overnight at 4 °C.

The following day, each incubated mixture was transferred to a fresh 1.5 ml tube containing 60 µl of protein-A-agarose beads, washed twice with 1X PBS and mixed. The tube was incubated on the shaker for two hours at 4°C. After incubation, the tube was centrifuged at 6000 rpm for 30 seconds at RT. The beads were washed with 1 ml of low salt buffer (1 % Triton, 0.1 % SDS, 150 mM NaCl, 2 mM EDTA, and 20 mM Tris), the tube was mixed on the shaker for 5 min at RT and then centrifuged at 6000 rpm for 30 s at 4 °C. The buffer was discarded each time. This process was repeated three times.

Finally, the beads were washed once with 1 ml of high salt buffer (1 % Triton, 0.1 % SDS, 500 mM NaCl, 2 mM EDTA, and 20 mM Tris). The tube was mixed on the shaker for 5 min at RT and centrifuged at 6000 rpm for 30 s at 4 °C, and the buffer was discarded. 150 µl of elution buffer (1 % SDS, and 100 mM NaHCO₃) was added to each tube and mixed by tapping. The tube was incubated in a 65 °C water bath for 10 min. The tube was centrifuged at 6000 rpm for 30 s at RT. The supernatant was collected into a fresh labelled 1.5 ml tube. A further 150 µl of the elution buffer was added and the tube was incubated in a 65 °C water bath for 10

min. The supernatant was collected and combined with the first supernatant. The total volume was 300 µl.

300 µl of the elution buffer was added to the INPUT sample after thawing. 30 µl of the sample was transferred to a fresh 1.5 ml tube labelled as “Western Blot” and stored at -80 °C for future use.

1.2 µl of 50 mg/ml proteinase K was added to each sample. The sample was incubated in a 37 °C water bath for 30 min and the tube was transferred to a 65 °C water bath overnight (16 hours). This step was to reverse the DNA protein cross linking.

2.4.5 DNA Phenol /Chloroform extraction

Genomic DNA was extracted (Sambrook *et al.* 1989) by adding 270 µl of equilibrated phenol (Sigma) to each sample. The sample was mixed on the shaker for 5 min at RT, and centrifuged at 13,000 rpm for 5 min at RT. The upper aqueous phase was collected into a fresh 1.5 ml tube containing 300 µl of CHCl₃ / IAA (chloroform/ isoamyl-alcohol). The tube was vortexed briefly and centrifuged at 13,000rpm for 5 min at RT. The aqueous phase was collected into a fresh 1.5 ml tube containing (4 µl of 20 µg/ µl glycogen + 30µl of 2 M sodium acetate + and 600 µl absolute ethanol) and the sample was incubated at -80°C for 10 min. The tube was centrifuged at 13,000 rpm for 30 min at 4 °C and the supernatant was discarded. The pellet was washed with 500 µl of 70% (v/v) ethanol and centrifuged as described previously; and the ethanol was discarded. The pellet was left to air-dry for 10-15 min and then suspended in 50 µl elution buffer (10 mM Tris, Qiagen), 100 µl for the INPUT, and stored at 4 °C or -20 °C to be used for the quantitative Real-Time PCR.

2.4.6 DNA quality check

Further PCR amplification was carried out to in order check the quality of the DNA sample, using 4 different sets of primers depending on the sample type used. The following sets of primers were used:

FXN promoter PCR

FXN proF 5'-CCCCACATACCCAACTGCTG-3'

FXN proR 5'-GCCCGCCGCTTCTAAAATTC-3'

GAA upstream PCR

FXN upF 5'-GAAACCCAAAGAATGGCTGTG-3'

FXN upR 5'-TTCCCTCCTCGTGAAACACC-3'

GAA downstream PCR

FXN downF 5'-CTGGAAAAATAGGCAAGTGTGG-3'

FXN downR 5'-CAGGGGTGGAAGGCCAATAC-3'

GAPDH (Human) PCR

GAPDH F 5'-CACCGTCAAGGCTGAGAACG-3'

GAPDH R 5'-ATACCCAAGGGAGGCCACACC-3'

GAPDH (Mouse) PCR

GapdhM-F 5'-TGACAAGAGGGCGAGCG-3'

GapdhM-R 5'-GGAAGCCGAAGTCAGGAAC-3'

For each sample the PCR reaction mix was made as follows:

Reagents	Concentration	Quantity in μ l
Kapa Master Mix	2X	12.5
FW primer	5 mM	1
RV primer	5 mM	1
dH ₂ O		9.5
DNA	-	1
Total	-	25

Controls were included every time this PCR was performed. They are as follows:

1- Genomic human placenta DNA

2- Blank (water) control

The amplification conditions were as follows:

Steps	Temperature	Duration	Cycles
Denaturation	94 °C	1 min	1
Denaturation	94 °C	20 s	
Annealing	60 °C	20 s	35
Elongation	72 °C	20 s	
Extension	72 °C	10 mins	1

10µl of PCR product was resolved on a 2% (w/v) agarose gel, which was photographed and evaluated. The ChIP DNA sample was evaluated and stored at -20 °C to be used for the quantitative Real-Time PCR.

2.5 Relative quantitative Real-time qPCR

Quantification was performed by using an ABI Prism® 7900 HT real-time PCR instrument (Applied Biosystems).

2.5.1 cDNA quantification

The cDNA sample from step 2.3.1 was quantified using real-time PCR in triplicate. Primers were used in this experiment were the same sets of primers were used in Section 2.3.2.

For each DNA sample, two PCR reaction master mixes were prepared (Fxn-RT + Gapdh) or (FRTIb + Gapdh) depending on the sample type used. Reaction mixes were prepared as follows:

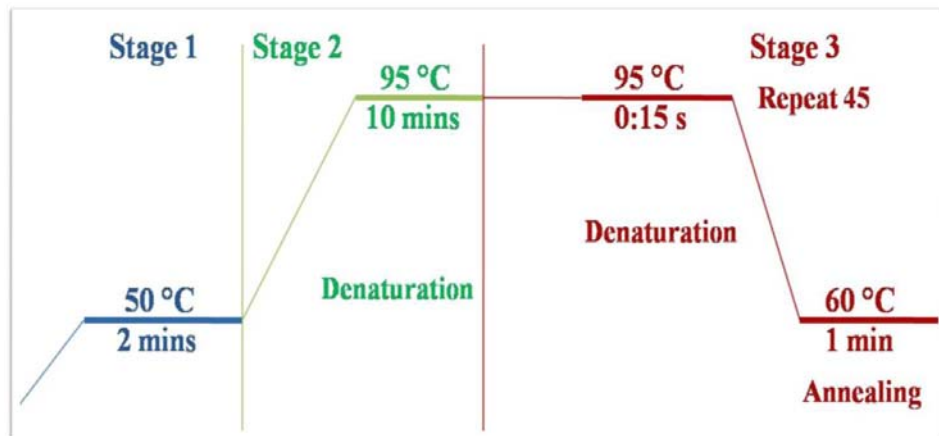
<i>Fxn-RT mix</i>		<i>Gapdh and FRT1b mixes</i>	
Reagents	Quantity in μ l	Quantity in μ l	Concentration
SYBR® Green Reagent Applied Biosystems	12.5	12.5	2X
FW primer	0.5	1	5 mM
RV primer	0.5	1	5 mM
dH₂O	10.5	9.5	
cDNA	1	1	-
Total	25	25	-

Controls were included every time this PCR was performed. They are as follows:

1- Human placenta cDNA

2- Blank (water) control

The q-PCR amplification conditions were as follows:



After amplification, 10 μ l of PCR product was resolved on a 2 % (w/v) agarose gel, which was photographed and evaluated.

2.5.2 ChIP genomic DNA quantification

The DNA sample from Section 2.4.5 was quantified using real-time PCR in triplicate. Primers that were used in this experiment are the same that were described in Section 2.4.6. For each DNA sample, four PCR reaction master mixes were prepared; *FXN* promoter; GAA upstream; GAA downstream; and GAPDH (Human

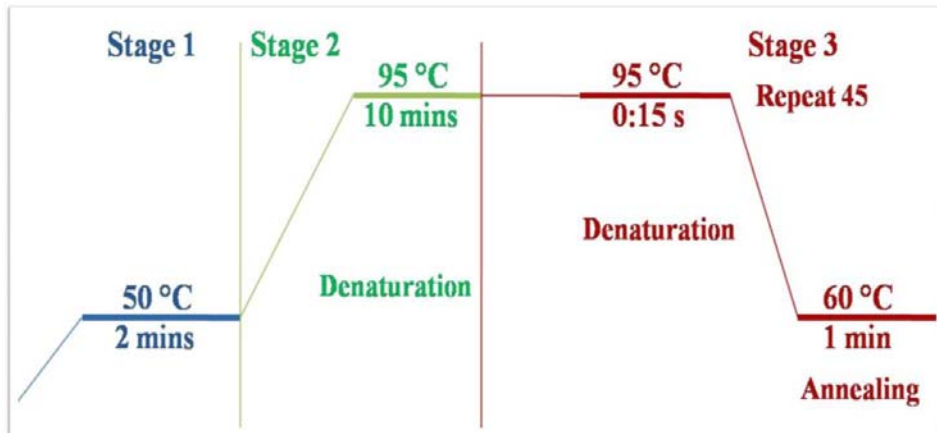
or Mouse) depending on the sample type used. Reaction mixes were prepared as follows:

Reagents	Concentration	Quantity in μ l
SYBR® Green Reagent Applied Biosystems	2X	12.5
FW primer	5 mM	1
RV primer	5 mM	1
dH₂O		9.5
ChIP DNA	-	1
Total	-	25

Controls were included every time this PCR was performed. They are as follows:

- 1- Genomic Human Placenta DNA 2- Blank (water) control

The q-PCR amplification conditions were as follows:



10 μ l of PCR product was resolved on a 2 % (w/v) agarose gel, which was photographed and evaluated. All Results were analysed using the ABI PRISM® 7900HT Sequence Detection System (SDS 2.1) software.

Chapter 3

Results

3.1 Genotyping of mice

The DNA samples from the transgenic rescued mice were PCR genotyped for the introduced (GAA·TTC)₁₉₀ and (GAA·TTC)₁₉₀₊₉₀ repeats and for the wild-type or *Fxn* knockout alleles. In order, to proceed with the project we had to make sure that we have the tissue sample, such as, brain, heart and liver from the transgenic mouse that contains the complete human *FXN* gene with the (GAA)n·(TTC)n on a null background (knockout), therefore, this is an essential confirmation step to be processed.

3.1.1 Screening for the (GAA)n·(TTC)n repeats

By using the GAA primers, we expected a PCR product size around 460bp, in addition to the (GAA)n(TTC)n repeat size. The size of the introduced expanded (GAA)n·(TTC)n repeat varies because of the genomic instability; as a result, different PCR products that range from approximately 800 bp to 1.6 kb were amplified. Selected samples from both transgenic mice lines YG8 and YG22 were screened for the repeat (Figure 3.1) to be used in this project.

3.1.2 Screening for the *Fxn* knockout alleles PCR

The DNA samples were screened for the *Fxn* mouse alleles. In this PCR we used three primers; the WJ5 and WN39 primers were used to amplify the normal allele and give a 520bp PCR product, whereas, the WJ5 and WC76 primers were used by the mutant allele to amplify and give a 245bp PCR product (KO). Different genotyping results including wild-type, homozygous and heterozygous knockout

were observed. The ratio between the three primers has to be adjusted to get an equal product from each allele and balanced intensity for each band. In figure 3.2 lanes 2, 5 and 6 represent this problem, the WT band is very weak compare with the KO band (Figure 3.2).

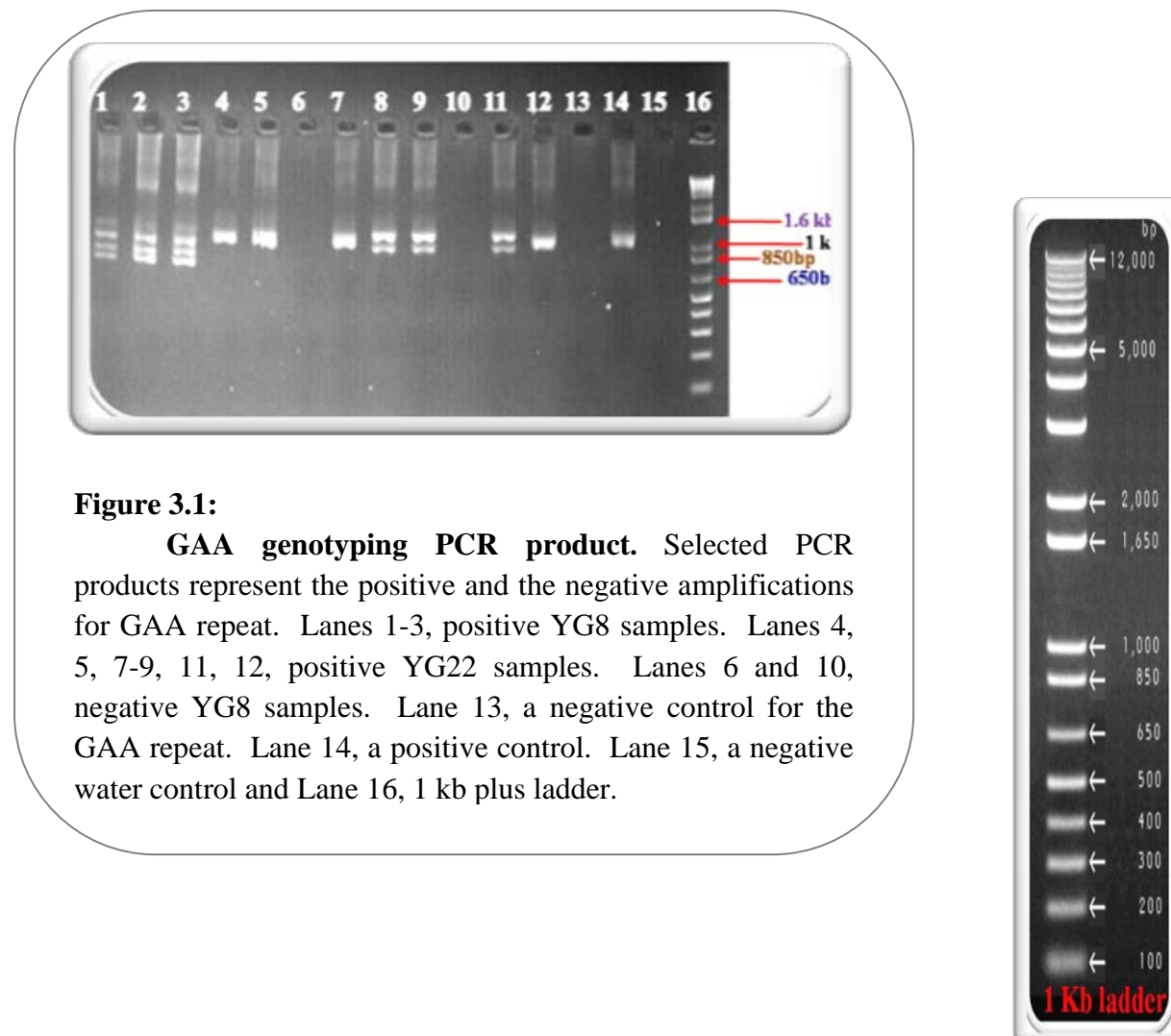


Figure 3.1:

GAA genotyping PCR product. Selected PCR products represent the positive and the negative amplifications for GAA repeat. Lanes 1-3, positive YG8 samples. Lanes 4, 5, 7-9, 11, 12, positive YG22 samples. Lanes 6 and 10, negative YG8 samples. Lane 13, a negative control for the GAA repeat. Lane 14, a positive control. Lane 15, a negative water control and Lane 16, 1 kb plus ladder.

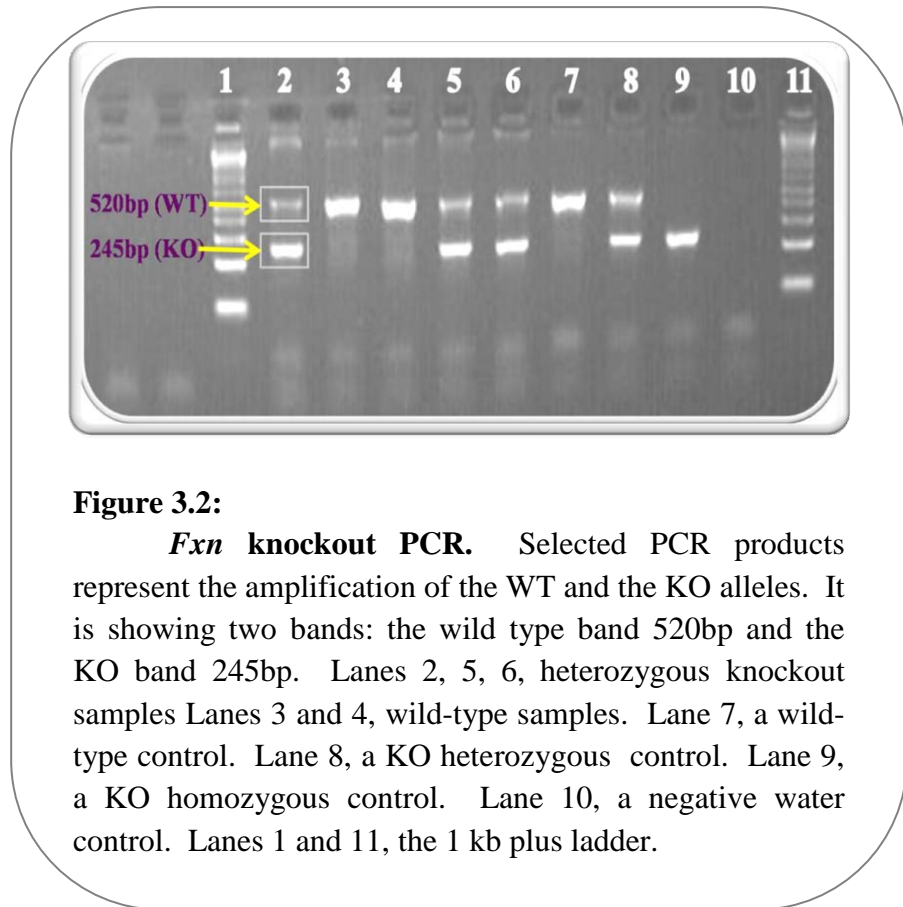
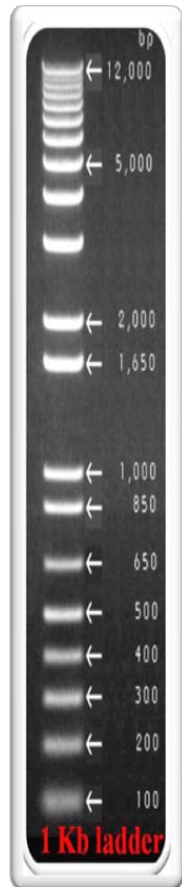


Figure 3.2:

***FXN* knockout PCR.** Selected PCR products represent the amplification of the WT and the KO alleles. It is showing two bands: the wild type band 520bp and the KO band 245bp. Lanes 2, 5, 6, heterozygous knockout samples Lanes 3 and 4, wild-type samples. Lane 7, a wild-type control. Lane 8, a KO heterozygous control. Lane 9, a KO homozygous control. Lane 10, a negative water control. Lanes 1 and 11, the 1 kb plus ladder.



3.2 *FXN* mRNA level in the human brain and transgenic mice brain, heart and liver tissues

The mRNA level in FRDA patients and in the transgenic mice was investigated previously by semi-quantitative RT-PCR. Studies have indicated a decreased level of frataxin mRNA and frataxin protein in most of the tissues in human and mouse (Al-Mahdawi *et al.* 2006; Gottesfeld 2007).

For a further more accurate investigation, we performed two quantitative RT-PCR experiments to detect the frataxin mRNA levels in human and mouse in different tissues. First, the detection of frataxin mRNA level in the brain tissue of a FRDA patient in comparison with a normal control. Second, the detection of the frataxin mRNA level in the brain and heart of three transgenic mice lines (Y47, YG8, YG22). RNA samples were extracted from the tissues, followed by the cDNA synthesis. This was followed by the quantification of the frataxin mRNA from the

cDNA was performed using real-time qPCR with a designed set of primers that are specific for the human *FXN* gene, human GAPDH and mouse GAPDH for the normalization.

3.2.1 RNA extraction quality check

A quality check step is an important procedure, ensuring us that there is a sufficient quantity and good quality of the RNA to further proceed with the experiment. Extra care is required in the RNA extraction protocol, especially with respect to DNase contamination, which may result in a certain degree of RNA degradation, as seen in all lanes in the picture (Figure 3.3). The OD₂₆₀ of the RNA samples was measured to check the purity of the RNA sample in addition to the quantity.

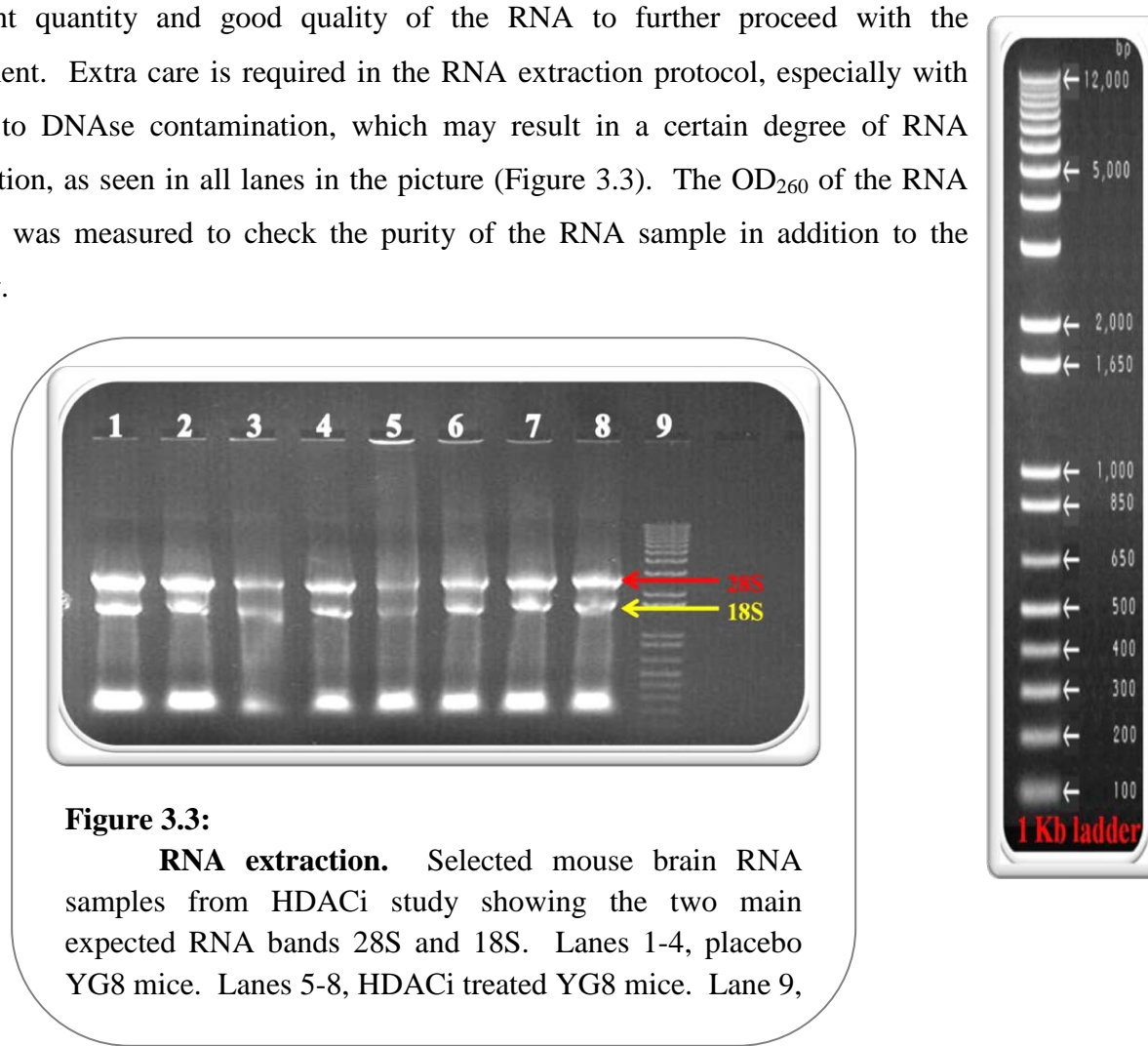
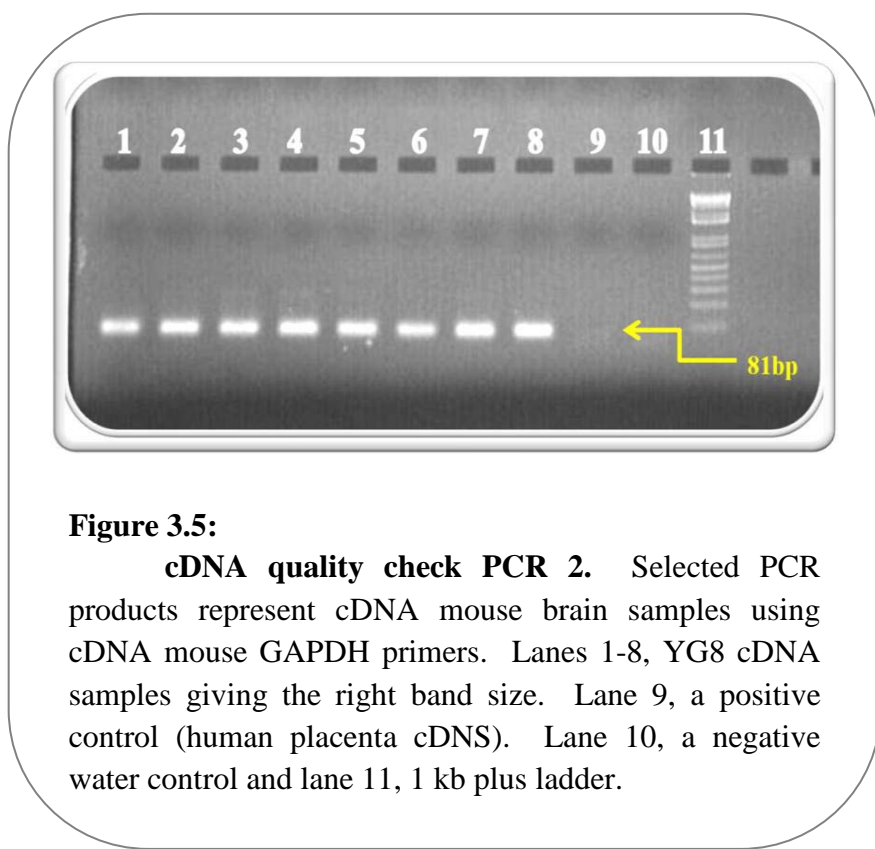
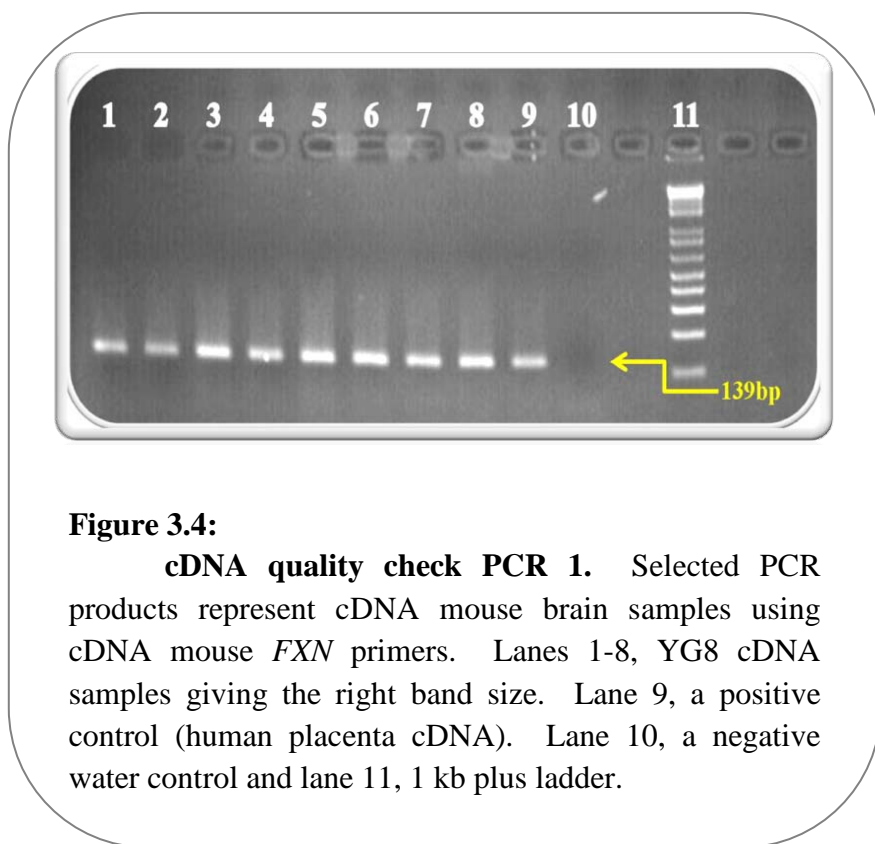


Figure 3.3:

RNA extraction. Selected mouse brain RNA samples from HDACi study showing the two main expected RNA bands 28S and 18S. Lanes 1-4, placebo YG8 mice. Lanes 5-8, HDACi treated YG8 mice. Lane 9,

3.2.2 cDNA synthesis quality check

The cDNA was synthesized and the quality of the DNA was checked by performing a PCR reaction using any set of the cDNA primers that are listed on page 87-88, Chapter 2). For examples, see Figures 3.4 and 3.5.



3.2.3 Relative quantitative, Real-time qRT-PCR

Reverse transcriptase quantitative PCR (qRT-PCR) has been the key technology for analyzing the gene expression because of its quick, high throughput, easiness and lower cost. The real-time PCR technique allows quantification of PCR products in real-time during each PCR cycle, so the quantitative measurement is accumulating during the reaction and then, a fluorescent detector molecule such as, SYBR green will carry out the measurement of the product. SYBR green is an intercalating dye; it binds to the product and emits a strong fluorescence. It is inexpensive, easy to use and can be used for any reaction (VanGuilder *et al.* 2008). The determination of the frataxin mRNA in the human and transgenic mouse tissues was conducted using this technique.

3.2.3.1 FXN mRNA level in the human brain and heart tissues

The *FXN* transcription level in the brain tissue of a FRDA patient with (GAA·TTC)_{750/650} repeats showed a dramatic decrease, it showed a mean value of 9% compared with a normal control, which was normalized to a 100 % (Figure 3.6). The decreased level of the frataxin mRNA was expected especially in the brain, as it is considered to be the primary affected organ in the body.

This result is in consensus with previous studies that indicated a reduced level of frataxin mRNA in different tissues in FRDA patients. It has been suggested that many factors are involved in reducing the frataxin transcription such as, DNA methylation patterns that located at upstream, downstream and at the promoter region around the (GAA)_n·(TTC)_n repeat. In addition, the histone modifications increase the trimethylation of H3K9 and decrease the acetylation of other histones in *FXN* gene (Greene *et al.* 2007; Al-Mahdawi *et al.* 2008).

The experiment for the human heart samples failed to produce a reliable mean values three consecutive times. Further adjustment and troubleshooting were required to proceed with the these samples were performed using the brain samples. However, we did not proceed further because of the time factor, in addition of the

concerns regarding about the transgenic mice; thus, these experiments should be considered in the future work.

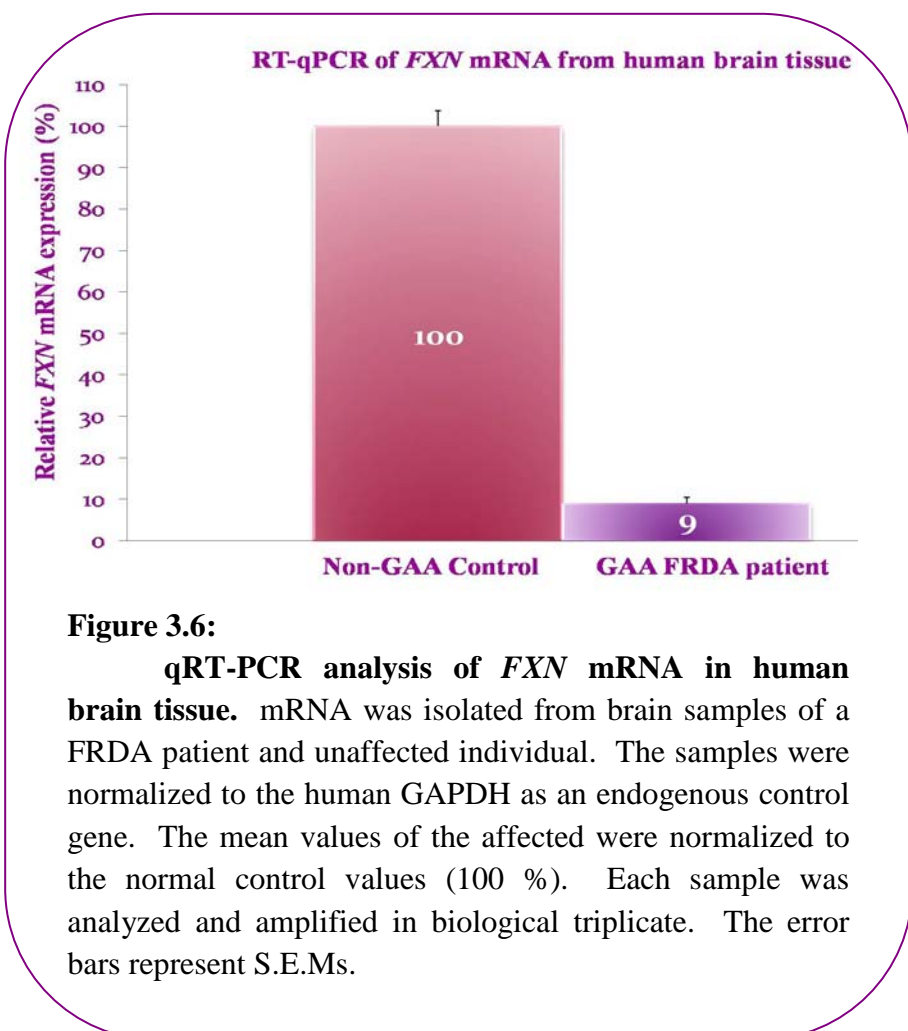


Figure 3.6:

qRT-PCR analysis of *FXN* mRNA in human brain tissue. mRNA was isolated from brain samples of a FRDA patient and unaffected individual. The samples were normalized to the human GAPDH as an endogenous control gene. The mean values of the affected were normalized to the normal control values (100 %). Each sample was analyzed and amplified in biological triplicate. The error bars represent S.E.Ms.

3.2.3.2 *FXN* mRNA level in the transgenic mice brain and heart tissues

The same experiment was conducted on the transgenic mice Y47, YG8 and YG22 to compare the frataxin mRNA profile in mouse within these three model lines and with the human profile. The frataxin mRNA level was investigated in the brain and heart tissues from each line. The results showed that the frataxin mRNA level in YG8 and YG22 lines is decreased by approximately 65 to 68 % compare with the Y47, which contains the normal repeat size. In addition, this pattern is similar to the human pattern in the previous section (Figure 3.7).

In conclusion, this experiment confirms that the expanded (GAA)_n·(TTC)_n repeats have a primary role in inhibiting frataxin transcription and it shows the effect of varying sizes of the repeat that can differentiate frataxin mRNA level. In addition, it confirms that these mice models are a reliable and useful model for FRDA research because of its similarity to the human system.

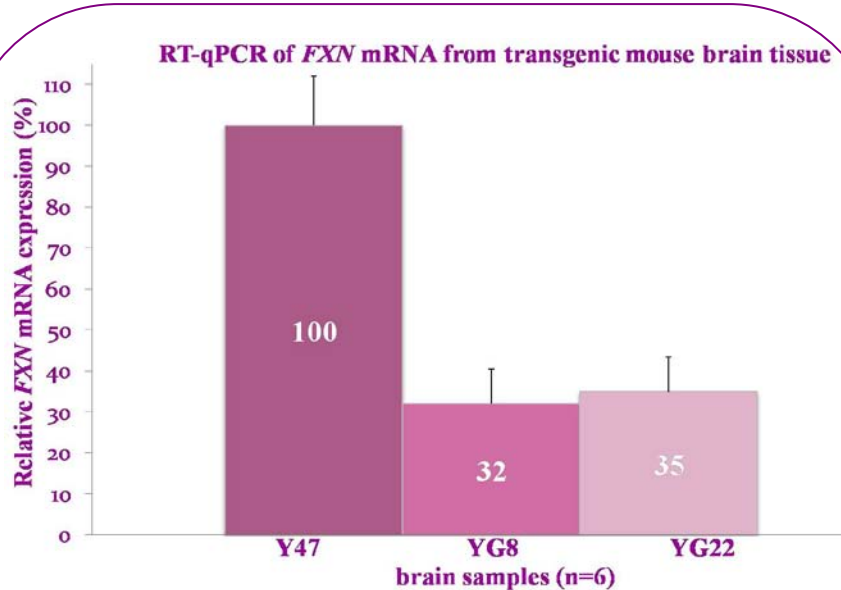


Figure 3.7:

qRT-PCR analysis of *FXN* mRNA in transgenic mouse brain tissues. Showing the values mRNA level which was isolated from six brain samples from each of Y47(GAA·TTC)₉, YG8 (GAA·TTC)₁₉₀₊₉₀ and YG22 (GAA·TTC)₁₉₀ repeat expansions. The samples were normalized to the mouse GAPDH as an endogenous control gene. The mean values of the affected were normalized to the normal control values (100 %). Each sample was analyzed and amplified in biological triplicate. The error bars represent S.E.Ms.

Similar interpretation was made with the mouse heart samples, the frataxin mRNA level in YG8 and YG22 was reduced by approximately 20 to 24 % compared with Y47 (Figure 3.8). The decreased range in the heart tissues is less than the decreased range in the brain tissues and that may explain that the cardiac symptoms,

which manifest themselves later in life rather than the symptoms of the neurodegeneration in the brain.

Due to the failure of the human heart experiment in (section 3.2.3.1), this result can be compared with a different semi-quantitative heart experiment that was conducted by Al-Mahadawi and colleagues, which indicated that a similar pattern of the frataxin mRNA level was observed in the heart tissues of two FRDA patients (Al-Mahdawi *et al.* 2008).

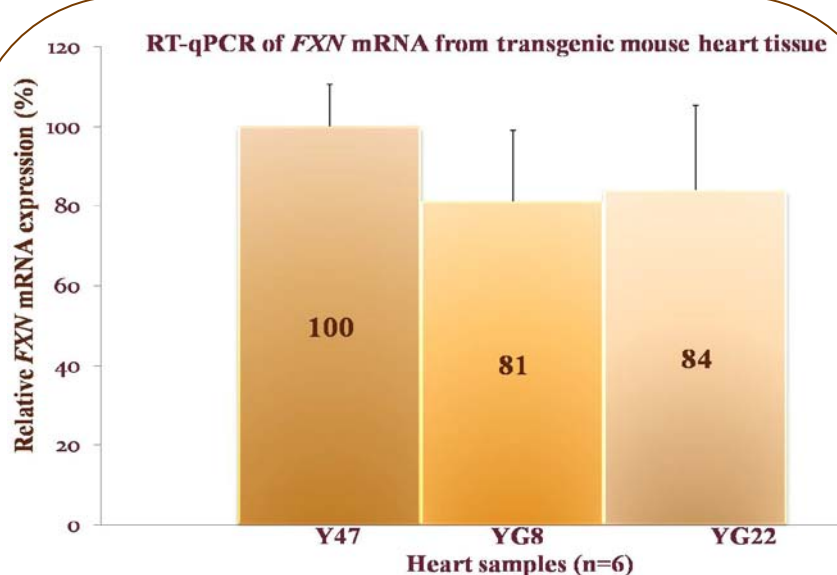


Figure 3.8:

qRT-PCR analysis of *FXN* mRNA in transgenic mouse heart tissues. Showing the values mRNA level which was isolated from six heart samples from each of Y47 (*GAA*ⁿ*TTC*)₉, YG8 (*GAA*ⁿ*TTC*)₁₉₀₊₉₀ and YG22 (*GAA*ⁿ*TTC*)₁₉₀ repeat expansions. The samples were normalized to the mouse GAPDH as an endogenous control gene. The mean values of the affected were normalized to the normal control values (100 %). Each sample were analyzed and amplified in biological triplicate. The error bars represent S.E.Ms.

The qPCR products were checked on an agarose gel, as a routine step (Figures 3.9 and 3.10). In the qPCR reaction SYBR green was used as a detective fluorescent as, this molecule can intercalate with any double stranded product.

Therefore, any presence of the non-specific products or primer dimers in the reaction can interfere with the products and gives a false positive result. Therefore, this routine step is essential in order to have the right evaluation for the quality of the qPCR, which includes, primer design, choosing the right annealing temperature, and the right concentration of the PCR mix contents.

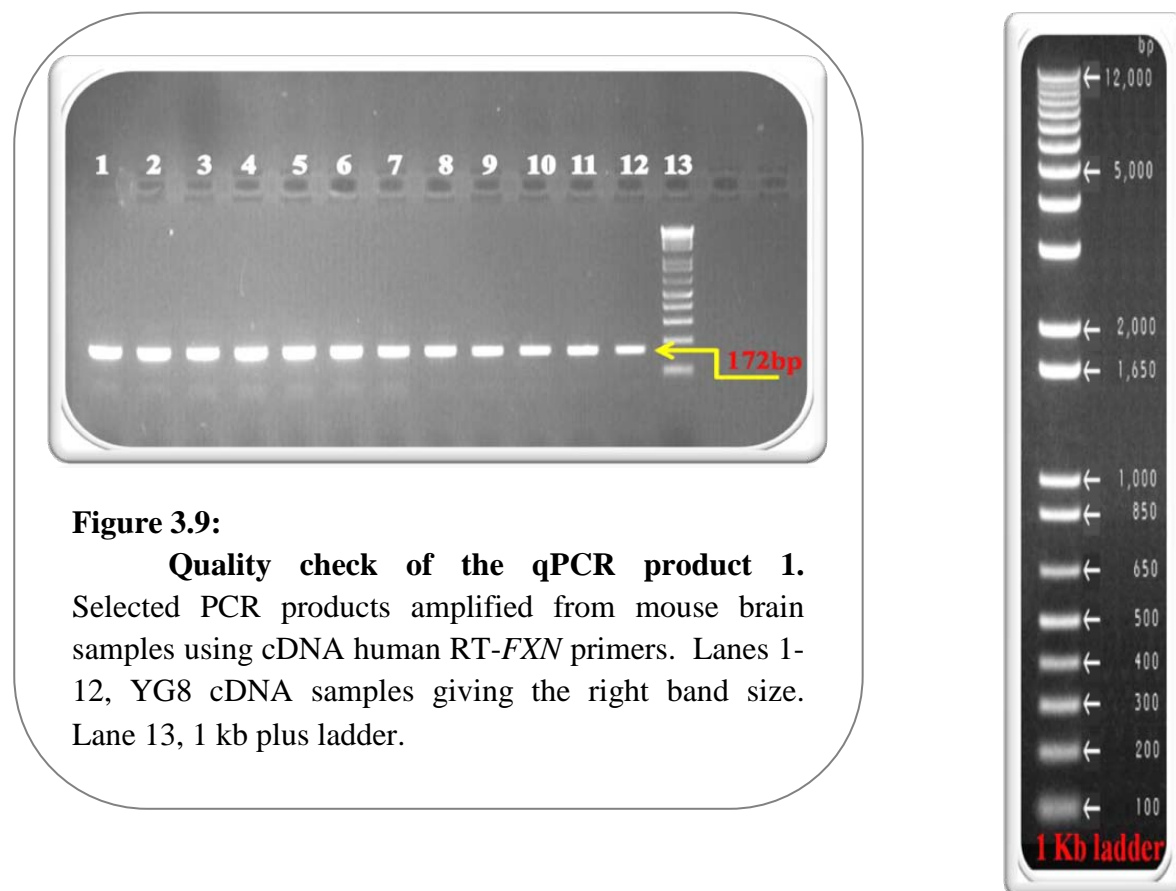
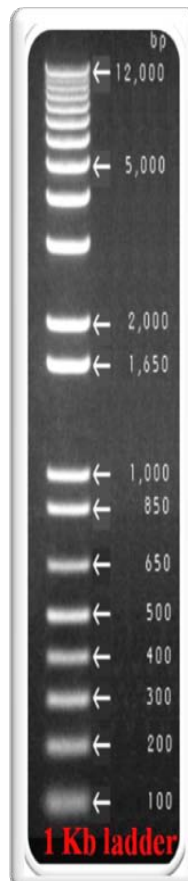
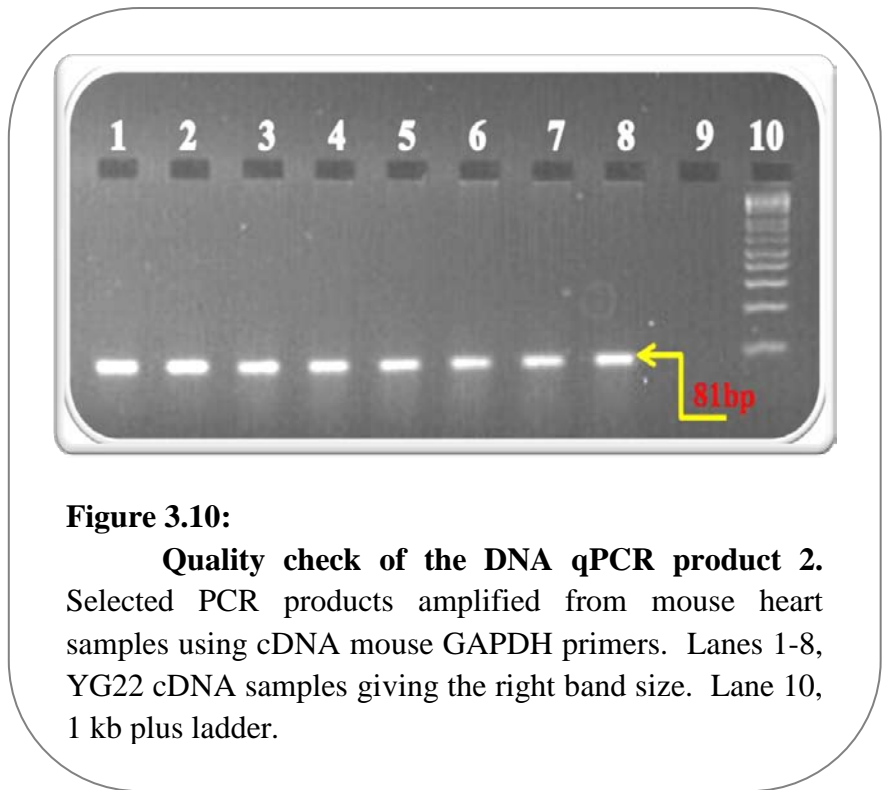


Figure 3.9:

Quality check of the qPCR product 1.

Selected PCR products amplified from mouse brain samples using cDNA human RT-FXN primers. Lanes 1-12, YG8 cDNA samples giving the right band size. Lane 13, 1 kb plus ladder.



3.3 Histone modifications of *FXN* in human and transgenic mouse brain tissues

Previous studies demonstrated that the heterochromatin formation and the histone modifications potentially regulate *FXN* transcription. Heterochromatin structure can block the access of necessary transcription factors and alter the modifications of the histone tails. In many studies it has been confirmed that very high trimethylation of H3K9 and hypoacetylation of H3K14, H4k5, H4K8 is a hallmark of the heterochromatin and gene silencing in FRDA (Gottesfeld 2007; Greene *et al.* 2007; Rai *et al.* 2008).

3.3.1 Chromatin immuno-precipitation assay (ChIP)

To investigate the histone modifications pattern in our mice model and compare the differences within the three different lines Y47, YG8, YG22 and with the human pattern, the chromatin immuno-precipitation assay (ChIP) was used. ChIP assay is quantitative, straightforward and is relatively standard. It is widely applied for measuring the association of proteins with specific genomic region to predict modified peptide, for instance, acetylation, methylation and phosphorylation. In this experiment, the formaldehyde is used to cross-link between the protein (histone) and DNA, and then the DNA is fragmented by sonication to give an average DNA length between 300 to 600 bp. Finally, samples are immunoprecipitated with a specific selected antibody (Struhl 2007). After preparing the ChIP sample, it is ready for the real-time qPCR.

The primer sets were used in this experiment, cover three main regions: promoter, upstream and downstream the (GAA)n(TTC)n repeat in the *FXN* gene. Therefore, the primer sets ‘genomic DNA ChIP primers’ were named as: *FXN* pro, *FXN* up, and *FXN* down (Figure 3.11) (Al-Mahdawi *et al.* 2008). In addition to the GAPDH primer sets for human and mouse to be used for the internal normalization control. For each sample, the three regions were investigated. The antibodies were anti- H3 and H4 acetylated and methylated (details in page 90, Chapter 2).

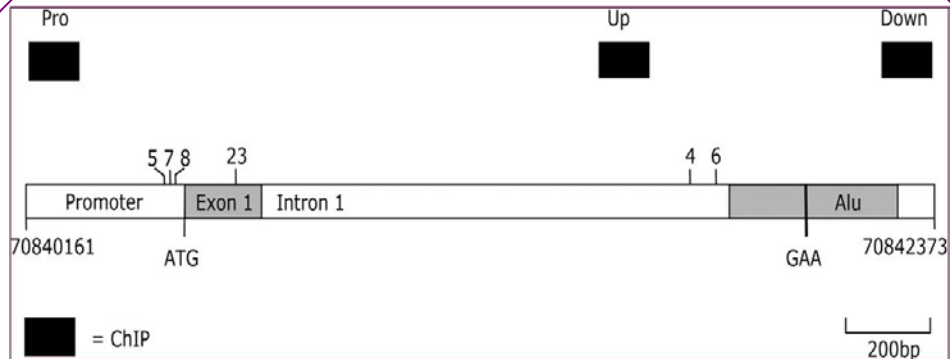


Figure 3.11:

Schematic representation of 2.2 kb at the 5'end of the FXN gene. This figure shows the promoter/exon 1 (Pro), upstream GAA (Up) and downstream GAA (Down) regions that were analysed by ChIP (black boxes). Numbers above indicate the position of CpG sites within the promoter and upstream GAA regions. The positions of the ATG translation start codon, exon 1 open reading frame and GAA repeat sequence within the Alu repeat sequence are shown. Numbers found below indicate the chromosome 9 base pair numbering according to the 2006 build of the UCSC human DNA sequence database. Modified from (Al-Mahdawi *et al.* 2008)

3.3.1.1 DNA shearing

After the DNA sample was crossed with the protein a shearing step was performed. The result of an ideal shearing step should give a range between 300 and 600bp fragments. In Figure 3.12 it is clear that more sonication was needed for the DNA samples, as seen in lanes 2, 4, 6, and 8. This step is considered the most critical step as it can determine the success of the ChIP experiment (Figure 3.12).

3.3.1.2 DNA quality check

The quality of the ChIP DNA samples were checked by performing a PCR reaction using any set of the genomic DNA ChIP primers that listed on page 93, Chapter 2 (Figure 3.13).

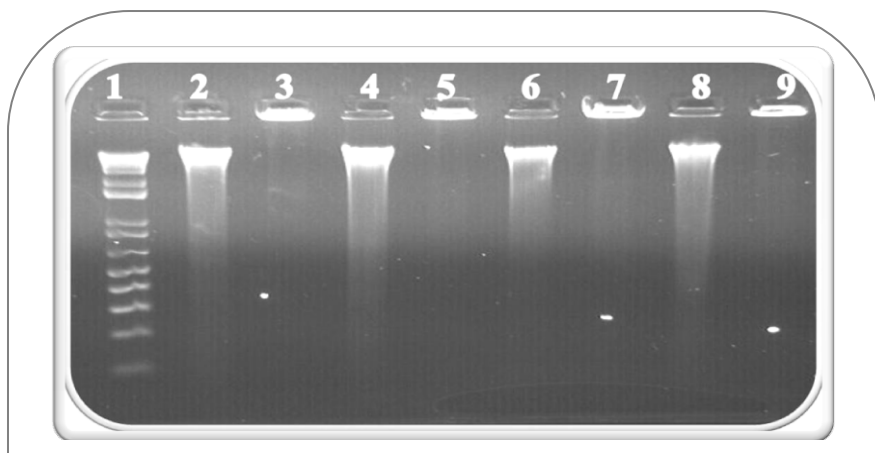


Figure 3.12:

DNA sonication. Selected DNA samples after the sonication. Lanes 2, 4, 6, and 8, represent sonicated DNA samples. Lanes 3, 5, 7, and 9, represent the same DNA samples before sonication. Lane 1, 1 kb plus ladder.

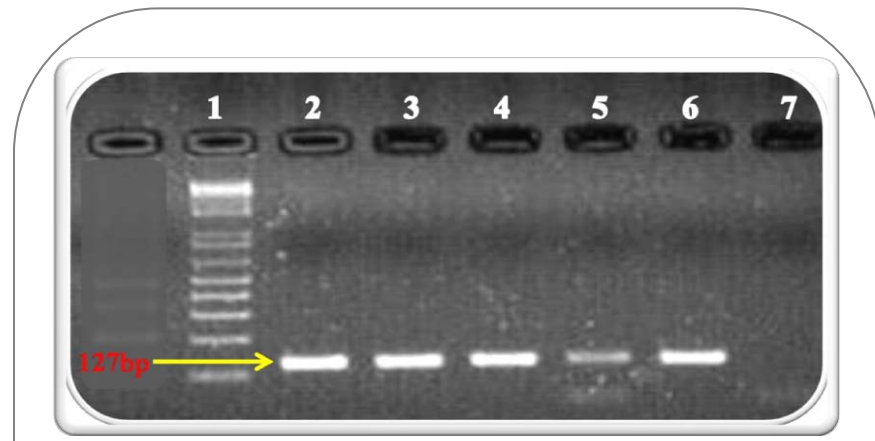
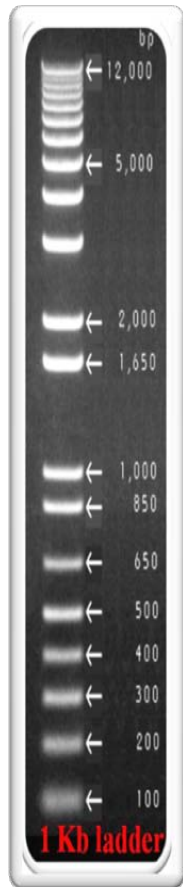


Figure 3.13:

ChIP DNA quality check PCR. Selected PCR products represent ChIP DNA human brain samples using DNA ChIP FXN promoter primers. Lane 2, Input DNA. Lane 3, DNA samples which was precipitated with H3K9 antibody. Lane 4, with H4K12 antibody. Lane 5, negative control (no antibody was added). Lane 6, a positive control (genomic human placenta). Lane 7, a water negative control and lane 1, 1 kb plus ladder.



3.3.2 Relative quantitative, Real-time qPCR

Previous investigations reinforced the connection between the presence of the histone modifications and the formation of the heterochromatin structure, as a result gene silencing. These observations were reported in FRDA cell lines (Herman *et al.* 2006; Gottesfeld 2007; Rai *et al.* 2008).

In this experiment, the same theory was applied to investigate the connection between the histone modifications and the gene silencing in the human and transgenic mice with different GAA repeats using real-time qPCR and covering all three regions (Promoter, upstream, and downstream) of the repeat. In addition, it was possible to compare the FRDA mouse histone modification profile with the human histone profile.

3.3.2.1 Histone modifications in human brain tissues

Histone modifications, such as acetylation and methylation, were investigated in a brain sample of FRDA patient with (GAA·TTC)_{750/650} repeats in comparison with a normal control using ChIP assay technology. The results showed interesting patterns, such as that the histone acetylation pattern was highest in the promoter and upstream region compared with the downstream region (Figure 3.14). Moreover, H3K9ac residue shows a dramatic decrease by 32, 65, and 84 % in the *FXN* promoter, upstream, and downstream, respectively. In addition, H4K16ac residue has shown to be decreased by 20, 29, and 61 % in the three regions respectively. The remaining four residues, H3K14ac, H4K5ac, H4K8ac, and H4K12ac all showed a slight increase in the *FXN* promoter and upstream region, whereas, they all showed a decrease between 40 to 90 % in the downstream area. In summary, there was a general decrease in the histone acetylation profile, specifically in downstream region (Figure 3.14). With regard to the methylation pattern, results indicated a dramatic increase in the H3K9me2 and H3K9me3 in all three regions in *FXN* gene in an FRDA patient. The increase in the di- and trimethylation of H3K9 is around 2 to 3 fold of the normal control (Figure 3.15). For example, the H3K9me3 in the

downstream region increased from 50 % in normal control to around 145 % in FRDA sample, while H3K9me2 increased from 200 % to 400 %. The methylation increase of residue H3K9me3 is more significant than the methylation of the H3K9me2 residue.

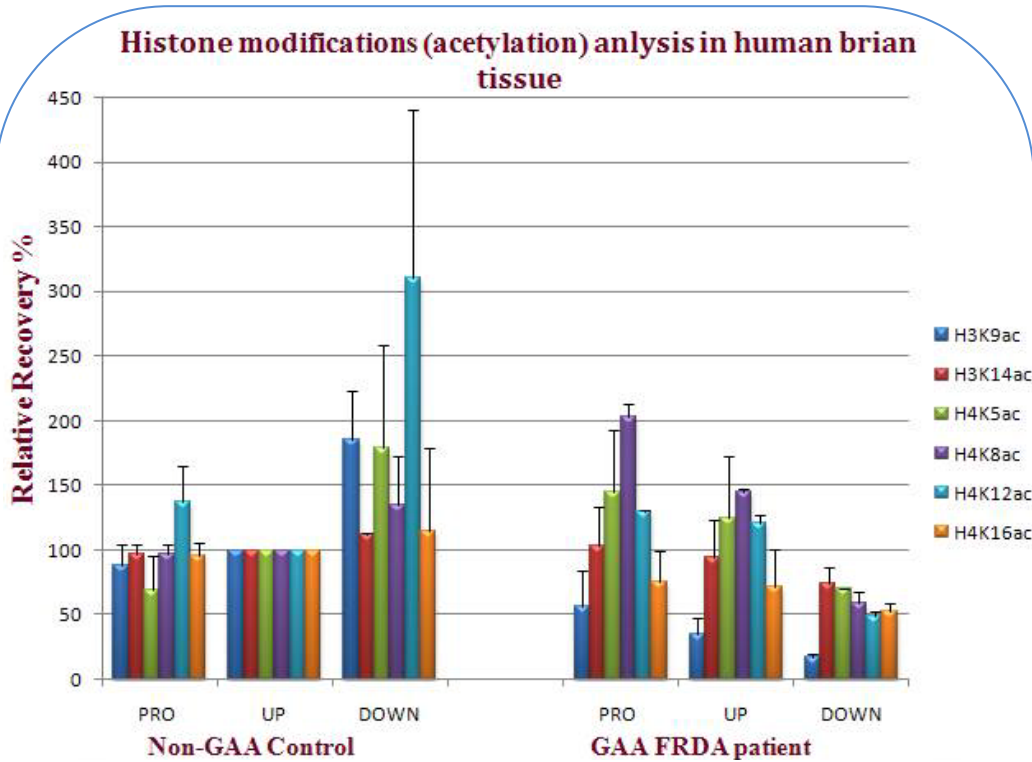


Figure 3.14:

Histone acetylation analysis in human brain tissue. ChIP DNA qPCR product represent acetylayment profile in three regions: FXN promoter (Pro), upstream GAA (Up) and downstream GAA (Down). All samples were normalized to the human GAPDH, then adjusted to the Upstream of normal control (100 %). Results show an overall decrease in H3ac and H4ac pattern of FRDA brain tissue, particularly in the downstream GAA region. Each sample was analysed in biological triplicate, bars represent S.E.Ms.

Many factors were taken into consideration when these results were interpreted. First, although each sample was investigated in biological triplicate, the results described are obtained only from one brain sample; thus, this experiment should be done with a larger number of samples in the future. Secondly, analysing results for the real-time qPCR have to be handled carefully to avoid being misled by

the false positive results. Thirdly, choosing the specific primers and the right endogenous control gene for the normalization could potentially affect the results. Finally, as with any other advanced techniques, the full attention is required in the experiment plan and with the calculations in the normalization of the anti-body precipitated DNA sample to the input DNA sample to obtain reliable results.

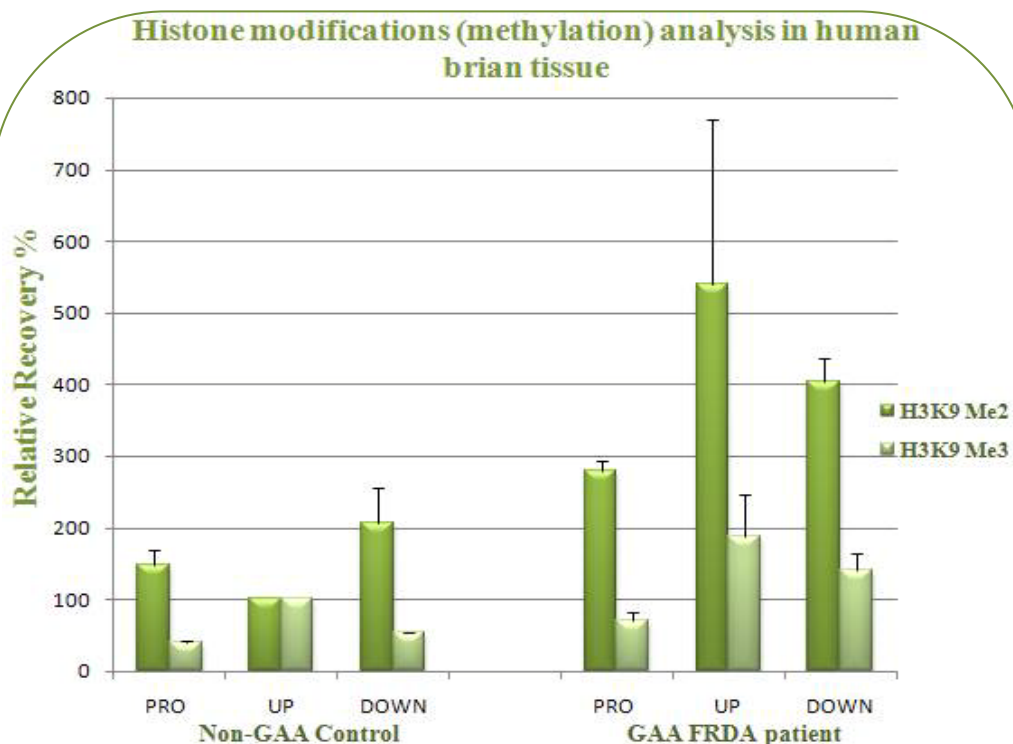


Figure 3.15:

Histone methylation analysis in human brain tissue. ChIP DNA qPCR product represent methylation profile in three regions: *FXN* promoter (Pro), upstream GAA (Up) and downstream GAA (Down). All samples were normalized to the human GAPDH, and then adjusted to the Upstream of normal control (100 %). Results indicate a dramatic increase in the H3K9me2 and H3K9me3 pattern in all three regions in a FRDA patient. Each sample was analysed in biological triplicate, bars represent S.E.Ms.

3.3.2.2 Histone modifications in transgenic mouse brain tissues

The same experiment were applied to the brain tissues from the transgenic mice Y47, YG8, YG22 by using the same techniques ChIP assay followed by real-time qPCR. Acetylation and methylation were investigated in the three regions in

FXN transgene Pro, Up, and Down. The results demonstrate that the acetylation of the H3K9ac residue decreased by around 15 % in the promoter and upstream regions, while it decreased more in the downstream region by around 25 to 30 % in both YG8 and YG22 in compare with Y47 (Figure 3.16). Moreover, the acetylation of H4K8ac in YG8 decreased slightly in all three regions, whereas it showed around 50% increase in YG22. In addition, H4K12ac behaved the same way H4K8ac did. However, the acetylation pattern for H3K14ac was inconsistent at all levels and H4K5ac showed a slight decreased by around 10 to 12 %. The last residue is H4K16ac which showed an increased by around 37, 62, 57 % in the *FXN* Pro, Up, and Down of YG8, respectively. Nevertheless, in YG22 H4K16ac showed a very high level of increase by around 70 % in the downstream region, and no observed increase in the other two regions (Figure 3.16).

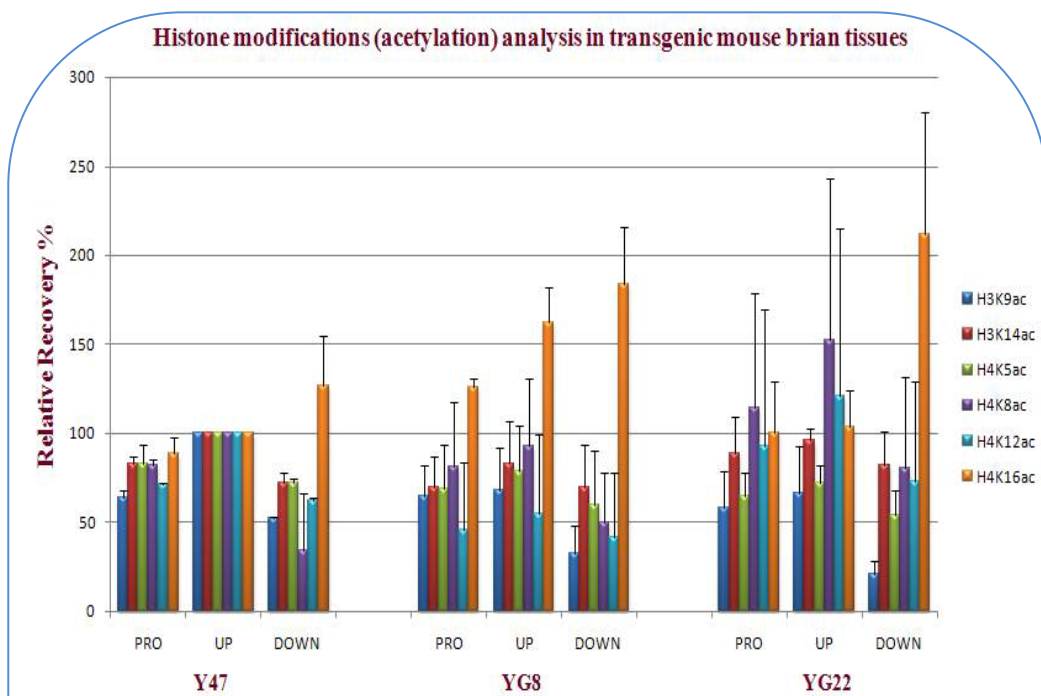


Figure 3.16:

Histone acetylation analysis in transgenic mouse brain tissue. ChIP DNA qPCR product represent acetyllyation profile in three regions: *FXN* promoter (Pro), upstream GAA (Up) and downstream GAA (Down). All samples were normalized to the mouse GAPDH, and then adjusted to the Upstream of Y47 (100 %). Results show a consistent decrease in H3K9ac pattern especially in downstream region and an overall increase in H4ac pattern in both YG8 and YG22 compared with Y47. Each sample was analysed in biological triplicate, bars represent S.E.Ms.

The histone methylation pattern in the transgenic mouse was also investigated in all three regions of FXN transgene. Both H3K9me2 and H3K9me3 showed a noticeable increase in the three regions of YG8 and YG22 (Figure 3.17). For example, the methylation of the H3K9me2 increased more significantly by 2 to 3 fold in the downstream region than it did the other two regions. Furthermore, H3K9me3 increased even more significantly by 3 to 5 fold than H3K9me2 did in all regions and more noticeable in YG8 than in YG22 (Figure 3.17).

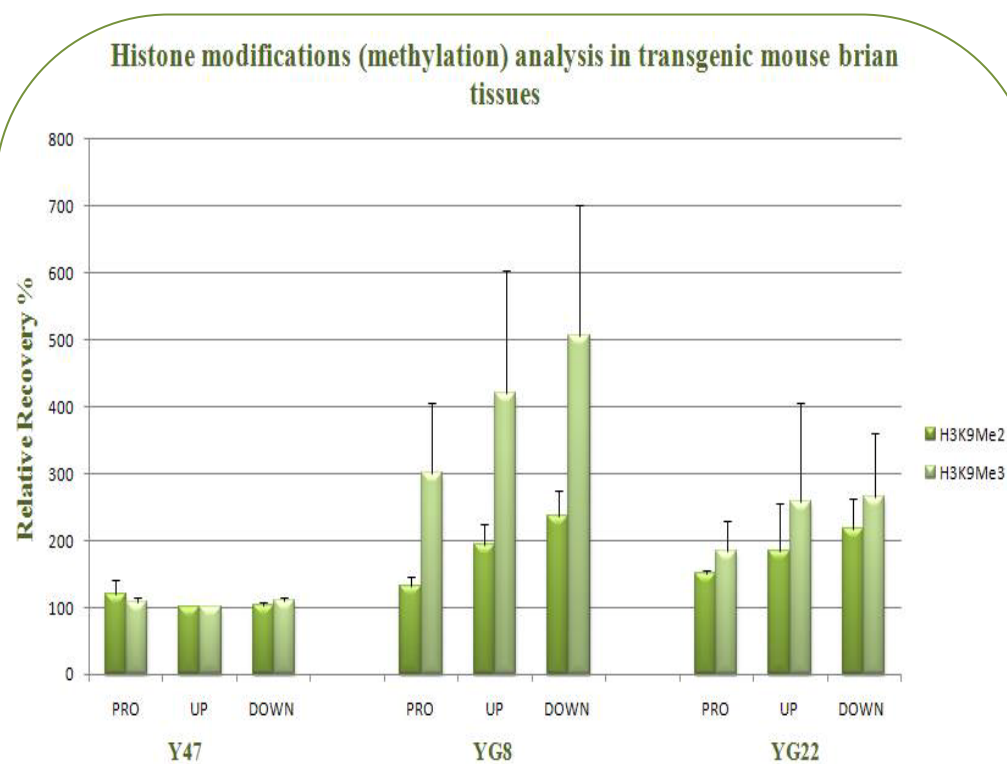


Figure 3.17:

Histone methylation analysis in transgenic mouse brain tissue. ChIP DNA qPCR product represent methylation profile in three regions: *FXN* promoter (Pro), upstream GAA (Up) and downstream GAA (Down). All samples were normalized to the mouse GAPDH, and then adjusted to the Upstream of Y47 (100 %). Results indicate a consistent increase in H3K9me2 and H3K9me3 pattern in both YG8 and YG22 compared with Y47. Each sample was analysed in biological triplicate, bars represent S.E.Ms.

In summary, although there are some specific differences between the human and the transgenic mice systems, there is an overall similarity between the human and the transgenic mice in the methylation and acetylation patterns of H3K9 residue. This observation confirms the potential of using the transgenic mice Y47, YG8, and YG22 for further studies in histone modification in studies of FRDA.

As a routine step, the qPCR products were checked and evaluated on agarose gel (Figure 3.18).

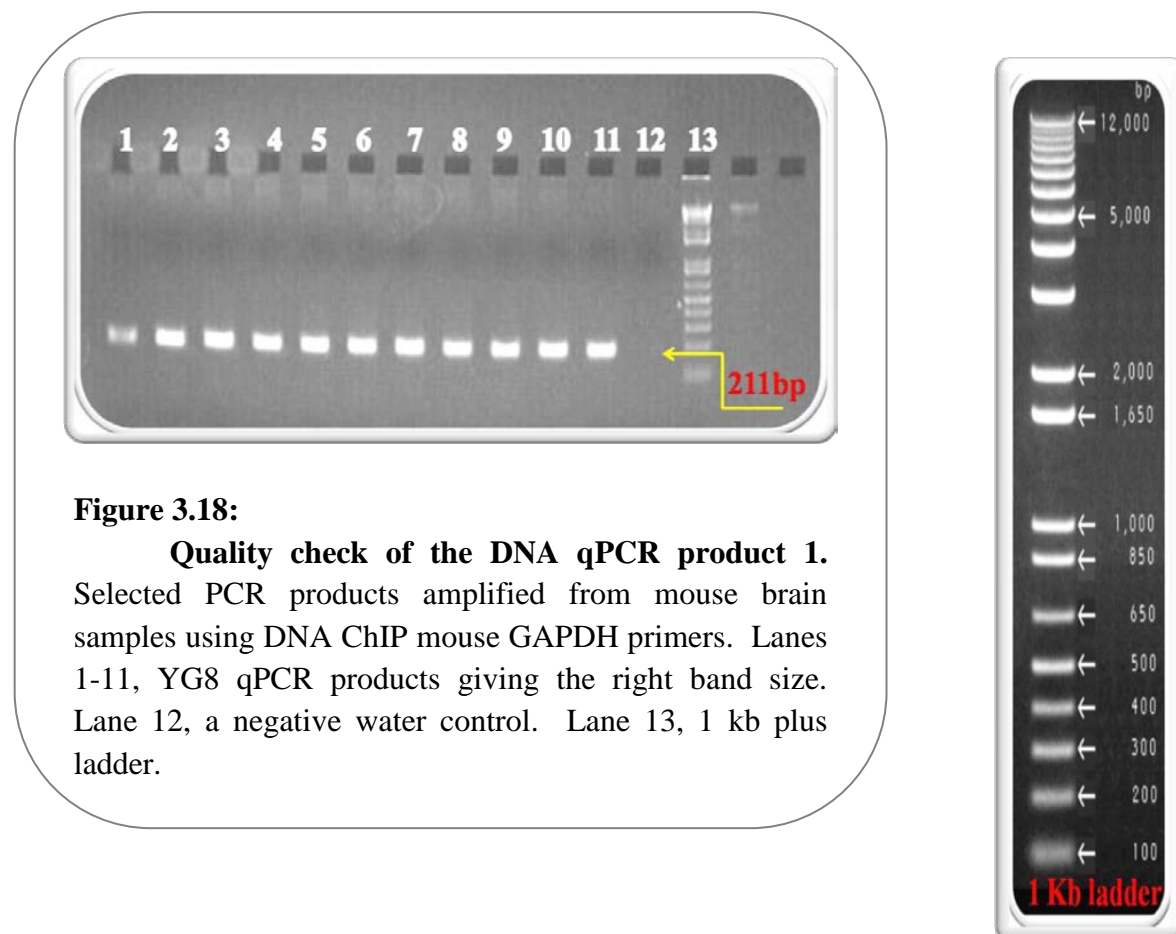


Figure 3.18:

Quality check of the DNA qPCR product 1.
Selected PCR products amplified from mouse brain samples using DNA ChIP mouse GAPDH primers. Lanes 1-11, YG8 qPCR products giving the right band size. Lane 12, a negative water control. Lane 13, 1 kb plus ladder.

The results presented in sections from 1.3 to 3.3 have recently published (Al-Mahdawi *et al.* 2008) (see Appendix 1).

3.4 An HDACi effect on *FXN* mRNA levels of in transgenic mouse brain, heart and liver tissues

Many previous studies have shown that HDACis can be effective in restoring *FXN* levels in FRDA cell lines and animal models. Many HDACis are currently under research investigations to be used as effective treatment in the future. HDACis have shown the ability to cross the blood-brain barriers and this is considered to be an essential characteristic as a treatment (Gottesfeld 2007; Rai *et al.* 2008).

For a further investigation of the role of HDACis in restoring *FXN* levels, we conducted a preliminary study to investigate the effect of one particular HDACi on the *FXN* mRNA transcription in our mice model. This HDACi is a benzamide compound, which is under licence to Repligen Corporation (Waltham, MA, USA), and it will only be referred to in this thesis as “HDACi”. Real-time qRT-PCR was used to detect the *FXN* mRNA level in brain, heart, and liver tissues of transgenic YG8 mice treated with three 150mg/kg doses of HDACi , given subcutaneously and orally (in water) once a day for three consecutive days. Other members of the Pook Ataxia research group did all of the animal work and tissue collection.

Different tissues were collected 24 hours after the last dose and then the mRNA was extracted using TRIZOL reagent followed by cDNA synthesis to have the cDNA samples ready for the quantification by real-time qRT-PCR reaction. The real-time qRT-PCR results demonstrate the HDACi effect in increasing the *FXN* transcription in different tissues of the YG8 transgenic mouse. In the brain tissues, 6 samples were collected for each placebo and HDACi treated group. The *FXN* mRNA indicated an increase of approximate 20 % in the treated group (Figure 3.19). Similar observations were reported in the heart and the liver tissues. In the liver tissues the *FXN* mRNA level increased by 18 % (Figure 3.20), while, in the heart tissues the increase was around 33 % only (Figure 3.21). These results concur with the previous studies that HDACi has a direct effect in activating the *FXN* transcription *in vivo* and *in vitro*. However the differences between the HDACi treated and placebo results were not statistically significant.

When the brain tissues were been collected after only four hours from the last dose the result was surprisingly different. The results showed a 49 % decrease in the *FXN* mRNA level in HDACi treated group (Figure 3.22), but again this was not statistically significant.

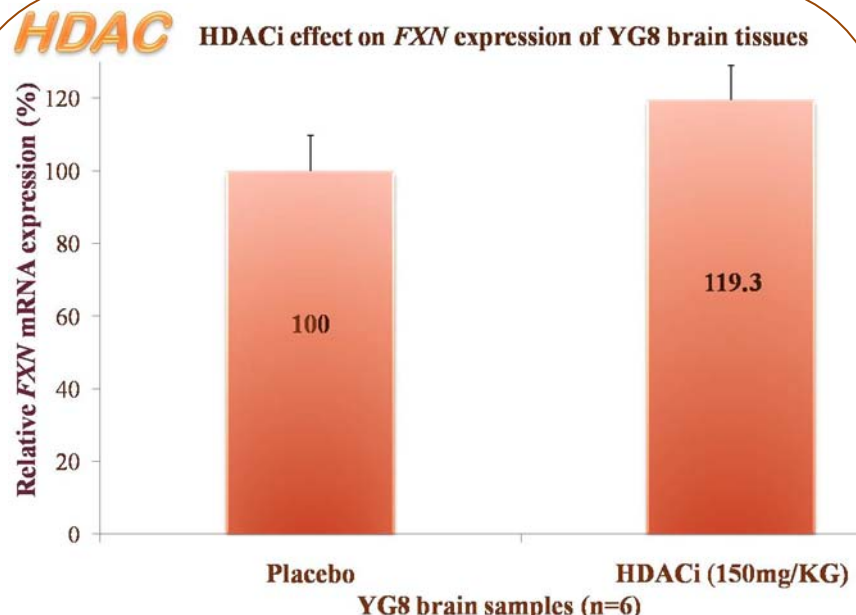
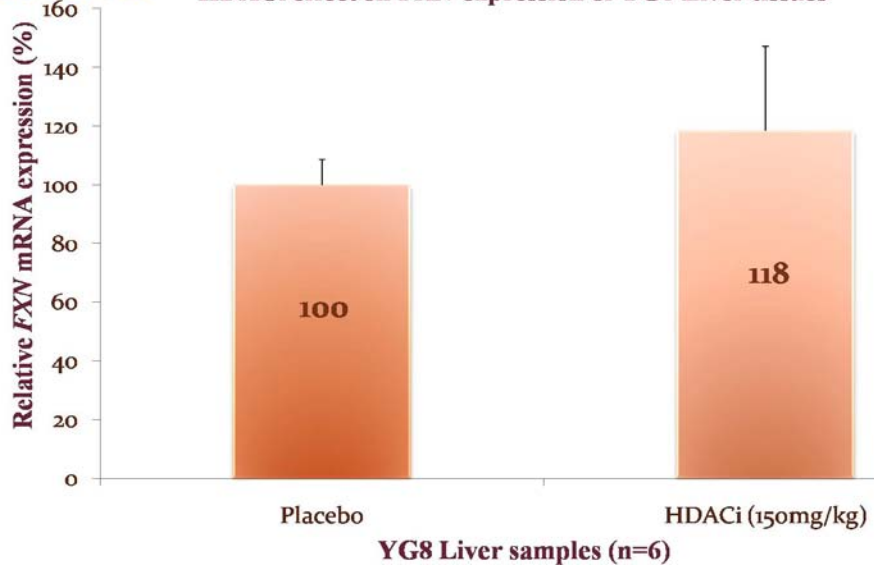
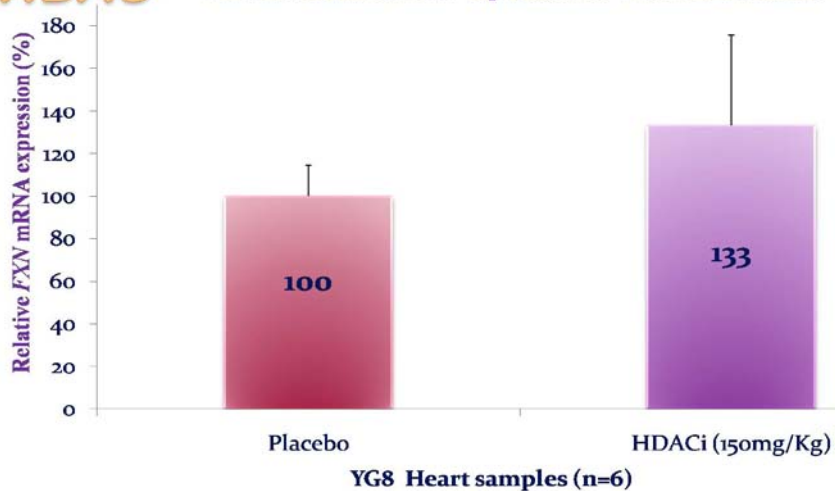


Figure 3.19:

HDACi effect on FXN mRNA of YG8 brain tissues.
Each sample was analysed in biological duplicate. Bars represent S.E.Ms.

HDAC**HDACi effect on *FXN* expression of YG8 Liver tissues****Figure 3.20:****HDACi effect on FXN mRNA of YG8 liver tissues.**

Each sample was analysed in biological duplicate, bars represent S.E.Ms.

HDAC**HDACi effect on *FXN* expression of YG8 Heart tissues****Figure 3.21:****HDACi effect on FXN mRNA of YG8 heart tissues.**

Each sample was analysed in biological duplicate, bars represent S.E.Ms.

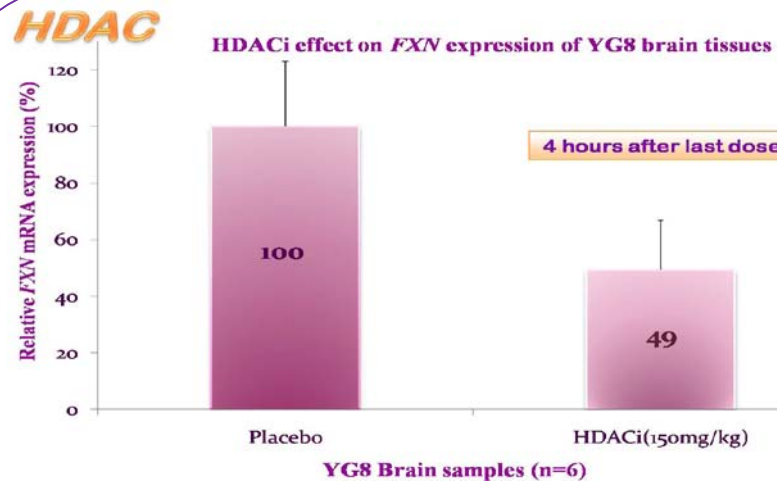


Figure 3.22:

HDACi effect on FXN mRNA of YG8 brain tissues.

After 4 hours from the last dose. P value = 0.014. Each sample was analysed in biological duplicate, bars represent S.E.Ms.

In summary, this is only preliminary data and further experiments are required to have more statistically significant data for this area of research to understand the mechanism of the drug in more depth.

3.5 The HDACi effect on histone modifications of *FXN* in transgenic mouse brain tissues

Chromatin structural changes and histone de-acetylation is involved in many neurological disorders, therefore, using HDACi as a treatment to reverse the heterochromatin region to an active form and restore the transcriptional activity is a recommended approach.

An earlier study using FRDA lymphoblastoid cells showed the affect of HDACis on the state of *FXN* transcription by modifying the histone acetylation profile. It suggested that HDACis will inhibit HDAC enzymes and that will lead to the increase levels of *FXN* histine acetylation leading to increase *FXN* transcription (Herman *et al.* 2006; Gottesfeld 2007).

We investigated the acetylation profile of H3K9ac and H4K12ac in the YG8 transgenic mouse brain tissues for two groups: placebo and HDACi treated for three days at 150mg/kg dose. Some samples were collected at 24 hours after the last dose and the other were collected at 4 hours after the last dose. Samples were processed for ChIP assay followed by the real-time qPCR to obtain our results; DNA samples were precipitated using H3K9ac and H4K12ac anti-bodies.

The results for this experiment are still in their infancy, so this experiment will be continued in the future. However, the preliminary results indicated that the HDACi increased the acetylation pattern of the H3K9ac and the H4K12ac in the *FXN* promoter and upstream the GAA repeat, while, in the downstream region there was no noticeable change in the acetylation profile for both residues (Figure 3.23). The same pattern was observed with the 4 hours brain samples (Figure 3.24), but for this group there is only the preliminary acetylation results for H3K9ac. Overall, these results suggest limited efficiency of the HDACi used in this thesis as a treatment for FRDA disorder. Further HDACis will be explored in the future.

In conclusion, there are still many questions to be answered in this area of research and other areas that can interact to support us with valuable information to move forward toward eliminating the symptoms of neurodegenerative disorders.

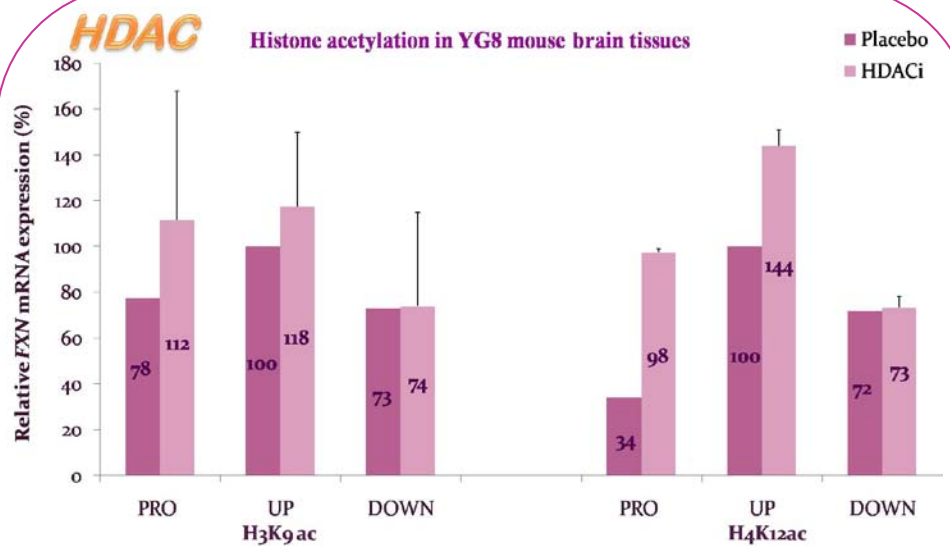


Figure 3.23:

Histone acetylation in YG8 mouse brain tissues.

Represent the acetylation of H3K9ac and H4K12ac after 24 hours from last dose. Each sample was analysed only once in triplicate reactions, bars represent S.E.Ms.

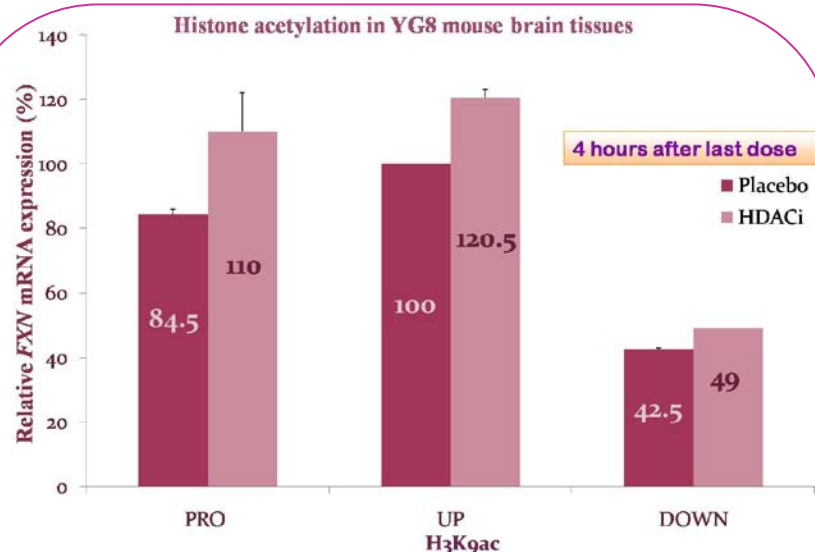


Figure 3.24:

Histone acetylation in YG8 mouse brain tissues.

Represent the acetylation of H3K9ac after 4 hours from last dose. Each sample was analysed only once in triplicate reactions, bars represent S.E.Ms.

Chapter 4

Discussion

Epigenetic modifications and FXN mRNA transcription profile in FRDA human tissues and YG8 and YG22 transgenic mouse tissues

Epigenetic modifications including histone acetylation and methylation in both FRDA human and transgenic mouse brain tissues were demonstrated using ChIP assay analysis and real-time qPCR. The results are aligned with previous studies that showed a decrease in the acetylation pattern of H3K9ac, H3K14ac and H4K16ac in the upstream GAA region in FRDA human cell lines (Herman *et al.* 2006; Greene *et al.* 2007; Rai *et al.* 2008). Our results verify these changes in three regions of the *FXN* gene: *FXN* promoter, upstream GAA and more clearly, in the downstream GAA region of FRDA human and transgenic mice brain tissues. In addition, the results confirmed the increase in the di- and trimethylation patterns of the H3K9me2 and the H3K9me3 residues in the all three regions of the *FXN* gene, which had been reported previously. Moreover, the *FXN* mRNA transcription profile was investigated and indicated a reduced level of the transcription process in the brain, heart and liver tissues of the YG8 and YG22 transgenic mice and in a FRDA human brain tissue. The reduced level of the *FXN* mRNA transcription had been referred previously to the presence of the (GAA)_n·(TTC)_n repeat, as a consequence heterochromatin formation occur leading to the gene silencing.

These results cover the integration of the chromatin modifications and the transcription and expression profile. However, they represent only two sides of a 3-dimension (3D) triangle. In order to have a better understanding of the mechanisms by which the expanded (GAA)_n·(TTC)_n repeats cause the heterochromatin formation, leading to *FXN* gene silencing, the integration of the third factor is required. DNA methylation forms the third side of the triangle, contributing to FRDA disease mechanisms and its contribution is well explained in a recent study on FRDA human and YG8 and YG22 transgenic mice brain and heart tissues (Al-Mahdawi *et al.* 2008). Results showed an overall shift in the DNA methylation

profile, hypomethylation in the downstream the repeat and hypermethylation in the upstream GAA tracts. As a result, DNA methylation is corresponding and correlating with the other changes: chromatin modifications and the expression profile. However, further studies are required to more accurately identify the relationship between these three factors. Moreover, having a clearer understanding of the integration mechanisms between chromatin structure, DNA methylation and expression profiles will lead to a comprehensive understanding of FRDA disease progression and will lead to the identification of new therapeutic approaches.

HDACi effect on epigenetic modifications and FXN mRNA transcription profile in YG8, YG22 transgenic mice tissues

Our preliminary results that demonstrate that the effect of one particular HDACi, which is one of the promising therapeutic approaches, on *FXN* mRNA transcriptional levels and histone modifications (acetylation) in YG8 transgenic mouse brain, heart and liver tissues are harmonized with the results from a previous study. The results for this study, which was conducted using KIKI mouse brain, cerebellum and heart tissues, indicated an increase in the *FXN* mRNA level and in the histone acetylation patterns for 24 hours after last injection with a similar HDACi (Rai *et al.* 2008). Our results showed an increase in the *FXN* mRNA level in different tissues such as, brain, heart and liver of the YG8 transgenic mice after 24 hours from the last HDACi treatment. Furthermore, an increase in the histone acetylation of H3K9ac and H4K12ac mainly in the *FXN* promoter, upstream GAA of the YG8 mice brain tissues was observed. The only exception is the decrease of the *FXN* mRNA transcription level after 4 hours of the last HDACi dose was injected. Here the importance of further investigation of the drug mechanism *in vivo* in more detail becomes an essential step forward in the near future.

In summary, although there are promising results described within this thesis and within other studies that HDACis have the ability to correct the frataxin deficiency and restore it to its normal level, the level of the specificity of the HDACi or any other epigenetic drug must be increased. In our study, it was important to

have this point in our consideration because we used the GAPDH gene as an endogenous reference gene and effecting the expression of this gene will affect our results. In a recent high-density microarray analysis study the results showed that other gene expression levels had been effected with HDACi drug treatment (Rai *et al.* 2008). Therefore, it would be a good idea in future to repeat all of the quantitative PCR experiments using a different housekeeping gene as the endogenous reference. Furthermore, the design of the epigenetic drug molecules to target a specific gene and to know the exact mechanism by which this drug interacts with the transcriptional factors and causes the change will require more substantial studies in the future.

Further recommendations

Due to the time limitation for this project it was not possible to investigate for all histone modifications in a larger sample number. In future, it is important to obtain statistically significant results by analysing these modifications on a larger sample number and analysing each sample as a biological triplicate. In addition, it would be interesting to expand the investigation of the acetylation and methylation modifications of different residues such as, H3K4me1, H3K4me2, H3K9me1 and H3K9me2 of the *FXN* locus in our transgenic mice model. A recent study showed that increase the methylation of H3K4me1,2 and decrease the methylation of H3K9me1,2 is related with the gene activation in human colon cancer cells (Huang *et al.* 2007). What this research group need to obtain for a cancer therapy will be the opposite of what we need for FRDA therapy, so considering these histone modifications and expanding the knowledge about them may be a useful tool leading to another line of efficient therapy for FRDA.

In addition, experiments for the quantitation of the *FXN* mRNA transcriptional level and histone modifications (acetylation) patterns in the FRDA transgenic mouse brain are worth continuing. This will provide important information about the mechanism and the activity of the epigenetic drugs *in vivo*, especially considering the unexpected effect that we saw of the HDACi drug after 4

hours from the last dose. Moreover, it is sensible to design different experiments with different doses of the HDACi for different time ranges to check for the drug activity and toxicity. Other such creative studies are currently underway to produce more efficient therapies for FRDA.

References

- Al-Mahdawi, S., Pinto, R.M., Ismail, O., Varshney, D., Lymperi, S., Sandi, C., Trabzuni, D. and Pook, M. (2008). "The Friedreich ataxia GAA repeat expansion mutation induces comparable epigenetic changes in human and transgenic mouse brain and heart tissues." *Hum Mol Genet* **17**(5): 735-46.
- Al-Mahdawi, S., Pinto, R.M., Ruddle, P., Carroll, C., Webster, Z. and Pook, M. (2004). "GAA repeat instability in Friedreich ataxia YAC transgenic mice." *Genomics* **84**(2): 301-10.
- Al-Mahdawi, S., Pinto, R.M., Varshney, D., Lawrence, L., Lowrie, M.B., Hughes, S., Webster, Z., *et al.* (2006). "GAA repeat expansion mutation mouse models of Friedreich ataxia exhibit oxidative stress leading to progressive neuronal and cardiac pathology." *Genomics* **88**(5): 580-90.
- Andermann, E., Remillard, G.M., Goyer, C., Blitzer, L., Andermann, F. and Barbeau, A. (1976). "Genetic and family studies in Friedreich's ataxia." *Can J Neurol Sci* **3**(4): 287-301.
- Babady, N.E., Carelle, N., Wells, R.D., Rouault, T.A., Hirano, M., Lynch, D.R., Delatycki, M.B., *et al.* (2007). "Advancements in the pathophysiology of Friedreich's Ataxia and new prospects for treatments." *Mol Genet Metab* **92**(1-2): 23-35.
- Baldi, P., Brunak, S., Chauvin, Y. and Pedersen, A.G. (1999). "Structural basis for triplet repeat disorders: a computational analysis." *Bioinformatics* **15**(11): 918-29.
- Baralle, M., Pastor, T., Bussani, E. and Pagani, F. (2008). "Influence of Friedreich ataxia GAA noncoding repeat expansions on pre-mRNA processing." *Am J Hum Genet* **83**(1): 77-88.
- Bencze, K.Z., Yoon, T., Millan-Pacheco, C., Bradley, P.B., Pastor, N., Cowan, J.A. and Stemmler, T.L. (2007). "Human frataxin: iron and ferrochelatase binding surface." *Chem Commun (Camb)*(18): 1798-800.
- Berger, S.L. (2007). "The complex language of chromatin regulation during transcription." *Nature* **447**(7143): 407-12.
- Bidichandani, S.I., Ashizawa, T. and Patel, P.I. (1997). "Atypical Friedreich ataxia caused by compound heterozygosity for a novel missense mutation and the GAA triplet-repeat expansion." *Am J Hum Genet* **60**(5): 1251-6.
- Bird, A. (2007). "Perceptions of epigenetics." *Nature* **447**(7143): 396-8.
- Bock, C. and Lengauer, T. (2008). "Computational epigenetics." *Bioinformatics* **24**(1): 1-10.
- Box, H., Bonney, H. and Greenfield, J. (2005). "The patient's journey: the progressive ataxias." *Bmj* **331**(7523): 1007-9.
- Boyer, S.t., Chisholm, A.W. and Va, M. (1962). "Cardiac aspects of Friedreich's ataxia." *Circulation* **25**: 493-505.
- Branda, S.S., Cavardini, P., Adamec, J., Kalousek, F., Taroni, F. and Isaya, G. (1999). "Yeast and human frataxin are processed to mature form in two sequential steps by the mitochondrial processing peptidase." *J Biol Chem* **274**(32): 22763-9.

- Brice, A. (1998). "Unstable mutations and neurodegenerative disorders." *J Neurol* **245**(8): 505-10.
- Campuzano, V., Montermini, L., Molto, M.D., Pianese, L., Cossee, M., Cavalcanti, F., Monros, E., et al. (1996). "Friedreich's ataxia: autosomal recessive disease caused by an intronic GAA triplet repeat expansion." *Science* **271**(5254): 1423-7.
- Chakravarty, A. (2003). "Friedreich's ataxia--yesterday, today and tomorrow." *Neurol India* **51**(2): 176-82.
- Chiurazzi, P., Pomponi, M.G., Pietrobono, R., Bakker, C.E., Neri, G. and Oostra, B.A. (1999). "Synergistic effect of histone hyperacetylation and DNA demethylation in the reactivation of the FMR1 gene." *Hum Mol Genet* **8**(12): 2317-23.
- Chiurazzi, P., Pomponi, M.G., Willemsen, R., Oostra, B.A. and Neri, G. (1998). "In vitro reactivation of the FMR1 gene involved in fragile X syndrome." *Hum Mol Genet* **7**(1): 109-13.
- Chomczynski, P. and Sacchi, N. (1987). "Single-step method of RNA isolation by acid guanidinium thiocyanate-phenol-chloroform extraction." *Anal Biochem* **162**(1): 156-9.
- Clark, R.M., De Biase, I., Malykhina, A.P., Al-Mahdawi, S., Pook, M. and Bidichandani, S.I. (2007). "The GAA triplet-repeat is unstable in the context of the human FXN locus and displays age-dependent expansions in cerebellum and DRG in a transgenic mouse model." *Hum Genet* **120**(5): 633-40.
- Coppola, G., Choi, S.H., Santos, M.M., Miranda, C.J., Tentler, D., Wexler, E.M., Pandolfo, M. and Geschwind, D.H. (2006). "Gene expression profiling in frataxin deficient mice: microarray evidence for significant expression changes without detectable neurodegeneration." *Neurobiol Dis* **22**(2): 302-11.
- Correia, A.R., Adinolfi, S., Pastore, A. and Gomes, C.M. (2006). "Conformational stability of human frataxin and effect of Friedreich's ataxia-related mutations on protein folding." *Biochem J* **398**(3): 605-11.
- Cossee, M., Puccio, H., Gansmuller, A., Koutnikova, H., Dierich, A., LeMeur, M., Fischbeck, K., Dolle, P. and Koenig, M. (2000). "Inactivation of the Friedreich ataxia mouse gene leads to early embryonic lethality without iron accumulation." *Hum Mol Genet* **9**(8): 1219-26.
- Crews, D. (2008). "Epigenetics and its implications for behavioral neuroendocrinology." *Front Neuroendocrinol* **29**(3): 344-57.
- D'Alessio, A.C. and Szyf, M. (2006). "Epigenetic tete-a-tete: the bilateral relationship between chromatin modifications and DNA methylation." *Biochem Cell Biol* **84**(4): 463-76.
- De Biase, I., Rasmussen, A., Endres, D., Al-Mahdawi, S., Monticelli, A., Cocozza, S., Pook, M. and Bidichandani, S.I. (2007a). "Progressive GAA expansions in dorsal root ganglia of Friedreich's ataxia patients." *Ann Neurol* **61**(1): 55-60.
- De Biase, I., Rasmussen, A., Monticelli, A., Al-Mahdawi, S., Pook, M., Cocozza, S. and Bidichandani, S.I. (2007b). "Somatic instability of the expanded GAA triplet-repeat sequence in Friedreich ataxia progresses throughout life." *Genomics* **90**(1): 1-5.

- De Michele, G., Di Maio, L., Filla, A., Majello, M., Cocozza, S., Cavalcanti, F., Mirante, E. and Campanella, G. (1996). "Childhood onset of Friedreich ataxia: a clinical and genetic study of 36 cases." *Neuropediatrics* **27**(1): 3-7.
- De Michele, G., Filla, A., Cavalcanti, F., Di Maio, L., Pianese, L., Castaldo, I., Calabrese, O., et al. (1994). "Late onset Friedreich's disease: clinical features and mapping of mutation to the FRDA locus." *J Neurol Neurosurg Psychiatry* **57**(8): 977-9.
- Delatycki, M.B., Camakaris, J., Brooks, H., Evans-Whipp, T., Thorburn, D.R., Williamson, R. and Forrest, S.M. (1999). "Direct evidence that mitochondrial iron accumulation occurs in Friedreich ataxia." *Ann Neurol* **45**(5): 673-5.
- Delatycki, M.B., Paris, D., Gardner, R.J., Forshaw, K., Nicholson, G.A., Nassif, N., Williamson, R. and Forrest, S.M. (1998). "Sperm DNA analysis in a Friedreich ataxia premutation carrier suggests both meiotic and mitotic expansion in the FRDA gene." *J Med Genet* **35**(9): 713-6.
- Delatycki, M.B., Williamson, R. and Forrest, S.M. (2000). "Friedreich ataxia: an overview." *J Med Genet* **37**(1): 1-8.
- Della Nave, R., Ginestroni, A., Giannelli, M., Tessa, C., Salvatore, E., Salvi, F., Dotti, M.T., et al. (2008a). "Brain structural damage in Friedreich's ataxia." *J Neurol Neurosurg Psychiatry* **79**(1): 82-5.
- Della Nave, R., Ginestroni, A., Tessa, C., Salvatore, E., Bartolomei, I., Salvi, F., Dotti, M.T., et al. (2008b). "Brain white matter tracts degeneration in Friedreich ataxia. An in vivo MRI study using tract-based spatial statistics and voxel-based morphometry." *Neuroimage* **40**(1): 19-25.
- Dhe-Paganon, S., Shigeta, R., Chi, Y.I., Ristow, M. and Shoelson, S.E. (2000). "Crystal structure of human frataxin." *J Biol Chem* **275**(40): 30753-6.
- Egger, G., Liang, G., Aparicio, A. and Jones, P.A. (2004). "Epigenetics in human disease and prospects for epigenetic therapy." *Nature* **429**(6990): 457-63.
- Feinberg, A.P. (2007). "Phenotypic plasticity and the epigenetics of human disease." *Nature* **447**(7143): 433-40.
- Foury, F. and Cazzalini, O. (1997). "Deletion of the yeast homologue of the human gene associated with Friedreich's ataxia elicits iron accumulation in mitochondria." *FEBS Lett* **411**(2-3): 373-7.
- Fraga, M.F., Ballestar, E., Paz, M.F., Ropero, S., Setien, F., Ballestar, M.L., Heine-Suner, D., et al. (2005). "Epigenetic differences arise during the lifetime of monozygotic twins." *Proc Natl Acad Sci U S A* **102**(30): 10604-9.
- Friedreich, N. (1863a,b). "Über degenerative Atrophie der spinalen Hinterstrange." *Virchow's Arch Pathol Anat* **26**: 391-419, 433-59.
- Friedreich, N. (1863c). "Über degenerative Atrophie der spinalen Hinterstrange." *Virchow's Arch Pathol Anat* **27**: 1-26.
- Friedreich, N. (1876). "Über ataxie mit besonderer berücksichtigung der hereditären formen." *Virchow's Arch Pathol Anat* **68**: 145-245.
- Friedreich, N. (1877). "Über ataxie mit besonderer berücksichtigung der hereditären formen." *Virchow's Arch Pathol Anat* **70**: 140-52.
- Gacy, A.M., Goellner, G.M., Spiro, C., Chen, X., Gupta, G., Bradbury, E.M., Dyer, R.B., et al. (1998). "GAA instability in Friedreich's Ataxia shares a common, DNA-directed and intraallelic mechanism with other trinucleotide diseases." *Mol Cell* **1**(4): 583-93.

- Gakh, O., Park, S., Liu, G., Macomber, L., Imlay, J.A., Ferreira, G.C. and Isaya, G. (2006). "Mitochondrial iron detoxification is a primary function of frataxin that limits oxidative damage and preserves cell longevity." *Hum Mol Genet* **15**(3): 467-79.
- Genschel, J., Littman, S.J., Drummond, J.T. and Modrich, P. (1998). "Isolation of MutSbeta from human cells and comparison of the mismatch repair specificities of MutSbeta and MutSalpha." *J Biol Chem* **273**(31): 19895-901.
- Geoffroy, G., Barbeau, A., Breton, G., Lemieux, B., Aube, M., Leger, C. and Bouchard, J.P. (1976). "Clinical description and roentgenologic evaluation of patients with Friedreich's ataxia." *Can J Neurol Sci* **3**(4): 279-86.
- Giovannangeli, C., Perrouault, L., Escude, C., Gryaznov, S. and Helene, C. (1996). "Efficient inhibition of transcription elongation in vitro by oligonucleotide phosphoramidates targeted to proviral HIV DNA." *J Mol Biol* **261**(3): 386-98.
- Gomez-Sebastian, S., Gimenez-Cassina, A., Diaz-Nido, J., Lim, F. and Wade-Martins, R. (2007). "Infectious delivery and expression of a 135 kb human FRDA genomic DNA locus complements Friedreich's ataxia deficiency in human cells." *Mol Ther* **15**(2): 248-54.
- Gordon, D.M., Shi, Q., Dancis, A. and Pain, D. (1999). "Maturation of frataxin within mammalian and yeast mitochondria: one-step processing by matrix processing peptidase." *Hum Mol Genet* **8**(12): 2255-62.
- Gottesfeld, J.M. (2007). "Small molecules affecting transcription in Friedreich ataxia." *Pharmacol Ther* **116**(2): 236-48.
- Gottlieb, G. (2007). "Probabilistic epigenesis." *Dev Sci* **10**(1): 1-11.
- Grabczyk, E., Mancuso, M. and Sammarco, M.C. (2007). "A persistent RNA.DNA hybrid formed by transcription of the Friedreich ataxia triplet repeat in live bacteria, and by T7 RNAP in vitro." *Nucleic Acids Res* **35**(16): 5351-9.
- Grabczyk, E. and Usdin, K. (2000). "The GAA*TTC triplet repeat expanded in Friedreich's ataxia impedes transcription elongation by T7 RNA polymerase in a length and supercoil dependent manner." *Nucleic Acids Res* **28**(14): 2815-22.
- Grant, L., Sun, J., Xu, H., Subramony, S.H., Chaires, J.B. and Hebert, M.D. (2006). "Rational selection of small molecules that increase transcription through the GAA repeats found in Friedreich's ataxia." *FEBS Lett* **580**(22): 5399-405.
- Greene, E., Mahishi, L., Entezam, A., Kumari, D. and Usdin, K. (2007). "Repeat-induced epigenetic changes in intron 1 of the frataxin gene and its consequences in Friedreich ataxia." *Nucleic Acids Res* **35**(10): 3383-90.
- Grewal, S.I. and Elgin, S.C. (2007). "Transcription and RNA interference in the formation of heterochromatin." *Nature* **447**(7143): 399-406.
- Harding, A. (1984). "The Hereditary Ataxias and Related Disorders" *Edinburgh: Churchill Livingstone*,: 174-90.
- Harding, A.E. (1981). "Friedreich's ataxia: a clinical and genetic study of 90 families with an analysis of early diagnostic criteria and intrafamilial clustering of clinical features." *Brain* **104**(3): 589-620.
- Hebert, M.D. (2007). "Targeting the gene in Friedreich ataxia." *Biochimie*.
- Hebert, M.D. (2008). "Targeting the gene in Friedreich ataxia." *Biochimie* **90**(8): 1131-9.

- Hebert, M.D. and Whittom, A.A. (2007). "Gene-based approaches toward Friedreich ataxia therapeutics." *Cell Mol Life Sci* **64**(23): 3034-43.
- Heintzman, N.D., Stuart, R.K., Hon, G., Fu, Y., Ching, C.W., Hawkins, R.D., Barrera, L.O., et al. (2007). "Distinct and predictive chromatin signatures of transcriptional promoters and enhancers in the human genome." *Nat Genet* **39**(3): 311-8.
- Herman, D., Jenssen, K., Burnett, R., Soragni, E., Perlman, S.L. and Gottesfeld, J.M. (2006). "Histone deacetylase inhibitors reverse gene silencing in Friedreich's ataxia." *Nat Chem Biol* **2**(10): 551-8.
- Holliday, R. (1987). "The inheritance of epigenetic defects." *Science* **238**(4824): 163-70.
- Holliday, R. (2006). "Epigenetics: a historical overview." *Epigenetics* **1**(2): 76-80.
- Holliday, R. and Pugh, J.E. (1975). "DNA modification mechanisms and gene activity during development." *Science* **187**(4173): 226-32.
- Huang, Y., Greene, E., Murray Stewart, T., Goodwin, A.C., Baylin, S.B., Woster, P.M. and Casero, R.A., Jr. (2007). "Inhibition of lysine-specific demethylase 1 by polyamine analogues results in reexpression of aberrantly silenced genes." *Proc Natl Acad Sci U S A* **104**(19): 8023-8.
- Huynen, M.A., Snel, B., Bork, P. and Gibson, T.J. (2001). "The phylogenetic distribution of frataxin indicates a role in iron-sulfur cluster protein assembly." *Hum Mol Genet* **10**(21): 2463-8.
- Jaenisch, R. and Bird, A. (2003). "Epigenetic regulation of gene expression: how the genome integrates intrinsic and environmental signals." *Nat Genet* **33 Suppl**: 245-54.
- Jiralerspong, S., Liu, Y., Montermini, L., Stifani, S. and Pandolfo, M. (1997). "Frataxin shows developmentally regulated tissue-specific expression in the mouse embryo." *Neurobiol Dis* **4**(2): 103-13.
- Karthikeyan, G., Santos, J.H., Graziewicz, M.A., Copeland, W.C., Isaya, G., Van Houten, B. and Resnick, M.A. (2003). "Reduction in frataxin causes progressive accumulation of mitochondrial damage." *Hum Mol Genet* **12**(24): 3331-42.
- Keverne, E.B. and Curley, J.P. (2008). "Epigenetics, brain evolution and behaviour." *Front Neuroendocrinol* **29**(3): 398-412.
- Kim, D. and Rossi, J. (2008). "RNAi mechanisms and applications." *Biotechniques* **44**(5): 613-6.
- Koutnikova, H., Campuzano, V., Foury, F., Dolle, P., Cazzalini, O. and Koenig, M. (1997). "Studies of human, mouse and yeast homologues indicate a mitochondrial function for frataxin." *Nat Genet* **16**(4): 345-51.
- Kovacs, A., Kandala, J.C., Weber, K.T. and Guntaka, R.V. (1996). "Triple helix-forming oligonucleotide corresponding to the polypyrimidine sequence in the rat alpha 1(I) collagen promoter specifically inhibits factor binding and transcription." *J Biol Chem* **271**(3): 1805-12.
- Kovtun, I.V. and McMurray, C.T. (2001). "Trinucleotide expansion in haploid germ cells by gap repair." *Nat Genet* **27**(4): 407-11.
- Kramer, P.R., Pearson, C.E. and Sinden, R.R. (1996). "Stability of triplet repeats of myotonic dystrophy and fragile X loci in human mutator mismatch repair cell lines." *Hum Genet* **98**(2): 151-7.

- Krasilnikova, M.M. and Mirkin, S.M. (2004). "Replication stalling at Friedreich's ataxia (GAA)n repeats in vivo." *Mol Cell Biol* **24**(6): 2286-95.
- Kulkarni, A. and Wilson, D.M., 3rd (2008). "The involvement of DNA-damage and - repair defects in neurological dysfunction." *Am J Hum Genet* **82**(3): 539-66.
- Kunkel, T.A. (1993). "Nucleotide repeats. Slippery DNA and diseases." *Nature* **365**(6443): 207-8.
- Lamarche, J.B., Cote, M. and Lemieux, B. (1980). "The cardiomyopathy of Friedreich's ataxia morphological observations in 3 cases." *Can J Neurol Sci* **7**(4): 389-96.
- Laskowski, R.A. and Thornton, J.M. (2008). "Understanding the molecular machinery of genetics through 3D structures." *Nat Rev Genet* **9**(2): 141-51.
- Lesuisse, E., Santos, R., Matzanke, B.F., Knight, S.A., Camadro, J.M. and Dancis, A. (2003). "Iron use for haeme synthesis is under control of the yeast frataxin homologue (Yfh1)." *Hum Mol Genet* **12**(8): 879-89.
- Lim, F., Palomo, G.M., Mauritz, C., Gimenez-Cassina, A., Illana, B., Wandosell, F. and Diaz-Nido, J. (2007). "Functional recovery in a Friedreich's ataxia mouse model by frataxin gene transfer using an HSV-1 amplicon vector." *Mol Ther* **15**(6): 1072-8.
- Lopez-Arlandis, J.M., Vilchez, J.J., Palau, F. and Sevilla, T. (1995). "Friedreich's ataxia: an epidemiological study in Valencia, Spain, based on consanguinity analysis." *Neuroepidemiology* **14**(1): 14-9.
- Miranda, C.J., Santos, M.M., Ohshima, K., Smith, J., Li, L., Bunting, M., Cossee, M., et al. (2002). "Frataxin knockin mouse." *FEBS Lett* **512**(1-3): 291-7.
- Mirkin, S.M. (2007). "Expandable DNA repeats and human disease." *Nature* **447**(7147): 932-40.
- Muller-Felber, W., Rossmanith, T., Spes, C., Chamberlain, S., Pongratz, D. and Deufel, T. (1993). "The clinical spectrum of Friedreich's ataxia in German families showing linkage to the FRDA locus on chromosome 9." *Clin Investig* **71**(2): 109-14.
- Murrell, A., Rakyan, V.K. and Beck, S. (2005). "From genome to epigenome." *Hum Mol Genet* **14 Spec No 1**: R3-R10.
- Musco, G., Stier, G., Kolmerer, B., Adinolfi, S., Martin, S., Frenkel, T., Gibson, T. and Pastore, A. (2000). "Towards a structural understanding of Friedreich's ataxia: the solution structure of frataxin." *Structure* **8**(7): 695-707.
- Muse, G.W., Gilchrist, D.A., Nechaev, S., Shah, R., Parker, J.S., Grissom, S.F., Zeitlinger, J. and Adelman, K. (2007). "RNA polymerase is poised for activation across the genome." *Nat Genet* **39**(12): 1507-11.
- Mysid. (2007). "Ideogram of the human chromosome 9." Retrieved May 9, 2008, from [\[http://ghr.nlm.nih.gov/chromosome=9\]](http://ghr.nlm.nih.gov/chromosome=9), National Library of Medicine.
- Nafee, T.M., Farrell, W.E., Carroll, W.D., Fryer, A.A. and Ismail, K.M. (2008). "Epigenetic control of fetal gene expression." *Bjog* **115**(2): 158-68.
- Nair, M., Adinolfi, S., Pastore, C., Kelly, G., Temussi, P. and Pastore, A. (2004). "Solution structure of the bacterial frataxin ortholog, CyaY: mapping the iron binding sites." *Structure* **12**(11): 2037-48.
- Napierala, M., Bacolla, A. and Wells, R.D. (2005). "Increased negative superhelical density in vivo enhances the genetic instability of triplet repeat sequences." *J Biol Chem* **280**(45): 37366-76.

- Napoli, E., Taroni, F. and Cortopassi, G.A. (2006). "Frataxin, iron-sulfur clusters, heme, ROS, and aging." *Antioxid Redox Signal* **8**(3-4): 506-16.
- Ohshima, K., Kang, S., Larson, J.E. and Wells, R.D. (1996). "Cloning, characterization, and properties of seven triplet repeat DNA sequences." *J Biol Chem* **271**(28): 16773-83.
- Ohshima, K., Montermini, L., Wells, R.D. and Pandolfo, M. (1998). "Inhibitory effects of expanded GAA.TTC triplet repeats from intron I of the Friedreich ataxia gene on transcription and replication in vivo." *J Biol Chem* **273**(23): 14588-95.
- Pandolfo, M. (1998). "Molecular genetics and pathogenesis of Friedreich ataxia." *Neuromuscul Disord* **8**(6): 409-15.
- Pandolfo, M. (2001). "Molecular basis of Friedreich ataxia." *Mov Disord* **16**(5): 815-21.
- Pandolfo, M. (2003). "Friedreich ataxia." *Semin Pediatr Neurol* **10**(3): 163-72.
- Pandolfo, M. (2006). "Iron and Friedreich ataxia." *J Neural Transm Suppl*(70): 143-6.
- Pandolfo, M. (2008). "Drug Insight: antioxidant therapy in inherited ataxias." *Nat Clin Pract Neurol* **4**(2): 86-96.
- Parniewski, P., Bacolla, A., Jaworski, A. and Wells, R.D. (1999). "Nucleotide excision repair affects the stability of long transcribed (CTG*CAG) tracts in an orientation-dependent manner in Escherichia coli." *Nucleic Acids Res* **27**(2): 616-23.
- Paves, H. (2003). "Dorsal root ganglion neurons of an embryonic rat (100x)." Retrieved March 25, 2008, from Laboratory of Molecular Genetics, National Institute of Chemical Physics and Biophysics in Tallinn, Estonia [<http://www.nikonsmallworld.com/gallery.php?grouping=year&year=2003&imageid=68>].
- Pearson, C.E., Nichol Edamura, K. and Cleary, J.D. (2005). "Repeat instability: mechanisms of dynamic mutations." *Nat Rev Genet* **6**(10): 729-42.
- Pelletier, R., Krasilnikova, M.M., Samadashwily, G.M., Lahue, R. and Mirkin, S.M. (2003). "Replication and expansion of trinucleotide repeats in yeast." *Mol Cell Biol* **23**(4): 1349-57.
- Pianese, L., Cavalcanti, F., De Michele, G., Filla, A., Campanella, G., Calabrese, O., Castaldo, I., Monticelli, A. and Cocozza, S. (1997). "The effect of parental gender on the GAA dynamic mutation in the FRDA gene." *Am J Hum Genet* **60**(2): 460-3.
- Pollard, L.M., Bourn, R.L. and Bidichandani, S.I. (2008). "Repair of DNA double-strand breaks within the (GAA*TTC)n sequence results in frequent deletion of the triplet-repeat sequence." *Nucleic Acids Res* **36**(2): 489-500.
- Pook, M.A., Al-Mahdawi, S., Carroll, C.J., Cossee, M., Puccio, H., Lawrence, L., Clark, P., et al. (2001). "Rescue of the Friedreich's ataxia knockout mouse by human YAC transgenesis." *Neurogenetics* **3**(4): 185-93.
- Potaman, V.N., Oussatcheva, E.A., Lyubchenko, Y.L., Shlyakhtenko, L.S., Bidichandani, S.I., Ashizawa, T. and Sinden, R.R. (2004). "Length-dependent structure formation in Friedreich ataxia (GAA)_n*(TTC)_n repeats at neutral pH." *Nucleic Acids Res* **32**(3): 1224-31.
- Ptak, C. and Petronis, A. (2008). "Epigenetics and complex disease: from etiology to new therapeutics." *Annu Rev Pharmacol Toxicol* **48**: 257-76.

- Puccio, H. and Koenig, M. (2002). "Friedreich ataxia: a paradigm for mitochondrial diseases." *Curr Opin Genet Dev* **12**(3): 272-7.
- Rai, M., Soragni, E., Jenssen, K., Burnett, R., Herman, D., Coppola, G., Geschwind, D.H., Gottesfeld, J.M. and Pandolfo, M. (2008). "HDAC inhibitors correct frataxin deficiency in a Friedreich ataxia mouse model." *PLoS ONE* **3**(4): e1958.
- Robertson, K.D. (2005). "DNA methylation and human disease." *Nat Rev Genet* **6**(8): 597-610.
- Rolfsmeier, M.L., Dixon, M.J. and Lahue, R.S. (2000). "Mismatch repair blocks expansions of interrupted trinucleotide repeats in yeast." *Mol Cell* **6**(6): 1501-7.
- Rotig, A., de Lonlay, P., Chretien, D., Foury, F., Koenig, M., Sidi, D., Munnich, A. and Rustin, P. (1997). "Aconitase and mitochondrial iron-sulphur protein deficiency in Friedreich ataxia." *Nat Genet* **17**(2): 215-7.
- Sakamoto, N., Ohshima, K., Montermini, L., Pandolfo, M. and Wells, R.D. (2001). "Sticky DNA, a self-associated complex formed at long GAA*TTC repeats in intron 1 of the frataxin gene, inhibits transcription." *J Biol Chem* **276**(29): 27171-7.
- Sambrook, J., Fritsch, E.F. and Maniatis, T. (1989). Molecular Cloning: a laboratory manual. 2nd edition. New York, Cold Spring Harbor Laboratory, Cold Spring Harbor Laboratory Press. 1659 p. ISBN 0-87969-309-6.
- Santos-Reboucas, C.B. and Pimentel, M.M. (2007). "Implication of abnormal epigenetic patterns for human diseases." *Eur J Hum Genet* **15**(1): 10-7.
- Sarsero, J.P., Holloway, T.P., Li, L., McLenachan, S., Fowler, K.J., Bertoncello, I., Vouillaire, L., Gazeas, S. and Ioannou, P.A. (2005). "Evaluation of an FRDA-EGFP genomic reporter assay in transgenic mice." *Mamm Genome* **16**(4): 228-41.
- Saveliev, A., Everett, C., Sharpe, T., Webster, Z. and Festenstein, R. (2003). "DNA triplet repeats mediate heterochromatin-protein-1-sensitive variegated gene silencing." *Nature* **422**(6934): 909-13.
- Schones, D.E. and Zhao, K. (2008). "Genome-wide approaches to studying chromatin modifications." *Nat Rev Genet* **9**(3): 179-91.
- Scrimgeour, E.M., Krishna, A.G., Gasim, A., Zawawi, T.H., Johnston, W.J., Barron, L. and Brock, D.J. (1996). "Friedreich's ataxia, with retained lower limb tendon reflexes, in a Saudi Arabian family." *Clin Neurol Neurosurg* **98**(1): 8-11.
- Seznec, H., Wilson, R.B. and Puccio, H. (2004). "2003 International Friedreich's Ataxia Research Conference, 14-16 February 2003, Bethesda, MD, USA." *Neuromuscul Disord* **14**(1): 70-82.
- Sharma, R., Bhatti, S., Gomez, M., Clark, R.M., Murray, C., Ashizawa, T. and Bidichandani, S.I. (2002). "The GAA triplet-repeat sequence in Friedreich ataxia shows a high level of somatic instability in vivo, with a significant predilection for large contractions." *Hum Mol Genet* **11**(18): 2175-87.
- Simon, D., Seznec, H., Gansmuller, A., Carelle, N., Weber, P., Metzger, D., Rustin, P., Koenig, M. and Puccio, H. (2004). "Friedreich ataxia mouse models with progressive cerebellar and sensory ataxia reveal autophagic neurodegeneration in dorsal root ganglia." *J Neurosci* **24**(8): 1987-95.

- Sinden, R.R., Potaman, V.N., Oussatcheva, E.A., Pearson, C.E., Lyubchenko, Y.L. and Shlyakhtenko, L.S. (2002). "Triplet repeat DNA structures and human genetic disease: dynamic mutations from dynamic DNA." *J Biosci* **27**(1 Suppl 1): 53-65.
- Spivakov, M. and Fisher, A.G. (2007). "Epigenetic signatures of stem-cell identity." *Nat Rev Genet* **8**(4): 263-71.
- Struhl, K. (2007). "Interpreting Chromatin Immunoprecipitation Experiments." In *Evaluating Techniques in Biochemical Research*, D. Zuk, ed: 29-33.
- Stuffrein-Roberts, S., Joyce, P.R. and Kennedy, M.A. (2008). "Role of epigenetics in mental disorders." *Aust N Z J Psychiatry* **42**(2): 97-107.
- Sturm, B., Stupphann, D., Kaun, C., Boesch, S., Schranzhofer, M., Wojta, J., Goldenberg, H. and Scheiber-Mojdehkar, B. (2005). "Recombinant human erythropoietin: effects on frataxin expression in vitro." *Eur J Clin Invest* **35**(11): 711-7.
- Tamkun, J.W. (2007). "Stalled polymerases and transcriptional regulation." *Nat Genet* **39**(12): 1421-2.
- Taroni, F. and DiDonato, S. (2004). "Pathways to motor incoordination: the inherited ataxias." *Nat Rev Neurosci* **5**(8): 641-55.
- Thompson, L.M. (2008). "Neurodegeneration: a question of balance." *Nature* **452**(7188): 707-8.
- VanGuilder, H.D., Vrana, K.E. and Freeman, W.M. (2008). "Twenty-five years of quantitative PCR for gene expression analysis." *Biotechniques* **44**(5): 619-26.
- Waddington, C.H. (1942). "Canalization of development and the inheritance of acquired characters." *Nature* **150**: 563-565.
- Waldvogel, D., van Gelderen, P. and Hallett, M. (1999). "Increased iron in the dentate nucleus of patients with Friedreich's ataxia." *Ann Neurol* **46**(1): 123-5.
- Wang, Z. and Storm, D.R. (2006). "Extraction of DNA from mouse tails." *Biotechniques* **41**(4): 410, 412.
- Warren, S.T. (1997). "Polyalanine expansion in synpolydactyly might result from unequal crossing-over of HOXD13." *Science* **275**(5298): 408-9.
- Wells, R.D. (2008). "DNA triplets and Friedreich ataxia." *Faseb J* **22**(6): 1625-34.
- Wells, R.D., Dere, R., Hebert, M.L., Napierala, M. and Son, L.S. (2005). "Advances in mechanisms of genetic instability related to hereditary neurological diseases." *Nucleic Acids Res* **33**(12): 3785-98.
- Zeitlinger, J., Stark, A., Kellis, M., Hong, J.W., Nechaev, S., Adelman, K., Levine, M. and Young, R.A. (2007). "RNA polymerase stalling at developmental control genes in the *Drosophila melanogaster* embryo." *Nat Genet* **39**(12): 1512-6.

Appendix 1

The Friedreich ataxia GAA repeat expansion mutation induces comparable epigenetic changes in human and transgenic mouse brain and heart tissues

Sahar Al-Mahdawi, Ricardo Mouro Pinto, Ozama Ismail, Dhaval Varshney, Stefania Lympéri, Chiranjeevi Sandi, Daniah Trabzuni and Mark Pook*

Hereditary Ataxia Group, Centre for Cell & Chromosome Biology and Brunel Institute of Cancer Genetics & Pharmacogenomics, Division of Biosciences, School of Health Sciences & Social Care, Brunel University, Uxbridge UB8 3PH, UK

Received September 20, 2007; Revised November 17, 2007; Accepted November 25, 2007

Friedreich ataxia (FRDA) is caused by a homozygous GAA repeat expansion mutation within intron 1 of the *FXN* gene, leading to reduced expression of frataxin protein. Evidence suggests that the mutation may induce epigenetic changes and heterochromatin formation, thereby impeding gene transcription. In particular, studies using FRDA patient blood and lymphoblastoid cell lines have detected increased DNA methylation of specific CpG sites upstream of the GAA repeat and histone modifications in regions flanking the GAA repeat. In this report we show that such epigenetic changes are also present in FRDA patient brain, cerebellum and heart tissues, the primary affected systems of the disorder. Bisulfite sequence analysis of the *FXN* flanking GAA regions reveals a shift in the FRDA DNA methylation profile, with upstream CpG sites becoming consistently hypermethylated and downstream CpG sites becoming consistently hypomethylated. We also identify differential DNA methylation at three specific CpG sites within the *FXN* promoter and one CpG site within exon 1. Furthermore, we show by chromatin immunoprecipitation analysis that there is overall decreased histone H3K9 acetylation together with increased H3K9 methylation of FRDA brain tissue. Further studies of brain, cerebellum and heart tissues from our GAA repeat expansion-containing FRDA YAC transgenic mice reveal comparable epigenetic changes to those detected in FRDA patient tissue. We have thus developed a mouse model that will be a valuable resource for future therapeutic studies targeting epigenetic modifications of the *FXN* gene to increase frataxin expression.

INTRODUCTION

FRDA is an autosomal recessive neurodegenerative disorder that is predominantly caused by a homozygous GAA repeat expansion mutation within intron 1 of the *FXN* gene (1). Normal individuals have 5–30 GAA repeat sequences, whereas affected individuals have from approximately 70 to more than 1000 GAA triplets (2). The GAA repeat shows somatic instability, with progressive expansion throughout life, particularly in the cerebellum and dorsal root ganglia (DRG) (3–5). The effect of the GAA expansion mutation is

to reduce the expression of frataxin (6), a mitochondrial protein that acts as an iron chaperone in iron–sulphur cluster and heme biosynthesis (7–9). Frataxin insufficiency leads to oxidative stress, mitochondrial iron accumulation and resultant cell death, with the primary site of pathology being in the large sensory neurons of the DRG and the dentate nucleus of the cerebellum (10). The outcome is progressive spinocerebellar neurodegeneration, causing symptoms of ataxia, dysarthria, muscle weakness and sensory loss, together with cardiomyopathy and diabetes. At present there is no effective treatment for FRDA, and affected individuals

*To whom correspondence should be addressed. Tel: +44 1895267243; Fax: +44 1895274348; Email: mark.pook@brunel.ac.uk

generally die in early adulthood from the associated heart disease.

Preclinical and clinical trials using antioxidants and iron chelators have demonstrated some limited success in alleviating FRDA heart pathology (11–16). However, a more effective overall therapeutic strategy may be to target the immediate effects of the GAA repeat expansion mutation to restore normal levels of frataxin expression. The exact mechanism by which the GAA repeat expansion leads to decreased frataxin expression is unknown, but several models have been put forward. First, it has been suggested that the GAA repeat expansion may adopt abnormal DNA or DNA/RNA hybrid structures that interfere with *FXN* gene transcription (17–20). Secondly, there is evidence that GAA repeat expansions produce a heterochromatin-mediated gene silencing effect (21). Epigenetic mechanisms, such as DNA methylation and the associated deacetylation and methylation of histones are known to affect gene expression by chromatin remodelling (22), and these epigenetic changes are likely to underpin any GAA repeat-induced heterochromatin-mediated gene silencing effects. In support of this hypothesis, research has recently shown increased DNA methylation of three specific CpG sites immediately upstream of the expanded GAA repeat sequence in FRDA patient lymphoblastoid cell lines and primary lymphocytes, and one of the three CpG sites was identified as an important enhancer of frataxin expression (23). Other studies have identified specific histone modifications that are associated with gene silencing within the GAA repeat expansion-flanking regions of the *FXN* intron 1 sequence in FRDA lymphoblastoid cell lines and primary lymphocytes (23,24). These changes include deacetylation of histone H3 and H4 lysine residues and increased di- and trimethylation of H3K9. Based on the hypothesis that the acetylation state of the core histones is responsible for gene silencing, novel histone deacetylase (HDAC) inhibitor compounds have been developed and have been shown to increase *FXN* transcription in FRDA lymphoblastoid cells and primary lymphocytes (24).

These previous epigenetic studies have provided valuable insights into the possible mechanism of GAA-induced transcription inhibition, but they do not address the issue of whether such epigenetic changes are actually present in the most clinically relevant FRDA tissues. Therefore, we decided to investigate epigenetic profiles of the *FXN* gene in FRDA patient autopsy brain, cerebellum and heart tissue. By bisulfite sequencing and ChIP analysis we now report changes in DNA methylation and histone modifications that are consistent with inhibition of *FXN* transcription. With a view to future epigenetic-based FRDA therapies, we also investigated the *FXN* epigenetic profiles within brain, cerebellum and heart tissue from our Y47, YG8 and YG22 FRDA YAC transgenic mouse models (25–27). We find that the GAA repeat expansion-containing FRDA mouse models (YG8 and YG22) exhibit comparable epigenetic changes to those detected in FRDA patient tissue. Therefore, these are excellent FRDA mouse models in which to investigate the therapeutic effects of epigenetically acting compounds, such as novel HDAC inhibitors or DNA methylation inhibitors.

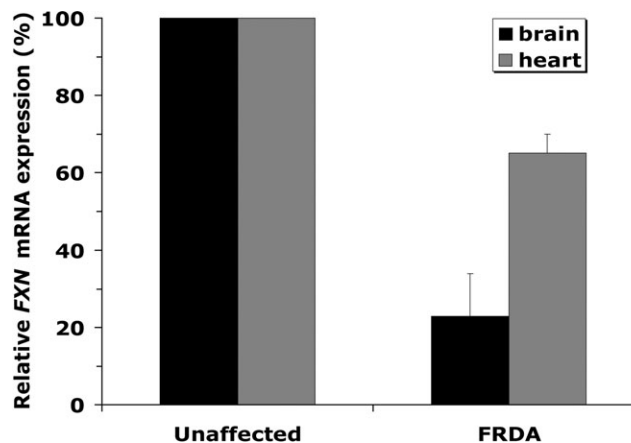


Figure 1. Quantitative RT–PCR analysis of *FXN* mRNA isolated from brain and heart autopsy samples of two FRDA patients (750/650 and 700/700 GAA repeats) and two unaffected individuals. The mean values of FRDA patient tissue data are normalized to the mean *FXN* mRNA level of the unaffected individuals taken as 100%. Two individual cDNA samples were analysed for each tissue and each reaction was carried out in triplicate. Bars represent SEMs.

RESULTS

FXN gene DNA methylation profiles are distinctly altered in human FRDA brain and heart tissues

A previous investigation of the *FXN* gene in FRDA patient lymphoblastoid cell lines and blood samples has detected hypermethylation at three specific CpG sites immediately upstream of the expanded GAA repeat sequence. One of the three CpG sites was further identified as an important enhancer element for frataxin expression (23). This same study also reported a lack of any DNA methylation in the promoter region of either FRDA or unaffected cells.

However, cultured cells are known to often develop non-physiological DNA methylation profiles. Furthermore, FRDA is a systemic disorder that is known to have differentially affected tissues and cell types. Therefore, we chose to investigate the DNA methylation status in two of the primary affected tissues in FRDA, namely brain and heart. We obtained brain and heart autopsy tissues from two FRDA patients (GAA repeat sizes of 750/650 and 700/700) and two unaffected individuals, and we first determined the *FXN* transcription levels of the samples by quantitative RT–PCR. The FRDA brain and heart samples showed mean values of 23 and 65% *FXN* expression, respectively, compared with the unaffected samples (Fig. 1). We then analysed the DNA methylation status of the samples by performing bisulfite sequence analysis of three regions of the *FXN* gene: (i) a 475 bp sequence that encompasses part of the *FXN* promoter, exon 1 and start of intron 1, containing 59 CpG sites; (ii) a 286 bp sequence upstream of the GAA repeat, containing 8 CpG sites and (iii) a 275 bp sequence downstream of the GAA repeat, containing 12 CpG sites (Fig. 2). A comparison of the bisulfite sequences from the FRDA patient and control brain and heart tissues reveals a certain degree of DNA methylation in all eight of the upstream GAA CpG sites (Fig. 3C and D) and all 12 of the downstream GAA CpG sites (Fig. 3E and F). However, the data show a

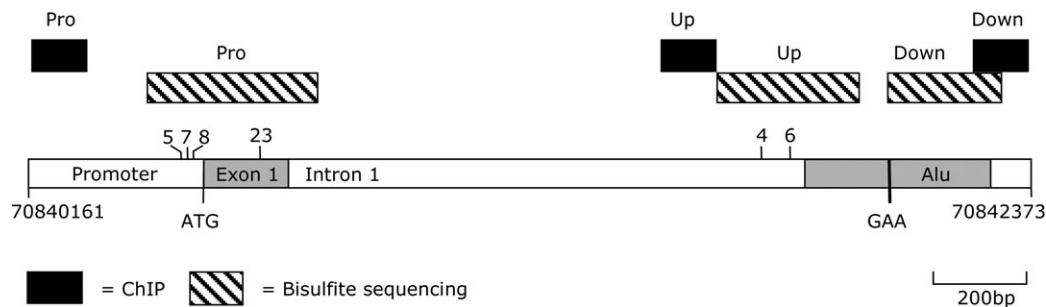


Figure 2. Schematic representation of 2.2 kb at the 5' end of the *FXN* gene, indicating the promoter/exon 1 (Pro), upstream GAA (Up) and downstream GAA (Down) regions that were analysed by ChIP (black boxes) and bisulfite sequencing (hatched boxes). Numbers above indicate the position of CpG sites within the promoter and upstream GAA regions. The positions of the ATG translation start codon, exon 1 open reading frame and GAA repeat sequence within the Alu repeat sequence are shown. Numbers below indicate the chromosome 9 base pair numbering according to the 2006 build of the UCSC human DNA sequence database.

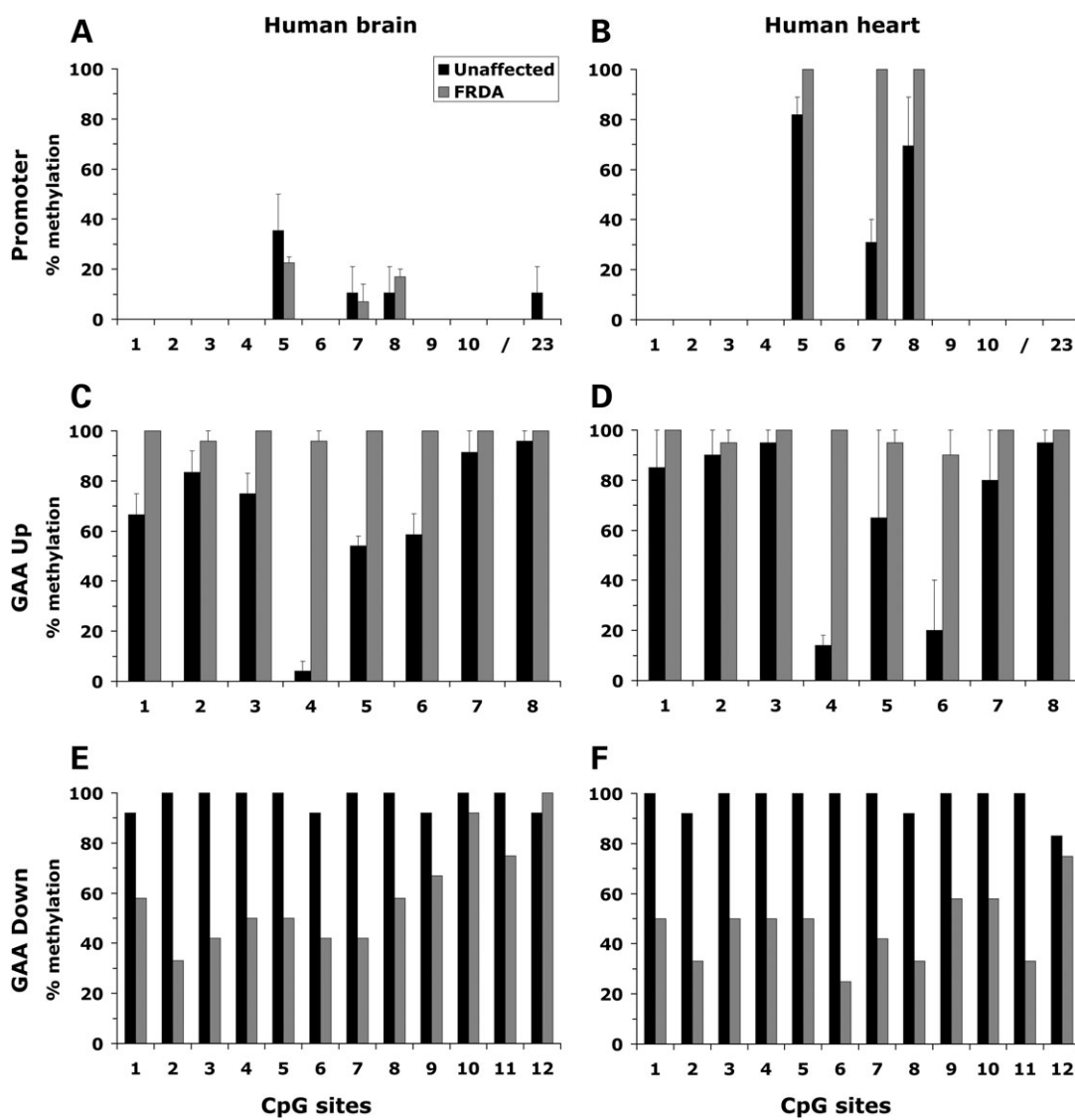


Figure 3. DNA methylation analysis of the *FXN* promoter (A and B), upstream GAA (C and D) and downstream GAA (E and F) regions of human brain and heart tissues. In each case for the *FXN* promoter and upstream GAA regions the mean percentage (+SEM) of methylated CpG sites is shown as determined from the analysis of two FRDA patients and two unaffected individuals, with 7–12 independent cloned DNA sequences analysed for each. For the downstream region the percentage of methylated CpG sites has been determined from one FRDA patient and one unaffected individual (12 independent cloned DNA sequences analysed for each). Only eleven CpG sites are represented for the promoter region (A and B), as sites 11–22 and 24–59 did not show any methylation in either FRDA or unaffected samples in brain or heart. FRDA brain tissues and both FRDA and unaffected heart tissues did not show any DNA methylation at CpG site 23.

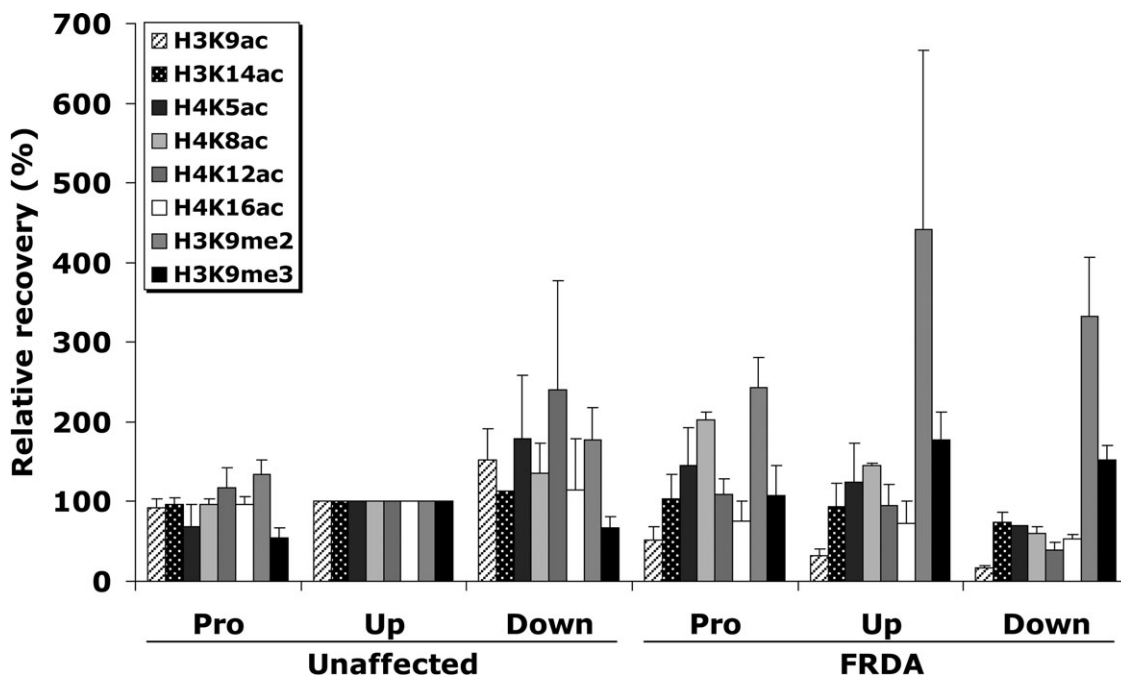


Figure 4. Analysis of histone modifications in human brain tissue. ChIP quantitative PCR results for the *FXN* promoter/exon1 (Pro), upstream GAA (Up) and downstream GAA (Down) amplified regions are represented as the relative amount of immunoprecipitated DNA compared with input DNA, having taken negligible –Ab control values into account. *FXN* values were normalized with human *GAPDH* and all values have been adjusted so that all of the Upstream GAA mean values from the unaffected individuals are 100%. In each case two individual ChIP samples from two FRDA patients and two unaffected controls were analysed in triplicate. The means and SEMs of these values are shown.

consistent shift in the DNA methylation pattern around the GAA repeat in both tissue types. The FRDA upstream GAA CpG sites are comparatively hypermethylated, whereas the FRDA downstream GAA CpG sites are comparatively hypomethylated (Fig. 3C–F). The greatest increases in DNA methylation within the upstream GAA region are seen at CpG sites 4, 5 and 6, the latter of which corresponds to the previously described E-box enhancer element (23). We observed 100% methylation at CpG site 6 in FRDA brain tissues (*FXN* mRNA level of 23%, Fig. 1) compared with a mean value of 90% methylation in heart tissue (*FXN* mRNA level of 65%, Fig. 1). Thus, the upstream GAA DNA methylation changes in both FRDA brain and heart are consistent with their proposed roles in inhibition of *FXN* transcription. However, the finding of decreased DNA methylation in the downstream GAA region (Fig. 3E and F) is somewhat unexpected, since all of the 12 CpG sites fall within an Alu repeat sequence and such sequences are usually repressed by heavy DNA methylation.

Another particularly interesting finding was the identification of differential DNA methylation at three specific CpG sites within the *FXN* promoter (sites 5, 7 and 8) and one CpG site within exon 1 (site 23) (Fig. 3A and B). All of the other 55 CpG sites in the total of 59 CpG sites analysed show complete lack of DNA methylation, as to be expected for a CpG island that is situated at the start of a gene. CpG sites 5, 7 and 8 show incomplete methylation in the unaffected heart, but complete methylation in the FRDA heart (Fig. 3B). Therefore, these CpG sites may be involved in reducing initiation of *FXN* gene transcription in FRDA heart. However, the DNA methylation pattern is different in brain

tissue. Here we identified mean values of 10–35% DNA methylation at the four CpG sites in the unaffected tissues, but very little overall change of DNA methylation in FRDA tissues, or even loss of methylation at CpG sites 5 and 23 (Fig. 3A). Furthermore, the fact that we have identified some degree of DNA methylation at all in this region contrasts with the previous report that DNA methylation is absent in the *FXN* promoter region of both FRDA and unaffected lymphoblastoid cells (23). Therefore, we have shown that the influence of DNA methylation on *FXN* gene expression is likely to be complex, with some similarities (CpG site usage) but also some distinct differences (degree of CpG methylation) identified between different somatic tissues.

FXN gene histone modifications are altered in human FRDA brain tissue

Previous studies of the promoter, upstream GAA and downstream GAA regions of the *FXN* gene have identified specific histone modifications that are associated with gene silencing within the GAA repeat expansion-flanking regions of the *FXN* intron 1 sequence in FRDA lymphoblastoid cell lines and primary lymphocytes (23,24). We have now investigated acetylated histone H3 and H4 and methylated histone H3K9 modifications by ChIP analysis of the *FXN* promoter, upstream GAA and downstream GAA regions (Fig. 2) in autopsy brain tissues from two FRDA patients and two unaffected individuals. Our results show overall decreased histone H3 and H4 acetylation of FRDA brain tissue, particularly in the downstream GAA region (Fig. 4). All of the six acetylated histone residues that we have examined show a GAA-induced gradient of

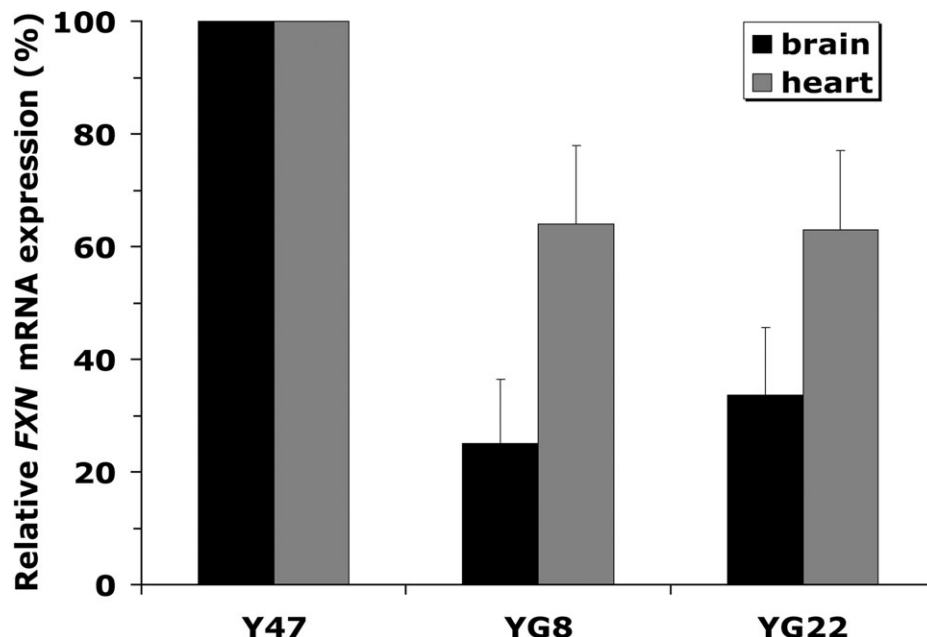


Figure 5. Quantitative RT–PCR analysis of transgenic *FXN* mRNA isolated from Y47 (9 GAA), YG8 (190+90 GAA) and YG22 (190 GAA) mouse brain and heart tissues. Data are normalized to the mean *FXN* mRNA level found in the non-GAA transgenic control samples taken as 100%. Two individual cDNA samples were analysed for each tissue from two mice of each line and each reaction was carried out in triplicate. The means and SEMs of these values are shown.

comparative acetylation that is highest in the *FXN* promoter and lowest in the downstream GAA region. The single most altered histone residue is H3K9, which exhibits progressive decreases in acetylation to comparative levels of 56, 32 and 11% in the *FXN* promoter, upstream GAA and downstream GAA regions, respectively. There is also a consistently increased H3K9 di- and tri-methylation of FRDA brain tissue in all three of the *FXN* gene regions (Fig. 4). These changes concur with the previous findings of increased H3K9 di- and tri-methylation in the upstream GAA region of other cell types (23,24). However, we have now extended these studies to show that in FRDA brain the H3K9 di- and tri-methylation spreads to both *FXN* promoter and downstream GAA regions.

DNA methylation profiles of *FXN* transgenic mouse brain and heart tissues resemble the profiles of human tissue

Having determined the epigenetic profiles around the human *FXN* gene, we then investigated the epigenetic profiles of the *FXN* transgene in brain and heart tissue isolated from YG8 and YG22 GAA repeat expansion-containing *FXN* YAC transgenic mice (26) compared with Y47 normal-sized GAA repeat-containing *FXN* YAC transgenic mice (27). Initial determination of *FXN* transgene expression showed YG8 (90+190 GAA repeats) and YG22 (190 GAA repeats) to have mean decreased mRNA levels of ~26 and 35% in brain and 57 and 56% in heart compared with Y47 (Fig. 5). Thus, inhibition of *FXN* expression in transgenic mouse brain and heart was comparable with the mean values of 23 and 65% observed in the human FRDA brain and heart samples, respectively (Fig. 1). DNA methylation analysis was then performed on the GAA repeat expansion-containing YG8 and YG22 GAA repeat transgenic mouse tissue samples compared with the Y47 non-GAA repeat

controls (3–4 individual mice for each group). As the mouse transgenes consist of entire human *FXN* gene sequence, we were able to investigate the DNA methylation profiles of exactly the same three regions of the *FXN* gene that we had previously analysed in human tissue (Fig. 2). Our data show that the DNA methylation profiles of upstream GAA regions of both YG8 and YG22 transgenic mouse brain and heart tissues closely resemble those found in human tissues (Fig. 6C and D). Namely, there is a consistent hypermethylation of the upstream GAA region induced by the GAA repeat expansion, with the most prominent hypermethylation at CpG sites 4, 5 and 6. However, the degree of DNA methylation at CpG sites 4 and 6 in YG8 and YG22 transgenic mouse brain tissue is less than that observed in FRDA human brain tissue, and indeed YG8 shows no difference at all at CpG site 6. The downstream GAA region differs from the human situation in that there is hypermethylation at all CpG sites, which is retained upon introduction of the GAA repeat expansion (Fig. 6E and F). Thus, there is no GAA-induced decrease in DNA methylation as detected in the human tissues. The promoter/exon 1 regions of the *FXN* transgenes in both mouse brain and heart tissues show a similarity to the human tissues in that DNA methylation is found at only four specific CpG sites: 5, 7, 8 and 23 (Fig. 6A and B). However, the changes in the DNA profiles of these four CpG sites upon introduction of the GAA repeat expansion differ markedly from those found in the human tissues. This time, the brain tissue shows either no change (CpG sites 5 and 7) or an increase (CpG sites 8 and 23) in DNA methylation, whereas the heart tissue shows an overall decrease in DNA methylation. Assessment of the entire mouse DNA methylation data indicates a similar overall DNA methylation profile around the start of the *FXN* gene that is consistent with inhibition of *FXN* transcription.

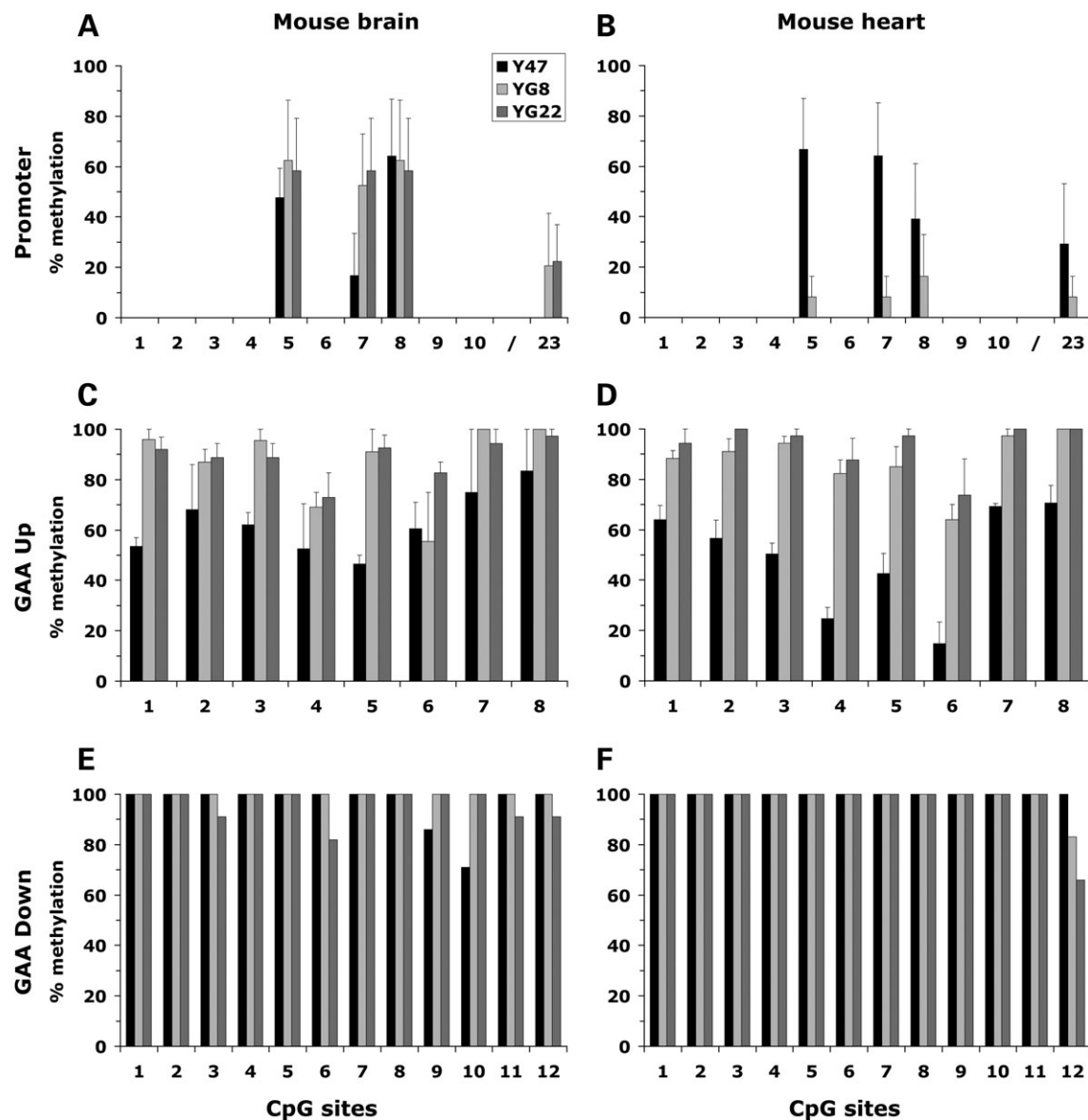


Figure 6. DNA methylation analysis of the *FXN* promoter (A and B), upstream GAA (C and D) and downstream GAA (E and F) regions of Y47 (black columns), YG8 (light grey columns) and YG22 (dark grey columns) transgenic mouse brain and heart tissues. In each case for the *FXN* promoter and upstream GAA regions, the mean percentage value (+SEM) of methylated CpG sites is shown as determined from the analysis of 7–12 independent cloned DNA sequences from each of 3–4 mice per group. For the downstream region the percentages of methylated CpG sites have been determined from one Y47, YG8 and YG22 mouse (12 independent cloned DNA sequences analysed for each). Only eleven CpG sites are represented for the promoter region, as sites 11–22 and 24–59 did not show any methylation in either FRDA or unaffected samples in brain or heart. Y47 brain tissues did not show any DNA methylation at CpG site 23, while YG22 heart tissues did not show any DNA methylation at any CpG site within the promoter region.

However, there are also some specific differences, which may result from epigenetic-control or transcriptional-control variations between the human and the mouse that will require further investigation.

DNA methylation profiles of the upstream GAA region in *FXN* human and transgenic mouse cerebellar tissues are comparable and more severely altered than in other brain tissue

To investigate potential variation within distinct regions of the brain we further analysed the DNA methylation profiles within

the upstream GAA region of cerebellar tissue from one FRDA patient compared with an unaffected control and two individual mice from each of the YG8 and YG22 lines compared with the Y47 control line. We chose to investigate the cerebellum because this structure is known to be involved in FRDA pathology (10) and we ourselves have observed increased GAA repeat instability primarily within the cerebellum of both human FRDA patient and FRDA transgenic mouse tissues (3,5,25). The results (shown in Fig. 7) reveal similar DNA methylation changes to those observed in both human and mouse brain tissues. However, the degree of hypermethylation change in the GAA repeat expansion-containing human and

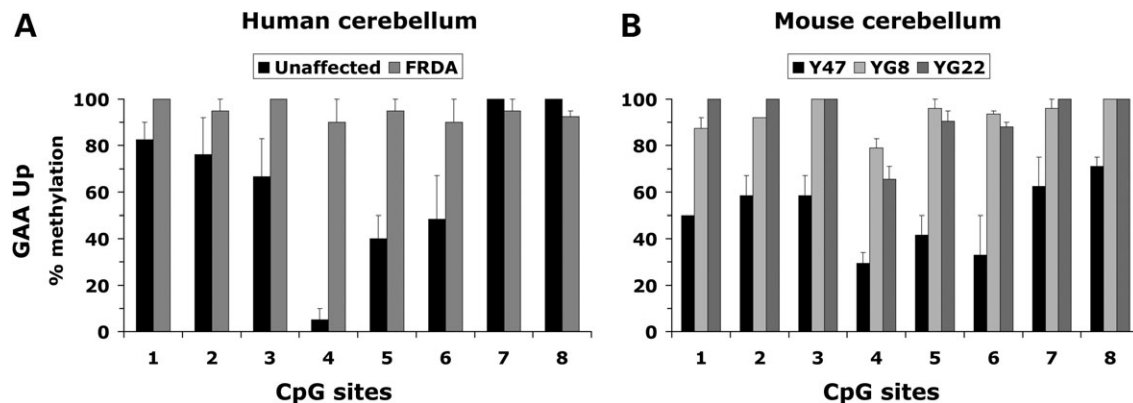


Figure 7. DNA methylation analysis of the upstream GAA regions of human (A) and transgenic mouse (B) cerebellar tissue. (A) In each case the mean percentage (+ SEM) of methylated CpG sites is shown as determined from the analysis of two FRDA patients (black columns) and two unaffected individuals (grey columns) with 10 independent cloned DNA sequences analysed for each. (B) Y47 (11 GAA) (black columns), YG8 (190+90 GAA) (light grey columns) and YG22 (190 GAA) (dark grey columns) transgenic mouse brain and heart tissues. In each case the mean percentage value (+SEM) of methylated CpG sites is shown as determined from the analysis of 7–12 independent cloned DNA sequences from each of two mice per group.

mouse cerebellar tissue is more severe, particularly at CpG sites 4, 5 and 6, compared with that seen in the brain tissues as a whole (Fig. 7A compared with Fig. 3C, and Fig. 7B compared with Fig. 6C). We have previously shown that frataxin expression in cerebellar tissue is reduced at both mRNA and protein levels compared with brain and brain stem tissue in our *FXN* transgenic mice (26). Therefore, the DNA hypermethylation patterns that we have now observed concur with the hypothesis that the upstream GAA region (CpG sites 4–6 in particular) is somehow involved in down-regulation of frataxin transcription.

Histone modifications of *FXN* transgenic mouse brain tissue are comparable with histone modifications of human tissue

Acetylated histone H3 and H4 and di- and tri-methylated histone H3K9 modifications were detected by ChIP analysis of the three regions of the *FXN* transgene (Fig. 2) in brain tissue isolated from both YG8 and YG22 GAA repeat expansion-containing *FXN* YAC transgenic mice (26) and Y47 normal-sized GAA repeat-containing *FXN* YAC transgenic mice (27). Our results show overall GAA repeat-induced decreases in histone H3K9 acetylation and increases in H3K9 methylation for both YG8 and YG22 transgenic mice (Fig. 8), as we previously identified in human FRDA tissue (Fig. 4). However, the level of deacetylation in the transgenic mouse tissue was not as great as that seen in the human tissue, possibly as a consequence of the smaller transgenic GAA repeat expansion sizes (190+90 for YG8 mice and 190 for YG22 mice, compared with 750/650 and 700/700 for FRDA patients). Also, H4K16 acetylation is actually increased in all three *FXN* transgene regions of YG8 mouse tissue compared with Y47. Furthermore, H4K8 acetylation and H4K12 acetylation are increased in all three *FXN* transgene regions of YG22 mouse tissue compared with Y47, which is somewhat different to the finding in human tissues. The greatest consistent histone residue changes that we found between the non-GAA (Y47) and both of the GAA (YG8 and YG22) transgenic brain tissue samples were decreases in acetylated H3K9

and increases in di- and tri-methylated H3K9. The H4K12 residue also showed a significant degree of deacetylation, but only in the YG8 transgenic tissue. All of these major histone residue changes in mouse brain tissue reflect the GAA repeat-induced histone residue changes that we detected in human tissue. Furthermore, as with the human samples, we similarly identified a GAA repeat-induced gradient of decreased H3K9 acetylation in both YG8 and YG22 transgenic mouse tissues, with the highest comparative levels of acetylation in the *FXN* promoter and the lowest comparative levels in the downstream GAA region. The increases in H3K9 di- and tri-methylation were consistent throughout all of the three *FXN* gene regions in both YG8 and YG22 transgenic mice, once again agreeing with our findings in human FRDA tissue.

DISCUSSION

For the consideration of future FRDA therapy, it is first essential to understand the mechanism of GAA-induced inhibition of *FXN* gene transcription. Previous studies of FRDA have implicated epigenetic changes, including the detection of increased DNA methylation of specific CpG sites upstream of the GAA repeat and histone modifications in regions flanking the GAA repeat that are both consistent with transcription inhibition (23,24). However, no DNA or histone methylation changes have previously been identified in the *FXN* promoter or downstream GAA regions, and clinically relevant FRDA brain and heart tissues have not previously been investigated. Different trinucleotide repeat expansion mutations have been shown to induce *cis*-acting epigenetic changes in several other human disorders (28,29). Thus, DNA methylation of the CGG repeat upstream of the *FMR1* gene has been identified as a main epigenetic switch in Fragile X syndrome, with histone acetylation playing an ancillary role (30). Decreased Sp1 interaction associated with DNA hypermethylation upstream of the CTG repeat in the *DMPK* gene has also been reported for congenital myotonic dystrophy type 1 (29). Furthermore, both CTG and GAA repeat expansions have

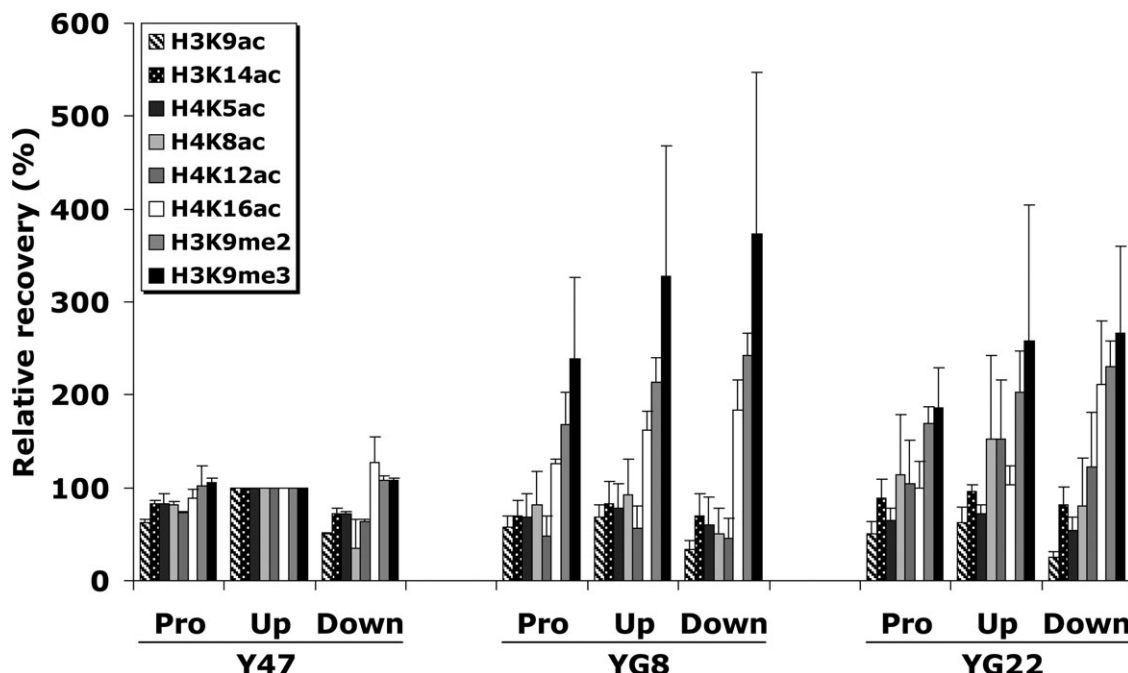


Figure 8. Analysis of histone modifications in transgenic mouse brain tissues. ChIP quantitative PCR results for the transgenic *FXN* promoter/exon1 (Pro), upstream GAA (Up) and downstream GAA (Down) amplified regions are represented as the relative amount of immunoprecipitated DNA compared with input DNA, having taken negligible –Ab control values into account. *FXN* values were normalized with mouse *GAPDH* and all values have been adjusted so that all of the upstream GAA values from the non-GAA transgenic mouse tissues (Y47) are 100%. In each case two individual ChIP samples were analysed in triplicate from each of two mice per group. The means and SEMs of these values are shown.

been shown to induce similar heterochromatin formation by position effect variegation studies of transgenic mice (21). However, it is still uncertain if different trinucleotide repeat sequences produce similar overall epigenetic effects or not.

Our investigations of the *FXN* gene in both FRDA human and transgenic mouse brain, cerebellum and heart tissues have now confirmed the presence of previously described DNA methylation changes (23) in the upstream GAA region of these clinically important tissues. Furthermore, our data have revealed an overall shift in the DNA methylation profile, moving from hypomethylation in the downstream GAA region towards hypermethylation in the upstream GAA region. This shift in DNA methylation profile could be explained by the known position of the GAA repeat within an Alu sequence, since Alu sequences have been shown to act as methylation centres leading to bi-directional spread of DNA methylation (31). Thus, the hypermethylation detected in the FRDA upstream GAA region may be due to the GAA repeat mutation enhancing the effect of a putative methylation centre at the 5' end of the Alu sequence. At the same time, the addition of the GAA repeat sequence would put extra distance between the methylation centre at the 5' end of the Alu sequence and the downstream GAA region. This may impede the spread of methylation to the downstream region when the distance is large enough (e.g. 2.25 kb for 750 human GAA repeats), but not when the distance is smaller (e.g. 600 bp for 190 transgenic mouse GAA repeats).

We have additionally identified differential DNA methylation at four specific CpG sites within the *FXN* promoter and exon 1 regions that have not previously been reported. The three CpG sites within the promoter region (sites 5, 7 and 8)

are immediately upstream of the ATG translation start site, at nucleotide positions -27, -18 and -11, respectively. CpG sites 5 and 7 are also contained within Sp1 transcription factor binding sites (32). Interestingly, the region between -64 and the start of translation has previously been suggested to contain sequences important for positive regulation of frataxin production, although no candidate sequences were identified (33). Therefore, the three differentially methylated CpG sites that we have now uncovered in the *FXN* promoter, and in particular the two Sp1 recognition sites, are likely to represent these important regulatory sequences.

In comparison with other instances of trinucleotide repeat-induced DNA methylation changes that inhibit transcription (28,29), one would have predicted general hypermethylation to be associated with the FRDA GAA repeat expansion mutation. However, we actually identified three occurrences in human tissues (promoter and downstream GAA regions in brain, and downstream GAA region in heart) and one occurrence in mouse tissues (promoter region in heart) where there was in fact GAA repeat expansion-induced decrease in DNA methylation. This suggests the possible occurrence of demethylation and resultant active *FXN* gene expression, at least for some cells within the tissue. DNA demethylation has previously been shown to occur both passively due to DNA replication upon cell division (34) and actively in a process that may involve RNA (35), although the DNA demethylating activity has yet to be identified. DNA demethylation has also previously been associated with processes of DNA damage and repair. The formation of 8-OH-dG by oxidative DNA damage has been shown to affect the activity of human DNA methyltransferase and

inhibit CpG methylation (36), and DNA demethylation has also been shown to occur as a result of homologous recombination repair of DNA damaged by double-strand breaks (37). However, DNA demethylation has not previously been considered for FRDA. A close inspection of our data reveals that potential DNA demethylation in the *FXN* promoter region occurs when the degree of DNA hypermethylation change in the upstream GAA region is greatest. Therefore, we now propose that the shutdown of transcription due to major epigenetic changes at the upstream GAA region may result in attempts to upregulate *FXN* transcription by Sp1 binding and subsequent DNA demethylation in the promoter region. In support of this proposal, Sp1 binding is known to occur independent of CpG methylation status (32), but at the same time has been shown to inhibit CpG methylation (38). Furthermore, DNA demethylation has previously been shown to occur when there are few methylated CpG sites within a CpG island, but not when all of the CpG sites are methylated (39), which is exactly the situation that we find for the *FXN* promoter region. However, the GAA repeat expansion-induced decreases in DNA methylation at the *FXN* promoter are not consistent throughout all human and mouse brain and heart tissues, suggesting the involvement of other factors. Such factors may include differential susceptibility of the brain and heart tissues to DNA damage and/or GAA repeat instability. Indeed, FRDA is a disorder that is known to involve both oxidative DNA damage (40) and somatic instability of GAA repeats (3–5). Therefore, cells that are initially methylated at the *FXN* promoter region may lose this methylation as part of the GAA repeat instability process, wherein demethylation subsequent to DNA damage repair (37) may be selected for due to beneficial effect of *FXN* expression and hence cell viability. The GAA repeat expansion-induced decreases in DNA methylation that we have observed in the downstream GAA region of human tissues, but not transgenic mouse tissues, are more likely due to differently sized GAA repeats within the Alu sequence, as we have previously discussed. However, potential DNA demethylation in this downstream GAA region could also indirectly lead to an increase in *FXN* transcription due to the removal of inhibitory effects on RNA polymerase II elongation.

Our investigations of histone modifications within *FXN* gene in both FRDA human and transgenic mouse brain tissues have now confirmed the changes previously reported for H3K9 deacetylation in the *FXN* promoter, upstream GAA and downstream GAA regions and H3K9 methylation in the upstream GAA region (23,24). Furthermore, we have extended the H3K9 methylation analysis to include the *FXN* promoter and downstream GAA regions that to our knowledge have not previously been reported for any FRDA tissue. Our findings from both human and transgenic mouse tissues indicate significant H3K9 deacetylation, which becomes more severe upon progression from the *FXN* promoter, through the upstream GAA region to the downstream GAA region. This correlates well with the results for both di- and trimethylation of H3K9, which show a generally similar gradient of progressive increase from the *FXN* promoter, through the upstream GAA region, to the downstream GAA region. The only exception is the very high level of di-methylated H3K9 in the upstream GAA region of human FRDA brain tissue, which is higher than that in the downstream GAA region.

All of the H3K9 changes correlate well with the DNA methylation changes in both human and transgenic mouse brain tissues. Thus, the patterns of progressively increasing H3K9 deacetylation and increasing H3K9 di- and tri-methylation in transgenic mouse brain correspond exactly to the pattern of increasing DNA methylation. Similarly, the patterns of progressively increasing H3K9 deacetylation and increasing H3K9 tri-methylation in human FRDA brain with a peak of H3K9 di-methylation in the upstream GAA region equate very well to the corresponding DNA methylation profiles. Therefore, our combined data thus far indicate major roles for DNA methylation, histone H3K9 deacetylation and histone H3K9 methylation in the inhibition of *FXN* transcription in brain and heart tissues, with a less prominent role for deacetylation of other histone residues. The more severe epigenetic changes within the *FXN* intron 1 region compared with the promoter region support a hypothesis of transcription inhibition due to interference with elongation rather than initiation. Further work will be required to determine the exact relationships between DNA methylation, histone acetylation and methylation, heterochromatin formation and transcription inhibition. However, our results are consistent with the generally described pathway for gene inactivation wherein initial histone H3K9 deacetylation leads to H3K9 methylation, recruitment of HP1, histone deacetylases, DNA methyltransferases and eventual long-term shut down of transcription by DNA methylation (41). However, this situation is not likely to be universal for all trinucleotide repeat disorders, as highlighted by research on the *FMR1* gene which has shown both histone deacetylation and H3K9 methylation in the absence of DNA methylation without interfering in active gene transcription (42).

For now, the exact mechanism by which the GAA repeat mutation inhibits frataxin expression remains elusive. However, accumulating evidence, including the findings of this report, now highlights the importance of epigenetic changes that lead to heterochromatin formation. The epigenetic changes that we and others have now identified in FRDA do not in any way negate the importance of any abnormal DNA or DNA/RNA hybrid structures in the inhibition of frataxin expression, but rather suggest the involvement of several combined mechanisms. Indeed the existence of abnormal DNA structures may help to explain why the GAA repeat mutation induces epigenetic changes in the first place. Thus, there are reports that non-B DNA structures such as hairpins may induce DNA methylation (43,44), and GAA repeats have been shown to form hairpins (45). Alternatively, small double-stranded RNA (dsRNA) has also been shown to induce transcriptional gene silencing through a mechanism that involves DNA methylation (46,47). However, dsRNA has failed to induce DNA methylation in a study of mouse oocytes (48) and dsRNA targeted to the *HD* gene does not induce DNA methylation at the target huntingtin genomic locus in human cells (49). Thus, further studies are still required to identify any possible involvement of non-B DNA structures (such as GAA hairpins or triplex structures), DNA/RNA hybrids or dsRNA in the establishment of epigenetic changes and heterochromatin formation in FRDA.

In light of the epigenetic changes that we and others have identified in FRDA tissues and cells, several novel epigenetic-

based therapeutic approaches can now be considered for FRDA. First, HDAC inhibitors can be used, and indeed these have already shown considerable promise by increasing acetylation of histones and thereby increasing *FXN* transcription in FRDA cells (24). Secondly, pharmacological approaches could be taken to decrease H3K9 methylation, as have recently been described for the combined use of mithramycin and cystamine in Huntington disease mice (50). Thirdly, therapies to decrease DNA methylation should now be considered for FRDA, as have previously been tried for other trinucleotide repeat disorders. In particular, 5-azadeoxycytidine (5-azadC) has been shown to remove DNA methylation of the CCG repeat expansion, increase H3 and H4 acetylation, decrease H3K9 methylation, increase H3K4 methylation and reactivate the *FMR1* gene (30,51). Combined HDAC inhibitor and 5-azadC treatment has also been shown to synergistically increase *FMR1* gene activity (52). Finally, short dsRNA molecules complementary to promoter sequences have recently been shown to induce gene activation (53,54), and such approaches may also prove effective in increasing *FXN* transcription. Our identification of a transgenic FRDA mouse model that shows comparable epigenetic changes to those seen in FRDA patients will now provide a valuable resource in the study of all such epigenetic-based FRDA therapies.

MATERIALS AND METHODS

Tissues

Human brain, cerebellum and heart tissue samples were obtained from autopsies of two FRDA patients (750/650 and 700/700 GAA repeats) and two non-FRDA individuals, in accordance with UK Human Tissue Authority ethical guidelines. Mouse brain and heart tissues were dissected from our previously reported *FXN* YAC transgenic mouse models: Y47 (two copies of nine GAA repeats); YG8 (2 copies of 90 and 190 GAA repeats) and YG22 (1 copy of 190 GAA repeats) (25,27).

mRNA expression analysis

Total RNA was isolated from frozen tissues by homogenization with Trizol (Invitrogen) and cDNA was then prepared by using AMV Reverse transcriptase (Invitrogen) with oligo-dT primers. Levels of human or mouse transgenic *FXN* mRNA expression were assessed by quantitative RT–PCR using an ABI7400 sequencer and SYBR® Green (Applied Biosystems) with the following primers: FxnRTF 5'-CAGAGGAAACGCTGGAC TCT-3' and FxnRTR 5'-AGCCAGATTGCTGTTGGC-3' (24). Human *GAPDH* or mouse *Gapdh* RT–PCR primers were used as control standards: human: GapdhF 5'-GAAGG TGAAGGTCGGAGT-3' and GapdhR 5'-GAAGATGGTGA TGGGATTT-3' mouse GapdhM 5'-ACCCAGAAGACTG TGGATGG-3' and GapdhR 5'-GGATGCAGGGATGAT GTTCT-3'.

Bisulfite sequencing

Genomic DNA was isolated from frozen tissue by standard phenol/chloroform extraction and ethanol precipitation. Two

micrograms of genomic DNA was digested with *Eco*RI prior to bisulfite treatment using the CpGenome kit (Calbiochem). Nested PCR was carried out on bisulfite-treated DNA to amplify three regions of the *FXN* gene using the following primers: Pro 1st primer pair: SL1F1 5'-TAGTTTTTAA GTTTTTTTGTTAG-3' and SL1R1 5'-CAAAACAAAAT ATCCCCCTTTC-3'; Pro 2nd primer pair: SL1F2 5'-GTTTT TTTATAGAAGAGTGTGTTG-3' and SL1R2 5'-CAAAAACC AATATAAATACAACC-3'; Up 1st primer pair: F1G 5'-GAG GGATTGTTGGTAAAG-3' and R1G 5'-ATACTAAAT TTCACCATATTAACC-3'; Up 2nd primer pair: F2G 5'-GA TTTGTTGGTAAAGGTTAG-3' and R2G 5'-CTCCCAA AATACTAAAATTATAAAC-3'; Down 1st primer pair: NH1F 5'-AAGAAGAAGAAGAAAATAAGAAAAG-3' and SLGR2 5'-TCCTAAAAAAATCTAAAAACCATC-3'; Down 2nd primer pair: NH2F 5'-AGAAGAAGAAAATAAA GAAAAGTTAG-3' and SLGR1 5'-AAAACCATCATAAC CACACTTAC-3'. PCR products were then resolved on agarose gels, purified with GeneClean (BIO101) and cloned into pCR4.0 (Invitrogen) prior to DNA sequencing. A minimum of seven clones were sequenced for each tissue sample.

ChIP analysis

Histone modifications at the three *FXN* gene regions were detected by ChIP analysis of FRDA human and mouse tissues. This procedure involved initial cross-linking of DNA and protein by formaldehyde treatment of homogenized frozen tissue samples. DNA was then sheared by sonication, followed by immunoprecipitation with commercially available anti-histone and anti-acetylated histone H3 and H4 antibodies: H3K9ac, H3K14ac, H4K5ac, H4K8ac, H4K12ac, H4K16ac and H3K9me2 (Upstate), and H3K9me3 (Diagenode). For each experiment, normal rabbit serum (SIGMA) was used as a minus antibody immunoprecipitation control. After reversal of cross-linking, quantitative RT–PCR amplification of the resultant co-immunoprecipitated DNA was carried out with SYBR® Green in an ABI7400 sequencer (Applied Biosystems) using three sets of *FXN* primers (Pro, Up and Down) and human *GAPDH* control for the human samples as previously described (24). For the analysis of transgenic mouse samples, the same three sets of *FXN* primers were used together with the following mouse *Gapdh* control primers: GapdhMF, 5'-TGACAAGAGGGCGAGCG-3' and GapdhMR, 5'-GGAAGCCGAAGTCAGGAAC-3'. Each tissue sample was subjected to two independent ChIP procedures, followed by triplicate quantitative PCR analysis.

Conflict of Interest statement. None declared.

FUNDING

This research has been supported by the Friedreich's Ataxia Research Alliance (FARA), the National Ataxia Foundation (NAF), Ataxia UK, GoFAR and the King Faisal Specialist Hospital and Research Center, KSA.

REFERENCES

- Campuzano, V., Montermini, L., Molto, M.D., Pianese, L., Cossee, M., Cavalcanti, F., Monros, E., Rodius, F., Duclos, F., Monticelli, A. et al. (1996) Friedreich's ataxia: autosomal recessive disease caused by an intronic GAA triplet repeat expansion. *Science*, **271**, 1423–1427.
- Pandolfo, M. (2002) The molecular basis of Friedreich ataxia. *Adv. Exp. Med. Biol.*, **516**, 99–118.
- Clark, R.M., De Biase, I., Malykhina, A.P., Al-Mahdawi, S., Pook, M. and Bidichandani, S.I. (2006) The GAA triplet-repeat is unstable in the context of the human FXN locus and displays age-dependent expansions in cerebellum and DRG in a transgenic mouse model. *Hum. Genet.*, **120**, 633–640.
- De Biase, I., Rasmussen, A., Endres, D., Al-Mahdawi, S., Monticelli, A., Cocozza, S., Pook, M. and Bidichandani, S.I. (2007) Progressive GAA expansions in dorsal root ganglia of Friedreich's ataxia patients. *Ann. Neurol.*, **61**, 55–60.
- De Biase, I., Rasmussen, A., Monticelli, A., Al-Mahdawi, S., Pook, M., Cocozza, S. and Bidichandani, S.I. (2007) Somatic instability of the expanded GAA triplet-repeat sequence in Friedreich ataxia progresses throughout life. *Genomics*, **90**, 1–5.
- Campuzano, V., Montermini, L., Lutz, Y., Cova, L., Hindelang, C., Jiralerspong, S., Trottier, Y., Kish, S.J., Faucheu, B., Trouillas, P. et al. (1997) Frataxin is reduced in Friedreich ataxia patients and is associated with mitochondrial membranes. *Hum. Mol. Genet.*, **6**, 1771–1780.
- Bulteau, A.L., O'Neill, H.A., Kennedy, M.C., Ikeda-Saito, M., Isaya, G. and Szewda, L.I. (2004) Frataxin acts as an iron chaperone protein to modulate mitochondrial aconitase activity. *Science*, **305**, 242–245.
- Gerber, J., Muhlenhoff, U. and Lill, R. (2003) An interaction between frataxin and Isu1/Nfs1 that is crucial for Fe/S cluster synthesis on Isu1. *EMBO Rep.*, **4**, 906–911.
- Yoon, T. and Cowan, J.A. (2004) Frataxin-mediated iron delivery to ferrochelatase in the final step of heme biosynthesis. *J. Biol. Chem.*, **279**, 25943–25946.
- Koeppen, A.H., Michael, S.C., Knutson, M.D., Haile, D.J., Qian, J., Levi, S., Santambrogio, P., Garrick, M.D. and Lamarche, J.B. (2007) The dentate nucleus in Friedreich's ataxia: the role of iron-responsive proteins. *Acta Neuropathol.*, **114**, 163–173.
- Hart, P.E., Lodi, R., Rajagopalan, B., Bradley, J.L., Crilley, J.G., Turner, C., Blamire, A.M., Manners, D., Styles, P., Schapira, A.H. et al. (2005) Antioxidant treatment of patients with Friedreich ataxia: four-year follow-up. *Arch. Neurol.*, **62**, 621–626.
- Mariotti, C., Solari, A., Torta, D., Marano, L., Fiorentini, C. and Di Donato, S. (2003) Idebenone treatment in Friedreich patients: one-year-long randomized placebo-controlled trial. *Neurology*, **60**, 1676–1679.
- Richardson, D.R., Mouralian, C., Ponka, P. and Becker, E. (2001) Development of potential iron chelators for the treatment of Friedreich's ataxia: ligands that mobilize mitochondrial iron. *Biochim. Biophys. Acta*, **1536**, 133–140.
- Rustin, P., Rotig, A., Munnich, A. and Sidi, D. (2002) Heart hypertrophy and function are improved by idebenone in Friedreich's ataxia. *Free Radic. Res.*, **36**, 467–469.
- Schols, L., Vorgerd, M., Schillings, M., Skipka, G. and Zange, J. (2001) Idebenone in patients with Friedreich ataxia. *Neurosci. Lett.*, **306**, 169–172.
- Seznec, H., Simon, D., Monassier, L., Criqui-Filipe, P., Gansmuller, A., Rustin, P., Koenig, M. and Puccio, H. (2004) Idebenone delays the onset of cardiac functional alteration without correction of Fe-S enzymes deficit in a mouse model for Friedreich ataxia. *Hum. Mol. Genet.*, **13**, 1017–1024.
- Bidichandani, S.I., Ashizawa, T. and Patel, P.I. (1998) The GAA triplet-repeat expansion in Friedreich ataxia interferes with transcription and may be associated with an unusual DNA structure. *Am. J. Hum. Genet.*, **62**, 111–121.
- Grabczyk, E., Mancuso, M. and Sammarco, M.C. (2007) A persistent RNA-DNA hybrid formed by transcription of the Friedreich ataxia triplet repeat in live bacteria, and by T7 RNAP *in vitro*. *Nucleic Acids Res.*, **35**, 5351–5359.
- Grabczyk, E. and Usdin, K. (2000) The GAA*TTC triplet repeat expanded in Friedreich's ataxia impedes transcription elongation by T7 RNA polymerase in a length and supercoil dependent manner. *Nucleic Acids Res.*, **28**, 2815–2822.
- Sakamoto, N., Ohshima, K., Montermini, L., Pandolfo, M. and Wells, R.D. (2001) Sticky DNA, a self-associated complex formed at long GAA*TTC repeats in intron 1 of the frataxin gene, inhibits transcription. *J. Biol. Chem.*, **276**, 27171–27177.
- Saveliev, A., Everett, C., Sharpe, T., Webster, Z. and Festenstein, R. (2003) DNA triplet repeats mediate heterochromatin-protein-1-sensitive variegated gene silencing. *Nature*, **422**, 909–913.
- Egger, G., Liang, G., Aparicio, A. and Jones, P.A. (2004) Epigenetics in human disease and prospects for epigenetic therapy. *Nature*, **429**, 457–463.
- Greene, E., Mahishi, L., Entezam, A., Kumari, D. and Usdin, K. (2007) Repeat-induced epigenetic changes in intron 1 of the frataxin gene and its consequences in Friedreich ataxia. *Nucleic Acids Res.*, **35**, 3383–3390.
- Herman, D., Jنسن, K., Burnett, R., Soragni, E., Perlman, S.L. and Gottesfeld, J.M. (2006) Histone deacetylase inhibitors reverse gene silencing in Friedreich's ataxia. *Nat. Chem. Biol.*, **2**, 551–558.
- Al-Mahdawi, S., Pinto, R.M., Ruddle, P., Carroll, C., Webster, Z. and Pook, M. (2004) GAA repeat instability in Friedreich ataxia YAC transgenic mice. *Genomics*, **84**, 301–310.
- Al-Mahdawi, S., Pinto, R.M., Varshney, D., Lawrence, L., Lowrie, M.B., Hughes, S., Webster, Z., Blake, J., Cooper, J.M., King, R. et al. (2006) GAA repeat expansion mutation mouse models of Friedreich ataxia exhibit oxidative stress leading to progressive neuronal and cardiac pathology. *Genomics*, **88**, 580–590.
- Pook, M.A., Al-Mahdawi, S., Carroll, C.J., Cossee, M., Puccio, H., Lawrence, L., Clark, P., Lowrie, M.B., Bradley, J.L., Cooper, J.M. et al. (2001) Rescue of the Friedreich's ataxia knockout mouse by human YAC transgenesis. *Neurogenetics*, **3**, 185–193.
- Greene, E., Handa, V., Kumari, D. and Usdin, K. (2003) Transcription defects induced by repeat expansion: fragile X syndrome, FRAXE mental retardation, progressive myoclonus epilepsy type 1, and Friedreich ataxia. *Cytogenet. Genome Res.*, **100**, 65–76.
- Steinbach, P., Glaser, D., Vogel, W., Wolf, M. and Schwemmle, S. (1998) The DMPK gene of severely affected myotonic dystrophy patients is hypermethylated proximal to the largely expanded CTG repeat. *Am. J. Hum. Genet.*, **62**, 278–285.
- Tabolacci, E., Pietrobono, R., Moscato, U., Oostra, B.A., Chiurazzi, P. and Neri, G. (2005) Differential epigenetic modifications in the FMR1 gene of the fragile X syndrome after reactivating pharmacological treatments. *Eur. J. Hum. Genet.*, **13**, 641–648.
- Graff, J.R., Herman, J.G., Myohanen, S., Baylin, S.B. and Vertino, P.M. (1997) Mapping patterns of CpG island methylation in normal and neoplastic cells implicates both upstream and downstream regions in *de novo* methylation. *J. Biol. Chem.*, **272**, 22322–22329.
- Clark, S.J., Harrison, J. and Molloy, P.L. (1997) Sp1 binding is inhibited by (m)Cp(m)CpG methylation. *Gene*, **195**, 67–71.
- Greene, E., Entezam, A., Kumari, D. and Usdin, K. (2005) Ancient repeated DNA elements and the regulation of the human frataxin promoter. *Genomics*, **85**, 221–230.
- Matsuo, K., Silke, J., Georgiev, O., Marti, P., Giovannini, N. and Rungger, D. (1998) An embryonic demethylation mechanism involving binding of transcription factors to replicating DNA. *EMBO J.*, **17**, 1446–1453.
- Weiss, A., Keshet, I., Razin, A. and Cedar, H. (1996) DNA demethylation in vitro: involvement of RNA. *Cell*, **86**, 709–718.
- Turk, P.W., Laayoun, A., Smith, S.S. and Weitzman, S.A. (1995) DNA adduct 8-hydroxyl-2'-deoxyguanosine (8-hydroxyguanine) affects function of human DNA methyltransferase. *Carcinogenesis*, **16**, 1253–1255.
- Cuozzo, C., Porcellini, A., Angrisano, T., Morano, A., Lee, B., Pardo, A.D., Messina, S., Iuliano, R., Fusco, A., Santillo, M.R. et al. (2007) DNA damage, homology-directed repair, and DNA methylation. *PLoS Genet.*, **3**, e110. First published on 22 May 2007, 10.1371/jgen.0030110.
- Macleod, D., Charlton, J., Mullins, J. and Bird, A.P. (1994) Sp1 sites in the mouse aprt gene promoter are required to prevent methylation of the CpG island. *Genes. Dev.*, **8**, 2282–2292.
- Choi, Y.C. and Chae, C.B. (1993) Demethylation of somatic and testis-specific histone H2A and H2B genes in F9 embryonal carcinoma cells. *Mol. Cell. Biol.*, **13**, 5538–5548.
- Schulz, J.B., Dehmer, T., Schols, L., Mende, H., Hardt, C., Vorgerd, M., Burk, K., Matson, W., Dichgans, J., Beal, M.F. et al. (2000) Oxidative stress in patients with Friedreich ataxia. *Neurology*, **55**, 1719–1721.

41. D'Alessio, A.C. and Szyf, M. (2006) Epigenetic tete-a-tete: the bilateral relationship between chromatin modifications and DNA methylation. *Biochem. Cell Biol.*, **84**, 463–476.
42. Pietrobono, R., Tabolacci, E., Zalfa, F., Zito, I., Terracciano, A., Moscato, U., Bagni, C., Oostra, B., Chiurazzi, P. and Neri, G. (2005) Molecular dissection of the events leading to inactivation of the FMR1 gene. *Hum. Mol. Genet.*, **14**, 267–277.
43. Chen, X., Mariappan, S.V., Catasti, P., Ratliff, R., Moysis, R.K., Laayoun, A., Smith, S.S., Bradbury, E.M. and Gupta, G. (1995) Hairpins are formed by the single DNA strands of the fragile X triplet repeats: structure and biological implications. *Proc. Natl Acad. Sci. USA*, **92**, 5199–5203.
44. Laayoun, A. and Smith, S.S. (1995) Methylation of slipped duplexes, snapbacks and cruciforms by human DNA(cytosine-5)methyltransferase. *Nucleic Acids Res.*, **23**, 1584–1589.
45. Heidenfelder, B.L., Makarov, A.M. and Topal, M.D. (2003) Hairpin formation in Friedreich's ataxia triplet repeat expansion. *J. Biol. Chem.*, **278**, 2425–2431.
46. Kawasaki, H. and Taira, K. (2004) Induction of DNA methylation and gene silencing by short interfering RNAs in human cells. *Nature*, **431**, 211–217.
47. Morris, K.V., Chan, S.W., Jacobsen, S.E. and Looney, D.J. (2004) Small interfering RNA-induced transcriptional gene silencing in human cells. *Science*, **305**, 1289–1292.
48. Svoboda, P., Stein, P., Filipowicz, W. and Schultz, R.M. (2004) Lack of homologous sequence-specific DNA methylation in response to stable dsRNA expression in mouse oocytes. *Nucleic Acids Res.*, **32**, 3601–3606.
49. Park, C.W., Chen, Z., Kren, B.T. and Steer, C.J. (2004) Double-stranded siRNA targeted to the huntingtin gene does not induce DNA methylation. *Biochem. Biophys. Res. Commun.*, **323**, 275–280.
50. Ryu, H., Lee, J., Hagerty, S.W., Soh, B.Y., McAlpin, S.E., Cormier, K.A., Smith, K.M. and Ferrante, R.J. (2006) ESET/SETDB1 gene expression and histone H3 (K9) trimethylation in Huntington's disease. *Proc. Natl Acad. Sci. USA*, **103**, 19176–19181.
51. Pietrobono, R., Pomponi, M.G., Tabolacci, E., Oostra, B., Chiurazzi, P. and Neri, G. (2002) Quantitative analysis of DNA demethylation and transcriptional reactivation of the FMR1 gene in fragile X cells treated with 5-azadeoxycytidine. *Nucleic Acids Res.*, **30**, 3278–3285.
52. Chiurazzi, P., Pomponi, M.G., Pietrobono, R., Bakker, C.E., Neri, G. and Oostra, B.A. (1999) Synergistic effect of histone hyperacetylation and DNA demethylation in the reactivation of the FMR1 gene. *Hum. Mol. Genet.*, **8**, 2317–2323.
53. Janowski, B.A., Younger, S.T., Hardy, D.B., Ram, R., Huffman, K.E. and Corey, D.R. (2007) Activating gene expression in mammalian cells with promoter-targeted duplex RNAs. *Nat. Chem. Biol.*, **3**, 166–173.
54. Li, L.C., Okino, S.T., Zhao, H., Pookot, D., Place, R.F., Urakami, S., Enokida, H. and Dahiya, R. (2006) Small dsRNAs induce transcriptional activation in human cells. *Proc. Natl Acad. Sci. USA*, **103**, 17337–17342.